Case Studies
in
Mathematical Modelling
for
Biological Conservation

A thesis
submitted in fulfilment
of the requirements for the Degree of
Doctor of Philosophy
in
Mathematics
at the
University of Canterbury

Britta Basse, M.Sc. (Hons.)

Department of Mathematics and Statistics
University of Canterbury
Christchurch, New Zealand
November 1999

North Island kokako *Callaeas cinerea wilsoni.*

Abstract

The use of mathematical modelling as a tool for investigating selected topics in conservation biology is the focus of this thesis.

A continuous system of partial and ordinary differential equations model the age structured population dynamics of a cohort of endemic, threatened New Zealand North Island brown kiwi, *Apteryx mantelli*. Critical predation and recruitment rates of immature birds are estimated. Stoats, *Mustela erminea*, are the main predator of immature kiwi. A refinement to the model allows the calculation of acceptable stoat densities. In order to reduce stoats to this critical density, a linear system of ordinary differential equations, representing an acute secondary poisoning regime, is solved. An optimal secondary poisoning scheme, which minimises the number of prey poisoned and the amount of poison used, is found. The minimum area required for pest control is estimated by simulating the dispersal of sub-adult kiwi using a discrete random walk approach. Simulations and a discrete age structured model are used to investigate pulsed management strategies for both kiwi and kokako, *Callaeas cinerea wilsoni*. Finally, a two dimensional discrete random walk is generalised and a continuous diffusion equation is derived. A diffusion equation is incorporated into a SIR (Susceptible, Infected, Recovered) model representing the natural spread of Rabbit Haemorrhagic Disease from a point source in rabbit, *Oryctolagus cuniculus cuniculus*, populations. The speed for the virus, dependant on certain model parameters, is found and the minimum initial population density, below which the wave of infection will not travel, is estimated.

All specific models discussed throughout the thesis are generic by nature and can be applied to a diverse range of subjects.

Acknowledgements

Firstly, I couldn't have asked for two better supervisors. To Graeme Wake, for convincing me that I should start my PhD and totally encouraging me throughout, thanks heaps! Also a big, big thankyou to John McLennan for his positivity, introducing us to kiwis at Lake Waikaremoana and motivating the project in the first place.

The following people were also involved at various times in the project and their help and advice was greatly appreciated: John Parkes (Landcare Research, Lincoln) and Nigel Barlow (AgResearch, Lincoln) for the RHD project; John Innes (Landcare Reseach, Hamilton) and Ian Flux (Department of Conservation, Wellington) for the kokako work; Ron Gribben (University of Brunei) for advice on the 'toes up stoats' poison model; Irene Hudson (University of Canterbury) for welcoming me to the Mathematics and Statistics department here and putting me on the right track for the population viability analysis; Mike Steel (University of Canterbury) for showing me how to convolute a bunch of two dimensional uniform probability density functions.

Thanks to Michael for checking my thesis and tolerating my thesis anxiety. Thanks to Kirsten and Beverley for the proofreading and constructive advice. Thanks to Dad, Mum, Kim, Lynn and Kirsten for their total support, encouragement over the years and believing I could do it. I'm especially grateful to Kirsten for coming down to Christchurch and looking after Lara while I was writing up. It could have taken months longer otherwise.

To the following institutions who made it possible for me to get through without a student loan. All amounts great and small helped, so thankyou: Landcare Research; Mathematics Department Auckland University; Statistics Department Auckland University; Department of Mathematics and Statistics University of Canterbury; New Zealand Federation of University Women for the Hariette Jenkins Award. University of Canterbury for the Laura J. Clad memorial scholarship.

This thesis is dedicated to Lara.

Contents

List of Figures

List of Tables

Chapter 1

Introduction

1.1 Mathematical biology and population dynamics

For centuries people have attempted to describe and predict biological and physical phenomena using a mathematical approach. In 1202, Fibonacci, an Italian mathematician, generated the Fibonacci sequence of numbers by investigating how many offspring are produced by a pair of rabbits in one year ([29]). In 1798, Malthus considered unlimited exponential growth as a model of population dynamics. This model was later refined by Pearl and Verhulst into a logistic growth model, incorporating carrying capacity ([80]). The word 'dynamic' generally implies change, movement or force and is derived from the Greek word 'dunamis' meaning power. The study of population dynamics encompasses everything relating to population change. For example one might analyse population densities or age structure, evolving throughout time and/or space. Another area of interest might be to follow a wave of infection travelling across a continent. The use of mathematics applied to population dynamics and many other areas of the biological sciences has grown substantially in recent years. A model of a dynamical system, such as a population, is usually a representation of either a part or the whole of the dynamical system of interest. Although models can take on many different forms, the emphasis in this thesis is on mathematical models where the dynamics of a system are represented by a set of equations. These equations can be used to predict the state of the system by computer simulation or numerical analysis.

Throughout this thesis, dynamical systems models and other mathematical and statistical tools are employed in order to examine topics associated with biological conservation and environmental management. The three specific areas of investigation were motivated by Landcare Research Limited, a New Zealand Crown Research Institute. The plight of the northern brown kiwi, *Apteryx mantelli*, an endangered flightless bird endemic to New Zealand, is the underlying theme in chapters 2 to 5. Chapter 6 examines pulsed management options for both kiwi and kokako birds, *Callaeas cinerea wilsoni*. Chapter 7 on the other hand, deals with the spread of the RHD (Rabbit Haemorrhagic Disease) virus which was illegally introduced into New Zealand in 1997 as a biological control for rabbits, *Oryctolagus cuniculus cuniculus*.

A diverse range of issues are discussed throughout the thesis but the underlying modelling has a generic nature and can be applied to a wider range of applications which may come from disciplines other than biological conservation.

The basis of all of the models derived throughout this thesis are conservation equations

of the type

$$\begin{pmatrix} \text{rate of} \\ \text{change} \end{pmatrix} = \begin{pmatrix} \text{rate} \\ \text{in} \end{pmatrix} - \begin{pmatrix} \text{rate} \\ \text{out} \end{pmatrix}. \tag{1.1}$$

Here the rate of change usually represents the change in population numbers during some time interval $\triangle t$. The 'rate in' is the number of individuals entering the population during that time interval through birth, immigration/dispersal or aging (if the 'population' is divided into age classes). The 'rate out' is the number of individuals leaving the population due to death, migration/dispersal or aging. More general and complicated forms of the conservation equation (1.1) are used to model processes from such a wide variety of applications that it is impossible to list them all here. Complex population models may have interactions which give rise to systems of conservation equations. A thorough overview of such mathematical models applied to biological fields is given by [66].

Conservation equations may be ordinary or partial, discrete or continuous, deterministic or stochastic. In section 1.3, differences between the stability of discrete and continuous models are discussed and in section 1.4 deterministic versus stochastic approaches to modelling are compared. In general, most of the models derived in chapters 2 to 7 are continuous and deterministic. In chapters 5 and 6, the underlying model is discrete and in chapter 7 a discrete approach is used for the derivation of a continuous diffusion equation. In chapters 4, 5 and 6 it was necessary to build a degree of stochasticity into the model. A chapter overview follows in section 1.2.

1.2 An overview of topics covered and techniques used in this thesis

In chapter 2, a continuous deterministic age structured kiwi population model is derived using equation (1.1) as a foundation. There are two sub-adult age classes; chicks and juveniles. Each conservation equation for sub-adults, representing the number density of individuals, $N(t, a)$, of a particular age, a, within an age class at time t, is of the form

$$\frac{\partial N}{\partial t} + \frac{\partial N}{\partial a} = \text{rate in} - \text{rate out}$$

where the left hand side represents a rate of change with respect to both age and time. Conservation equations for adults are differentiated by gender but are not age structured.

The model is partially analytically solved to find a temporal solution for female adults. The asymptotic behaviour of this solution depends on the control parameter representing juvenile predation. The latter being the crucial factor for the demise of the kiwi population. A critical value of the juvenile predation rate represents the boundary between survival and extinction of the entire cohort. Using this, the minimum number of chicks required for adult recruitment can be obtained. In the field, predation losses of juveniles greatly exceed the critical value estimated by the model and the recruitment of chicks to adults is well below the estimated minimum required for population maintenance.

Chapter 2 sets the scene for chapters 3 to 6, each of which relate to the reduction of predator densities to acceptable levels and the methods being considered for doing so. Kiwis are vulnerable to a wide range of predators throughout their life but the main cause of decline in mainland New Zealand forests is consistent excessive stoat, *Mustela erminea*, predation on immature birds ([60]). Stoat reduction and control is consequently viewed as essential for kiwi survival. Chapter 3 uses a modified version of the model developed in chapter 2 to estimate an acceptable stoat density. Stoat abundance varies between localities and years, apparently in response to changes in the availability of food. Measurements suggest that even when stoats are at the low point of their cycle, they are still sufficiently abundant to prevent adequate adult recruitment of kiwi ([60]) and the model verifies this.

Chapters 4, 5 and 6 explore optimal methods of stoat eradication. Chapter 4 aims to obtain an optimal secondary poisoning regime for stoat removal. Secondary poisoning is where the target species is poisoned via its prey species, rather than ingesting the poison directly. The main food source of stoats in most New Zealand forests is mice, *Mus musculus*. In this chapter, a simplified continuous system of differential equations is derived representing poison in the environment, poison in the mice and stoat pools, and mice and stoat densities. This system is a special case of the generic continuous model for multi-species interaction given in equation (1.2). A degree of stochasticity is built into the model via a contact rate. This was necessary in order to ensure that in an optimal regime, there is a high probability of an encounter between a stoat and a poisoned mouse. It is evident that an accurate mathematical analysis has advantages over field trials when it comes to developing a secondary poisoning regime however, the dichotomy is that field trials are required to verify the predictions of the model.

Up to this point in the thesis, each of the models formulated has been continuous by na-

ture. Chapter 5 uses a discrete approach to find an optimal (minimum) area to be eradicated of stoats to ensure survival of kiwi. Economically it is not a viable option to continually control pests on a large scale using current methods. The age structured model developed in chapter 2 is generalised and discretised. A discrete spatial structure is also added to represent the dispersal of sub-adult kiwi from their nest sites. A 10,000 hectare block of land, perhaps representing part of a national park is considered, inside which there is an area (termed the treatment block) eradicated of pests. Computer simulations and a population viability analysis are used to determine how big the treatment block should be to ensure a high probability of survival throughout the whole 10,000 hectare block. Population viability analysis (PVA), in general terms, is a technique used to estimate the probability of extinction of a population as described by [48]. Outcomes of different sub-adult dispersal scenarios are compared indicating that the suppression of dispersal decreases the size of the minimum treatment block area.

In chapter 6, the simulations from chapter 5 are used to consider pulsed management options for kiwi. Pulsed management strategies for North Island kokako are then compared. The comparison is performed via a difference equation for adult females, generalised and discretised from the age structured model in chapter 2. The productivity rate of female adults is sampled from a distribution leading to a stochastic difference equation. Simulations result in a density distribution of adult females in any particular snapshot year. The variance of the distribution increases with time so it is decided that ten years is an ample forecast.

Stochasticity is built into the simulation in chapter 5 via the sub-adult movement scenarios. In a time interval, each individual sub-adult disperses with a direction and distance sampled from a uniform distribution. A similar discrete spatial random walk approach leads to the derivation of the diffusion equation used in chapter 7. Each individual in a cell positioned within a grid or lattice has a certain probability of moving to a neighbouring cell in a particular time interval. This gives rise to a conservation equation that is discrete in both space and time. When both the time interval, Δt, and the distance between lattice points, Δx, tend towards zero, the diffusion equation is derived. Diffusion equations are continuous (both spatially and temporally) partial differential equations traditionally used in fluid dynamics. In chapter 7 however, diffusion equations are incorporated into an SIR (Susceptible, Infective, Recovered) model to represent the spread of the RHD (Rabbit Haemorrhagic Disease) virus in rabbits.

A basic SIR model has three continuous conservation equations of the type shown in equation (1.2), one for susceptible individuals, one for those who are infected with the disease and one for those recovered and perhaps immune. More complicated versions may include an age structure ([72]) or different types of immunity. In chapter 7, a spatial structure is added by incorporating diffusion terms. The solution of the system shows travelling waves of infection. Analysis of travelling waves has its origins in the physical sciences under fluid dynamics, however, many examples of the appearance of travelling waves in biological phenomena are listed in [66], with examples ranging from chemical reactions to insect dispersal.

Throughout chapters 2 to 7 the stability of each system is investigated. In chapters 2, 3, 5 and 6, parameters are perturbed and graphical sensitivity analyses are performed. In chapter 7, the stability of the system is vital because when numerical methods are used to solve the diffusion equations, instability can occur if time and spatial intervals are chosen incorrectly.

1.3 Discrete versus continuous models

Continuous population models can be used if birth is essentially a continuous process. A generic continuous mathematical model of multi-species interactions has the differential system

$$\frac{dN_j(t)}{dt} = F_j[N_1(t), N_2(t), \ldots, N_m(t)], \tag{1.2}$$

where $j = 1, 2, \ldots, m$ and $F_j(N_1, N_2, \ldots N_m)$ are a series of non-linear functions describing the interactions among the m species with population size $N_j(t)$. This generic system of equations is the basis for modelling the secondary poisoning regime discussed in chapter 4. Other examples include predator prey systems and SIR (Susceptible, Infected, Recovered) models of disease transmission ([66]).

If generations do not overlap, or if there is well defined breeding season, then a discrete system may be used ([52],[66]). The discrete analogue of equation (1.2) is given in equation (1.3), where the time step has been scaled to unity,

$$N_j(t+1) = N_j(t) + F_j[N_1(t), N_2(t), \ldots, N_m(t)]. \tag{1.3}$$

The classic paper by [52] investigates the general system of continuous differential equations, (1.2), and its homologous system of discrete difference equations, (1.3). The stability

of the discrete system implies that of the continuous system but the converse is not necessarily guaranteed. If the time lapse between successive generations in (1.3) becomes small, then the properties of the discrete system are usually the same as that of the continuous system. Thus, continuous models have advantages over discrete models which are generally less stable. In practise, as soon as a continuous system becomes difficult or impossible to solve, usually via the presence of a non-linearity, numerics are employed and the continuity is essentially discretised. This discretisation alone can unduly alter the behaviour of the dynamics.

1.4 Deterministic versus stochastic models

Stochasticity can be built into a deterministic mathematical model of population dynamics by considering some, or all, of the parameters as random variables. For example, suppose a deterministic equation for population dynamics is of the form

$$\frac{dx}{dt} = f(x,t), \tag{1.4}$$

where $f(x,t)$ is a function depending on some parameters which are themselves random variables, then the stochastic differential equation consists of the deterministic equation plus some noise, i.e.

$$dx = f(x,t)dt + \text{noise}. \tag{1.5}$$

The solution of equation 1.5 at a particular time, t, is the probability density function, $p(x,t)$ ([80]).

A stochastic model incorporates uncertainty of model parameters and gives an idea about the variability of the solution, for example in the form of variances or higher moments. Similar knowledge can be obtained from a deterministic model by perturbing parameters and performing a sensitivity analysis.

1.5 A brief overview of mathematical modelling

Suppose one has a dynamical system, part or all of which is to be mathematically modelled. The dynamical system could be, for example, a bird population or perhaps an electric circuit. Each of these systems has many characteristic parameters and state variables which may be

of interest, such as the population density in a particular area or the voltage and current at a point in the circuit. Due to the dynamic nature of the system, these state variables may change in time and can be described by a system of differential equations, often by making simplifying assumptions. By solving the system of differential equations, prediction of the values of the state variables at a desired time, and in terms of the other model parameters, can be obtained.

The process of mathematically modelling any dynamical system can be essentially categorised ([30],[89]) into four steps, each of which is vitally important:

1. Clarify the aims and objectives of the modelling and gain a thorough understanding of the problem to be solved.

2. Formulate a model, perhaps with simplifications, of the dynamical system. Formulate a mathematical model, usually a system of equations or a method of identification of relevant parameters in the dynamical system.

3. Solution. This step usually involves solving a system of differential equations or manipulating the mathematical model in order to gain a solution to the problem.

4. Interpret the solution and if possible test the validity of the solution using available data. If the solution does not make sense in a real world context, or if the aims and objectives from step one have not been satisfied, then the modelling process from step two onwards should be repeated. There is always a possibility that the aims and objectives should be reconsidered.

In chapters 2 to 7 of this thesis, these modelling steps are adhered to wherever possible. There is always more than one way of formulating a model and not always a 'best' direction or method. In an ideal world, it would be desirable to approach the problem from a number of different ways and compare solutions. Because of time constraints, this is rarely a reality.

Chapter 2

An age structured population model

Since the arrival of people in New Zealand and their subsequent introduction of mammalian predators, many populations of indigenous birds have become extinct or declined dramatically. Considered in this chapter is the population of one such species, the northern brown kiwi, *Apteryx mantelli*, whose chicks and juveniles are particularly vulnerable to stoat, *Mustela erminea*, predation in mainland forests of New Zealand. In most areas less than 5% of kiwi chicks survive to become adults. The adults, on the other hand, have high survival rates because they are large enough (2-3 kg) to defend themselves against stoats. A mathematical model is formulated which has two distinct age classes for immature kiwi, with different predation and natural mortality rates. For the adult population cohort, the possibility of different mortality rates for males and females is allowed.

Assuming predation and natural death rates are independent of population size, it is possible to calculate analytically the threshold of the predation rate, especially on chicks and juveniles, below which survival is assured and above which the cohort is doomed to extinction. The mathematical model leads to a linear delay-differential equation. Transform techniques reveal that the behaviour of the solution of the adult cohort will vary like $exp(\lambda t)$, where λ is related to a balance between the productivity rate of adult females and predation rates in various age classes. The sign of λ governs the asymptotic behaviour of the solution and λ equals zero determines the threshold between survival and extinction for this mathematical model ([9]). Analysis of the predation rate at the threshold predicts that a recruitment rate of approximately 19% is required to maintain population stability.

This work can be generalised to represent any such species and can provide useful information for management strategies.

2.1 Formulating the mathematical model

In this section a mathematical model is formulated which represents the changing dynamics of the kiwi population with respect to time. The model needs to have an age structure since immature kiwi (chicks and juveniles) are more susceptible to predation than adults and thus population growth of the immature kiwi needs to be differentiated from that of adults ([60]). Mortality rates for the two immature classes are markedly different which justifies having two immature age classes.

In order to set up a mathematical model, four classes are defined, chicks (dependent

young), juvenile kiwi, adult females and adult males. The chicks and juvenile classes are presumed to be structured by age a. Thus let

1. $m_1(t,a)$ be the number density of chicks of age a years in the population at time $t \geq 0$ years, $0 \leq a \leq a_1$;

2. $m_2(t,a)$ be the number density of juveniles of age a years in the population at time $t \geq 0$ years, $a_1 \leq a \leq a_2$;

3. $n_1(t)$ be the number of male adults in the population at time $t \geq 0$ years (not structured by age $a \geq a_2$);

4. $n_2(t)$ be the number of female adults in the population at time $t \geq 0$ years (not structured by age $a \geq a_2$).

To be mathematically rigourous, $m_i(t,a)da$ where $i \in \{1,2\}$, is the number of chicks or juveniles in the population at time t in the age interval $(a, a+da)$. Thus $m_i(t,a)$ is strictly a number density (i.e. a number in an age interval). For simplicity however, and because density is usually associated with a unit of area, $m_i(t,a)$ will in future be referred to as a number of individuals, as opposed to a number density. The division of the cohort into four compartments is shown in Figure 2.1. Death includes predation and natural mortality.

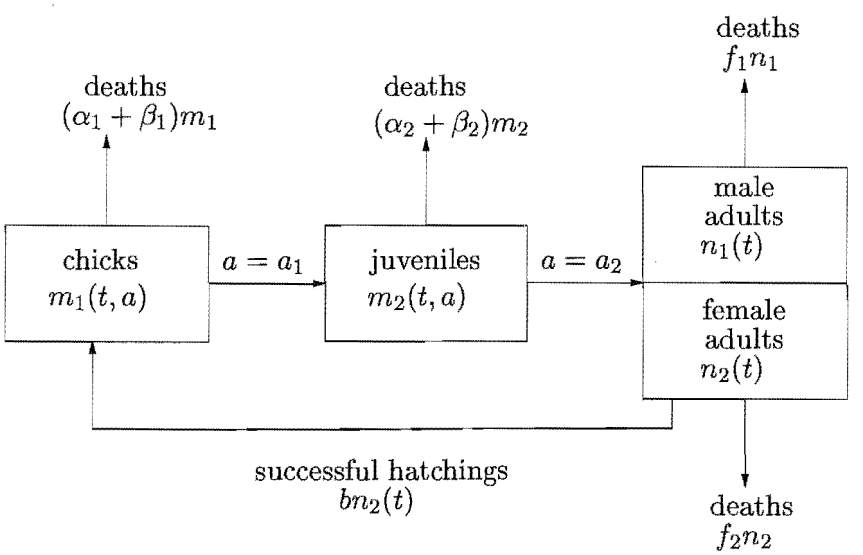

Figure 2.1: Schematic diagram showing the population compartments.

2.1.1 Finding differential equations for the chicks and juveniles

Since $m_1(t,a)$ is the number of chicks of age a in the cohort at time t (where age and time are both in years), then $m_1(t+dt, a+da) - m_1(t,a)$ is the change in population density in a time interval dt and an age interval da. Age and time increase at exactly the same rate so it is only necessary to consider an interval $h = dt = da$. Thus, the conservation equation for the change in population density in a time interval h, $m_1(t+h, a+h) - m_1(t,a)$, is equal to the number of chicks hatched in the time interval h less those chicks either becoming juveniles or dying in the time interval h. i.e.

$$m_1(t+h, a+h) - m_1(t,a) = \left(\begin{array}{c} \text{rate of} \\ \text{chicks in} \end{array} - \begin{array}{c} \text{rate of} \\ \text{chicks out} \end{array} \right) h \times m_1(t,a)$$

The number of chicks coming into the population in this time interval h is taken care of by imposing the initial condition $m_1(t,0) = bn_2(t)$ where b is the annual productivity rate per adult female, taken as a constant for simplicity, and $n_2(t)$ is the number of female kiwi at time t.

The breeding season for the northern brown kiwi is June to February ([56]). Females lay between 0-5 eggs in one breeding season but for a variety of reasons, including desertion and decay, not all eggs hatch. The productivity rate, b, on average is 0.85 eggs hatched per female per year.

The natural mortality rate and the predation rate for the chicks can initially be taken as a constant. Of particular interest are the values of the predation rates of the chicks and juveniles. These can be controlled by human intervention whereas most natural deaths (for example chicks tumbling out of nests) cannot.

The death rate of the chicks is partitioned into two parts: α_1 is the annual natural death rate and β_1 is the annual mortality rate of chicks due to predators. Hence, the number of chicks leaving the cohort in a time interval h due to death is $(\alpha_1 + \beta_1)h \times m_1(t,a)$. The conservation equation becomes

$$m_1(t+h, a+h) - m_1(t,a) = -(\alpha_1 + \beta_1)h \times m_1(t,a)$$

which can be rearranged as follows:

$$\begin{aligned} -(\alpha_1 + \beta_1)m_1(t,a) &= \frac{m_1(t+h, a+h) - m_1(t,a)}{h} \\ &= \frac{m_1(t+h, a+h) - m_1(t, a+h) + m_1(t, a+h) - m_1(t,a)}{h} \\ &= \frac{m_1(t+h, a+h) - m_1(t, a+h)}{h} + \frac{m_1(t, a+h) - m_1(t,a)}{h}. \end{aligned}$$

Letting $h \to 0$, the right hand side becomes the sum of two partial derivatives and *McKendricks'* equation ([55]) is obtained:

$$\frac{\partial m_1}{\partial t} + \frac{\partial m_1}{\partial a} = -(\alpha_1 + \beta_1)m_1(t, a), \tag{2.1}$$

which, with the inclusion of the initial condition $m_1(t, 0) = bn_2(t)$, represents the rate of change of population numbers in the chick's compartment. Note that the partial derivatives in equation (2.1) represent an instantaneous rate of change with respect to both age and time.

Using the same methodology, a similar partial differential equation can be derived representing the instantaneous rate of change with respect to age and time for the juvenile kiwi. This is *McKendricks'* equation for $m_2(t, a)$ where $m_2(t, a)$ is the number of juveniles of age a at time t. The equation is

$$\frac{\partial m_2}{\partial t} + \frac{\partial m_2}{\partial a} = -(\alpha_2 + \beta_2)m_2(t, a)$$

where α_2 is the natural death rate of the juveniles and β_2 is the death rate due to predators of the juveniles.

Northern brown kiwi chicks develop into independent juveniles when they leave the nest permanently, between approximately 18 and 25 days after hatching ([56]). Juveniles become adults at an age of about 18 months ([75]), therefore $a_1 = 0.06$ years (approximately three weeks) and $a_2 = 1.5$ years.

Instead of an initial condition, the continuity condition $m_1(t, a_1) = m_2(t, a_1)$, represents the number of chicks of age three weeks must be equal to the number of juveniles of age three weeks.

Parameter values for natural and predator mortality rates for the chicks and juveniles were obtained from a cohort of 171 radio tagged northern brown kiwi (*A. mantelli*) which live in mainland forests of the North and South Islands. Small sample sizes in each age class could lead to inaccuracies, however, this is currently the most comprehensive data set collected on any kiwi species in New Zealand ([60]). Data are scarce for kiwi because the birds are nocturnal, secretive and now so rare in mainland forests that they are difficult to locate and study.

The females produced 49 chicks that were observed for 100 days, 7 were not radio tagged and their fate was unknown so for the purposes of calculating mortality rates they were ignored from the data set. In the first three weeks (until the time that the chicks became

juveniles), 10 chicks were killed by predators (thus $\beta_1 = \frac{10}{42} \times \frac{1}{0.06} = 3.97$ per year) and 12 died due to natural causes (thus $\alpha_1 = \frac{12}{42} \times \frac{1}{0.06} = 4.76$ per year.) The remaining 20 chicks became juveniles after 3 weeks. 17 were killed by predators thus $\beta_2 = \frac{17}{20} \times \frac{365}{100} = 3.1$ per year. 2 died due to natural causes, thus $\alpha_2 = \frac{2}{20} \times \frac{365}{100} = 0.365$ per year. Only one juvenile survived.

2.1.2 Finding two differential equations for the adults

The same principle as the one described for the immature kiwi can be used to find a mathematical representation for the adult males and females. Let $n_1(t)$ and $n_2(t)$ be the number of male and female adult kiwi respectively at time t in years.

The rate of change of the adult females is equal to the rate of females coming into the adult population, via maturing juveniles, less the rate of females leaving the population through death. This can be expressed mathematically as

$$\frac{dn_2}{dt} = \frac{1}{2}m_2(t, a_2) - f_2 n_2(t)$$

where f_2 is the annual death rate of the female adults. It has been assumed that at age $a = a_2$, which is when a juvenile becomes an adult, half of the juveniles are females, thus the number of females coming into the adult population from the juvenile population is given by $\frac{1}{2}m_2(t, a_2)$.

Similarly for adult males:

$$\frac{dn_1}{dt} = \frac{1}{2}m_2(t, a_2) - f_1 n_1(t)$$

where f_1 is the annual death rate of male adults.

Since adult kiwi are better able to protect themselves and are less vulnerable than immature kiwi due to their increased body size, the male and female annual mortality rates, f_1 and f_2 respectively, are taken as constant and include both natural and predator mortality.

The gender breakdown for this cohort was 72 females and 99 males. Female mortality was 4.5% per year and male mortality was 10.3% per year. There was, however, no significant difference between these mortality rates so the average mortality rate for both genders was taken to be 8.2% per year ([60]). Thus $f_1 = f_2 = 0.082$ per year.

2.1.3 A summary of the mathematical model

The full mathematical model consists of two partial differential equations, based on *McKendricks'* equation for age classes, and two ordinary differential equations plus one initial condition and one continuity condition. This gives the following system of equations where the parameters and variables are summarised in Table 2.1:

$$\frac{\partial m_1(t,a)}{\partial t} + \frac{\partial m_1(t,a)}{\partial a} = -(\alpha_1 + \beta_1)m_1(t,a), \quad t \geq 0, 0 \leq a \leq a_1 \tag{2.2}$$

$$\frac{\partial m_2(t,a)}{\partial t} + \frac{\partial m_2(t,a)}{\partial a} = -(\alpha_2 + \beta_2)m_2(t,a), \quad t \geq 0, a_1 \leq a \leq a_2 \tag{2.3}$$

$$\frac{dn_1(t)}{dt} = \frac{1}{2}m_2(t,a_2) - f_1 n_1(t) \tag{2.4}$$

$$\frac{dn_2(t)}{dt} = \frac{1}{2}m_2(t,a_2) - f_2 n_2(t) \tag{2.5}$$

$$m_1(t,0) = bn_2(t) \tag{2.6}$$

$$m_2(t,a_1) = m_1(t,a_1). \tag{2.7}$$

parameter	description	value
$m_1(t,a)$	the number of chicks of age a at time t	
$m_2(t,a)$	the number of juveniles of age a at time t	
$n_1(t)$	the number of males at time t	
$n_2(t)$	the number of females at time t	
α_1	annual natural death rate of chicks	4.76
β_1	annual predation rate of chicks	3.97
α_2	annual natural death rate of juveniles	0.3650
β_2	annual predation rate of juveniles	3.1
f_1	annual death rate of adult males	0.082
f_2	annual death rate of adult females	0.082
b	number of young produced per adult female per year	0.85
a_1	age (in years) when a chick becomes a juvenile	0.06
a_2	age (in years) when a juvenile becomes an adult	1.5

Table 2.1: Summary of parameters and variables.

2.2 Solving the mathematical model

2.2.1 Solving for $m_1(t,a)$ and $m_2(t,a)$

Using the method of characteristics it is possible to solve equation (2.2), $\frac{\partial m_1}{\partial t} + \frac{\partial m_1}{\partial a} = -(\alpha_1 + \beta_1)m_1$, by comparing it to the total differential, $\frac{\partial m_1}{\partial t}dt + \frac{\partial m_1}{\partial a}da = dm_1$. Hence, $\frac{dt}{da} = 1, \quad \Rightarrow t = a + \text{constant}$ and $\frac{dm_1}{da} = -(\alpha_1 + \beta_1)m_1 \quad \Rightarrow m_1(t,a) = C_1 e^{-(\alpha_1+\beta_1)a}$ where, since $m_1(t,a)$, the number of chicks of age a at time t, is dependant on events at time $t-a$ (when they were hatched), $C_1 = C_1(t-a)$, which is found using the initial condition (2.6),

$$m_1(t,0) = bn_2(t) = C_1 e^{-(\alpha_1+\beta_1)0} = C_1(t).$$

Hence the solution of equation (2.2) is

$$m_1(t,a) = bn_2(t-a)e^{-(\alpha_1+\beta_1)a} \quad \text{where} \quad 0 \leq a \leq a_1. \tag{2.8}$$

Similarly by the method of characteristics $m_2(t,a) = C_2(t-a)e^{-(\alpha_2+\beta_2)a}$, and the continuity condition, (2.7), can be used to find $C_2(t-a)$ as follows:

$$\begin{aligned} m_2(t,a_1) &= m_1(t,a_1) \\ \Rightarrow C_2(t-a_1)e^{-(\alpha_2+\beta_2)a_1} &= bn_2(t-a_1)e^{-(\alpha_1+\beta_1)a_1} \\ \Rightarrow C_2(t-a_1) &= bn_2(t-a_1)e^{-(\alpha_1+\beta_1)a_1}e^{(\alpha_2+\beta_2)a_1} \\ &= bn_2(t-a)e^{(\alpha_2-\alpha_1)a_1}e^{(\beta_2-\beta_1)a_1}. \end{aligned}$$

The value for $C_2(t-a)$ can be substituted into the equation for $m_2(t,a)$ to obtain the solution of equation (2.3)

$$m_2(t,a) = bn_2(t-a)e^{(\alpha_2-\alpha_1)a_1}e^{(\beta_2-\beta_1)a_1}e^{-(\alpha_2+\beta_2)a} \quad a_1 \leq a \leq a_2. \tag{2.9}$$

2.2.2 Solving for $n_2(t)$

Substituting $m_2(t,a_2)$ into equation (2.5) gives

$$\frac{dn_2(t)}{dt} = \frac{1}{2}bn_2(t-a_2)e^{(\alpha_2-\alpha_1)a_1}e^{(\beta_2-\beta_1)a_1}e^{-(\alpha_2+\beta_2)a_2} - f_2 n_2(t) \quad a_2 \leq a < \infty.$$

This can be written as the differential-delay equation

$$\frac{dn_2(t)}{dt} = kn_2(t-a_2) - f_2 n_2(t) \tag{2.10}$$

where $a_2 \leq a < \infty$ and $k = \frac{b}{2} e^{(\alpha_2-\alpha_1)a_1+(\beta_2-\beta_1)a_1-(\alpha_2+\beta_2)a_2}$.

To solve equation (2.10), standard Laplace transform techniques are used ([82]), noting that the initial values of equation (2.10) are $n_2(a_2)$ and $\{n_2(u) : \quad (0 < u < a_2)\}$. The Laplace transform of $n_2(t)$ is denoted $\bar{n}_2(p) = \mathcal{L}[n_2(t)]$ and is defined as

$$\bar{n}_2(p) = \int_{a_2}^{\infty} n_2(t) e^{-pt} dt,$$

and the Laplace transform of the derivative, $\frac{dn_2}{dt}$, is $\mathcal{L}\left[\frac{dn_2}{dt}\right] = p\bar{n}_2(p) - n_2(a_2)$ ([82]). Taking the Laplace transform of both sides of equation (2.10) gives:

$$\begin{aligned}
p\bar{n}_2(p) - n_2(a_2) &= k\int_0^{\infty} n_2(t-a_2)e^{-pt}dt - f_2\bar{n}_2(p), \\
\text{let} \quad s = t - a_2, & \\
&= k\int_0^{\infty} n_2(s)e^{-p(s+a_2)}ds - f_2\bar{n}_2(p) \\
&= ke^{-pa_2}\int_0^{\infty} n_2(s)e^{-ps}ds - f_2\bar{n}_2(p) \\
&= ke^{-pa_2}\left[\int_0^{a_2} n_2(s)e^{-ps}ds + \int_{a_2}^{\infty} n_2(s)e^{-ps}ds\right] - f_2\bar{n}_2(p) \\
&= ke^{-pa_2}\left[\int_0^{a_2} n_2(s)e^{-ps}ds + \bar{n}_2(p)\right] - f_2\bar{n}_2(p).
\end{aligned}$$

Taking this equation and solving for $\bar{n}_2(p)$:

$$\begin{aligned}
p\bar{n}_2(p) - n_2(a_2) &= ke^{-pa_2}\left[\int_0^{a_2} n_2(s)e^{-ps}ds + \bar{n}_2(p)\right] - f_2\bar{n}_2(p) \\
\Rightarrow (p + f_2 - ke^{-pa_2})\bar{n}_2(p) &= ke^{-pa_2}\int_0^{a_2} n_2(s)e^{-ps}ds + n_2(a_2)
\end{aligned}$$

$$\Rightarrow \bar{n}_2(p) = \frac{ke^{-pa_2}\int_0^{a_2} n_2(s)e^{-ps}ds + n_2(a_2)}{(p + f_2 - ke^{-pa_2})}. \tag{2.11}$$

Now the inverse Laplace transform of equation (2.11) is taken to find $n_2(t)$. The inverse Laplace transform of $\bar{n}_2(p)$ is defined as

$$\mathcal{L}^{-1}[\bar{n}_2(p)] = \frac{1}{2\pi i}\int_{p=\gamma-i\infty}^{p=\gamma+i\infty} e^{pt}\bar{n}_2(p)dp, \tag{2.12}$$

where γ is a number chosen so that all singularities of $\bar{n}_2(p)$ lie to the left of the line $z = \gamma$ in the complex plane. In practise the integral in equation (2.12) is evaluated by first

representing it as a contour integral over the positively oriented contour, C, as depicted in Figure 2.2, and secondly using the residue theorem ([82],[21]). Hence, $n(t)$ can be solved for,

$$\begin{aligned} n(t) = \mathcal{L}^{-1}[\bar{n}_2(p)] &= \frac{1}{2\pi i}\oint_C e^{pt}\bar{n}_2(p)dp \\ &= \sum \text{residues of} \quad e^{pt}\bar{n}_2(p) \quad \text{at the poles of} \quad \bar{n}_2(p). \end{aligned}$$

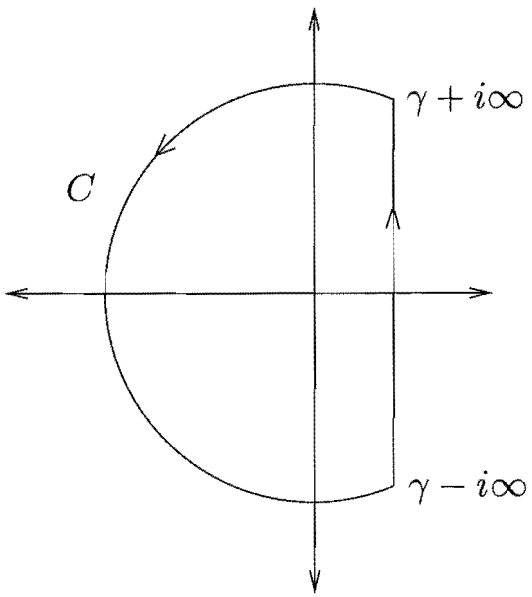

Figure 2.2: The positively oriented contour C.

To find the residues of $e^{pt}\bar{n}_2(p)$ the poles of $\bar{n}_2(p)$ need to be found. The poles of $\bar{n}_2(p)$ are the solutions of the equation $p + f_2 - ke^{-pa_2} = 0$. This equation cannot be solved analytically so other methods are employed.

2.2.3 Finding the residues of $e^{pt}\bar{n}_2(p)$

The poles of $\bar{n}_2(p)$ are the roots of $p + f_2 - ke^{-pa_2} = 0$ which shall be denoted p_j.
Since p_j is a simple pole of order one of $\bar{n}_2(p)$, then the residue of $e^{pt}\bar{n}_2(p)$ at p_j is given by:

$$\begin{aligned} \text{res}(p_j) &= \lim_{p\to p_j}(p - p_j)e^{pt}\bar{n}_2(p) \\ &= \lim_{p\to p_j}(p - p_j)e^{pt}\left[\frac{ke^{-pa_2}\int_0^{a_2} n_2(s)e^{-ps}ds + n_2(a_2)}{(p + f_2 - ke^{-pa_2})}\right] \\ &= \lim_{p\to p_j}\frac{(p - p_j)}{(p + f_2 - ke^{-pa_2})}\left[e^{pt}ke^{-pa_2}\int_0^{a_2} n_2(s)e^{-ps}ds + e^{pt}n_2(a_2)\right] \end{aligned}$$

(using L'Hopital's rule):

$$\begin{aligned} &= \lim_{p \to p_j} \frac{1}{(1 + ka_2 e^{-pa_2})} \left[e^{pt} k e^{-pa_2} \int_0^{a_2} n_2(s) e^{-ps} ds + e^{pt} n_2(a_2) \right] \\ &= \frac{e^{p_j t}}{(1 + ka_2 e^{-p_j a_2})} \left[k e^{-p_j a_2} \int_0^{a_2} n_2(s) e^{-p_j s} ds + n_2(a_2) \right]. \end{aligned}$$

Since p_j is a solution of $p - ke^{-pa_2} + f_2 = 0$, the expression $ke^{-p_j a_2} = p_j + f_2$ can be substituted into the equation. Hence

$$\begin{aligned} n_2(t) &= \sum_j \text{res}(p_j) \\ &= \sum_j \frac{e^{p_j t}}{(1 + a_2(p_j + f_2))} \left[(p_j + f_2) \int_0^{a_2} n_2(s) e^{-p_j s} ds + n_2(a_2) \right]. \end{aligned}$$

Because $n_2(t)$ depends on the term $e^{p_j t}$, the sign of each root, p_j, of $p + f_2 - ke^{-pa_2} = 0$ needs to be investigated. If each p_j is negative then $n_2(t) \to 0$ as $t \to \infty$ and the species will become extinct. If one p_j is positive then the species will survive.

2.2.4 p_j is a real root of $p + f_2 - ke^{-pa_2} = 0$

If $p + f_2 - ke^{-pa_2} = 0$ then $p = ke^{-pa_2} - f_2$ and the real roots can be found graphically by looking at the intersection of the graphs of the two functions $y_1(p) = p$ and $y_2(p) = ke^{-pa_2} - f_2$. The shape of the graph of y_2 can be found by considering its first derivative, $y_2' = -ka_2 e^{-pa_2}$, which is always non-zero so there are no critical points. The second derivative of y_2 is $y_2'' = ka_2^2 e^{-pa_2}$ which is always positive since $k > 0$ thus the graph of y_2 is concave up everywhere. The horizontal asymptote of y_2 is $y = -f_2$ since as $p \to \infty$, $y_2 = ke^{-pa_2} - f_2 \to -f_2$. Letting $p = 0$ gives the vertical axis intercept as $y = k - f_2$ which is positive if $k > f_2$ and negative if $k < f_2$ and setting $y_2 = 0$ gives the horizontal axis intercept:

$$\begin{aligned} ke^{-pa_2} &= f_2 \\ \Rightarrow p &= \frac{-1}{a_2} log\left(\frac{f_2}{k}\right). \end{aligned}$$

The graphs of $y_1 = p$ and $y_2 = ke^{-pa_2} - f_2$ are depicted in Figure 2.3. It can be seen that there is only one real root, p, which is positive if $k > f_2$ and negative if $k < f_2$.

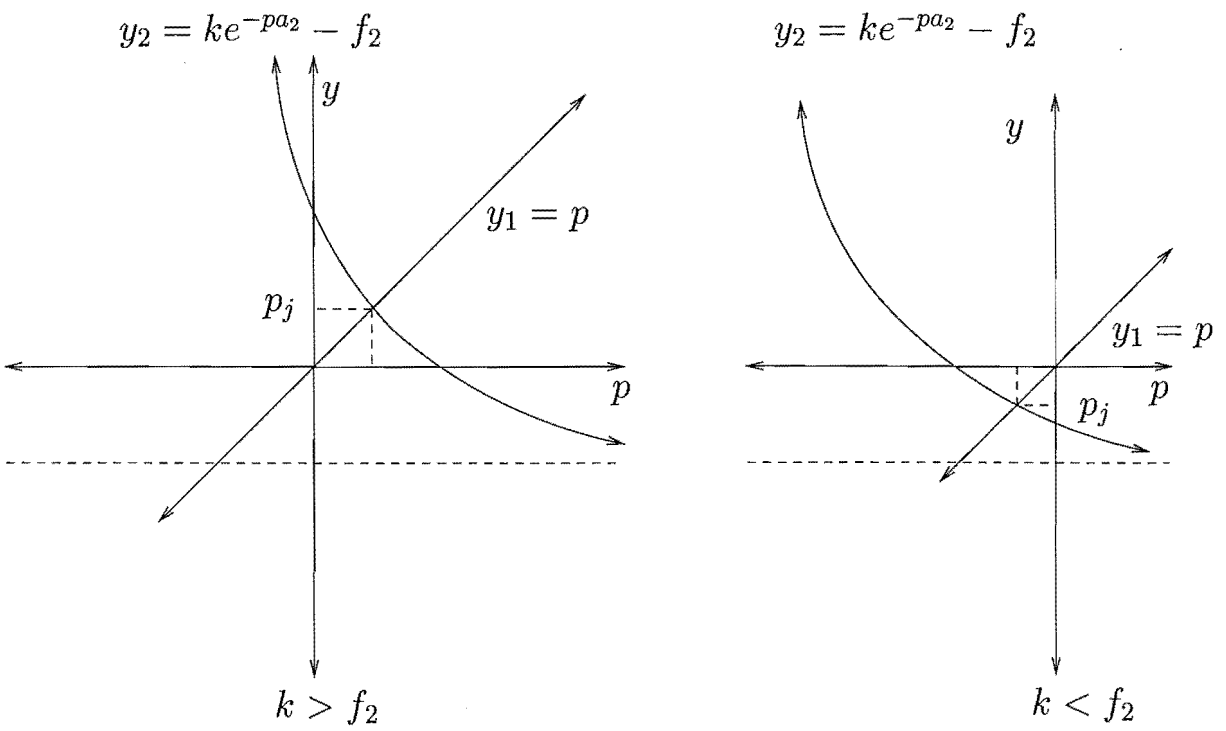

Figure 2.3: The graphs of $y_1(p) = p$ and $y_2(p) = ke^{-pa_2} - f_2$.

2.2.5 p_j is a complex root of $p + f_2 - ke^{-pa_2} = 0$

Theorem: All the roots of $p + f_2 - ke^{-pa_2} = 0$ have negative real parts iff

1. $-f_2a_2 < 1$

2. $-f_2a_2 < -a_2k < \sqrt{a^2 + f_2^2a_2^2}$ where a is the root of $a - p\tan a = 0$ with $0 < a < \frac{\pi}{2}$.

Proof: See ([11]).

For the mathematical model discussed here, assuming $f_2 \neq 0$, condition 1 above is satisfied because $f_2 > 0$ and $a_2 > 0 \Rightarrow -f_2a_2 \leq 0 < 1$. The second part of Condition 2 is also easily shown (assuming $b > 0$) since

$$k = \frac{b}{2}e^{(\alpha_2-\alpha_1)a_1+(\beta_2-\beta_1)a_1-(\alpha_2+\beta_2)a_2} > 0$$

and $a_2 > 0$ so,

$$\begin{aligned} a_2k &> 0 \\ \Rightarrow -a_2k &< 0 < \sqrt{a^2 + f_2^2a_2^2}. \end{aligned}$$

The first part of condition 2 is to show that $-f_2 a_2 < -a_2 k$ which is the same as showing that $f_2 > k$. So if $f_2 > k$ then the complex roots of $p + f_2 - ke^{-pa_2}$ have negative real part. Recall that if $f_2 > k$ then the real root is also negative. Similarly, if $f_2 < k$ then the complex roots of $p + f_2 - ke^{-pa_2}$ have positive real part. Recall that if $f_2 < k$ then the real root is also positive.

There is now a condition for whether the female kiwi population will survive or become extinct. This can be generalised to a condition of survival for the whole population. The condition is:

$$\begin{aligned} f_2 &> k \Rightarrow \quad \textbf{EXTINCTION} \\ f_2 &\leq k \Rightarrow \quad \textbf{SURVIVAL.} \end{aligned}$$

2.3 Results

A series expansion for the explicit number of females has been found, and thereby shown that a criterion for survival of the kiwi cohort (depending on the immature kiwi reaching adulthood) is given by the inequality $f_2 \leq k$ or $f_2 \leq \frac{b}{2} e^{(\alpha_2-\alpha_1)a_1+(\beta_2-\beta_1)a_1-(\alpha_2+\beta_2)a_2}$ which can be arranged as

$$\begin{aligned} 1 &\leq \frac{b}{2f_2} e^{(\alpha_2-\alpha_1)a_1+(\beta_2-\beta_1)a_1-(\alpha_2+\beta_2)a_2} \\ &= \frac{b}{2f_2} e^{-((a_1\alpha_1+(a_2-a_1)\alpha_2)+(\beta_1 a_1+(a_2-a_1)\beta_2))} \\ &= \frac{b}{2f_2} e^{-(\alpha+\beta)a_2} \end{aligned}$$

where α and β are defined to be the combined annual natural and predation rates for the combined classes of immature kiwi given by $\alpha = \frac{1}{a_2}(a_1\alpha_1 + (a_2 - a_1)\alpha_2) = 0.5$ and $\beta = \frac{1}{a_2}(a_1\beta_1 + (a_2 - a_1)\beta_2) = 3.1$. So for survival it is required that

$$\left(\frac{1}{f_2}\right) \frac{b}{2} e^{-(\alpha+\beta)a_2} \geq 1. \tag{2.13}$$

Expression (2.13) has a nice intuitive meaning. A female has an average life expectancy of $\frac{1}{f_2}$ years. Of the chicks hatched in her lifetime, $\frac{1}{f_2} \times \frac{b}{2} \times e^{-(\alpha+\beta)a_2}$ survive a_2 years to become female adults. Therefore, the criterion for survival of female kiwi can be derived using the principle that each female must, in her lifetime, produce on average at least one female chick that reaches maturity in order to replace herself.

Now β can be solved for in inequality (2.13) to find the threshold for the annual predation rate of immature kiwi:

$$\begin{aligned}\beta &\leq \frac{1}{a_2}\ln(\frac{b}{2f_2}) - \alpha \\ &= \frac{1}{1.5}\ln(\frac{0.85}{2 \times 0.082}) - 0.5 \\ &= 0.6.\end{aligned}$$

This gives a critical value $\gamma_c = 0.6$ per year for the annual predation rate of the immature kiwi. By critical it is meant that if the predation rate falls below this value then the female kiwi cohort can sustain itself and is in a survival regime, however if the predation rate is higher than this critical value then the female kiwi cohort will eventually become extinct. Since the entire cohort depends on the survival of each compartment then the criterion for survival for the entire cohort in terms of the control parameter, β, can be summarised as

$$\begin{aligned}\beta &\leq \gamma_c = 0.6 \quad \Rightarrow \quad \text{SURVIVAL} \\ \beta &> \gamma_c = 0.6 \quad \Rightarrow \quad \text{EXTINCTION.}\end{aligned}$$

Using the data set, the actual value of $\beta = 3.1$ is much greater than the critical value. This needs to be reduced by a factor of 5. An analysis of β as a function of b and f_2 shows that it is sensitive to small changes in b as $b \to 0$. In chapter 3 a graphical sensitivity analysis on β incorporating a scaling factor for predator abundance will be performed.

It has been possible to analytically solve (in part at least) the system of equations and find that $m_2(t, a_2)$, the number of juveniles of age $a_2 = 1.5$ years (or the number of chicks that reach adulthood), is

$$m_2(t, a_2) = bn_2(t - a_2)e^{-(\alpha+\beta)a_2}$$

where α and β are defined (as above) to be the combined annual natural and predation rates for both classes of immature kiwi given by $\alpha = \frac{1}{a_2}(a_1\alpha_1 + (a_2 - a_1)\alpha_2) = 0.5$ and $\beta = \frac{1}{a_2}(a_1\beta_1 + (a_2 - a_1)\beta_2) = 3.1$.

Using the data set for the northern brown kiwi with $bn(t - a_2) = 42$ being the number of kiwi hatched at time $(t - a_2)$, then for survival, using the threshold value of $\beta = \gamma_c = 0.6$, the number of immature kiwi becoming adults is required to be $m(t, a = 1.5) = 42e^{-1.1\times1.5} \approx 8$ which is about 19% of those hatched. The population can sustain an 81% drop in numbers from the kiwi hatched to those becoming adults. In reality though $m(t, a = 1.5) = 42e^{-3.6\times1.5} \approx 0$. Recall that only one chick survived more that 100 days. Obviously the

cohort is currently in the extinction regime to an extreme degree. Figure 2.4 shows how reducing the predation rate will increase the recruitment rate. The need to reduce β, the combined predation rate of chicks and juveniles, is evident.

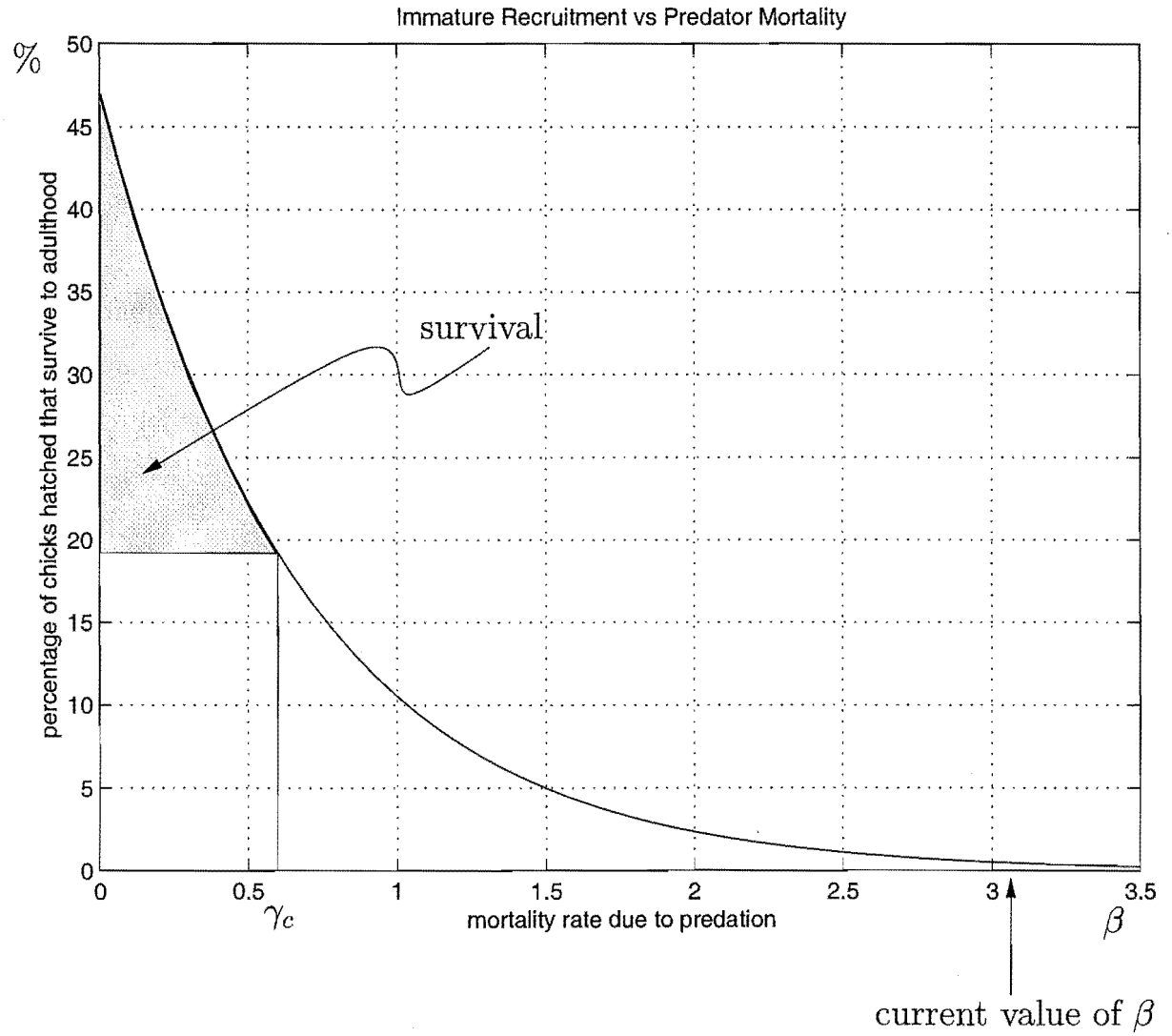

Figure 2.4: Immature recruitment versus predator mortality.

2.4 Generalisation of the mathematical model

In this section, the methodology is further generalised. Suppose there are i immature age classes, $a_0 = 0 \leq a \leq a_1, a_1 \leq a \leq a_2, \ldots, a_{i-1} \leq a \leq a_i$, with each class differentiated by gender. If $m_{fi}(t, a)$ is the number of immature females of age a at time t in age class i specified by $a_{i-1} \leq a \leq a_i$ and b_f, α_{fi} and β_{fi} are the respective productivity rate of female

adults, natural death and predation rates of females in that age class, then

$$m_{fi}(t,a) = b_f n_2(t-a)e^{-(\alpha_{f1}+\beta_{f1})a_1}e^{-(\alpha_{f2}+\beta_{f2})(a_2-a_1)}\ldots e^{-(\alpha_{fi}+\beta_{fi})(a-a_{i-1})}.$$

With a general mathematical model, equation (2.10) becomes

$$\frac{dn_2(t)}{dt} = b_f n_2(t-a_i)r_{f1}r_{f2}\ldots r_{fi} - f_2 n_2 \tag{2.14}$$

where $r_{fi} = \frac{m_{fi}(t,a_i)}{m_{fi}(t-(a_i-a_{i-1}),a_{i-1})} = e^{-(\alpha_{fi}+\beta_{fi})(a_i-a_{i-1})}$, is the recruitment rate in immature female age class $a_{i-1} \leq a \leq a_i$, or, in other words, the proportion of those individuals entering the age class at age a_{i-1} who then survive to become aged a_i.

In chapter 6, this general mathematical model is used to consider pulsed management strategies for kiwi and another threatened bird, the North Island kokako, *Callaeas cinerea wilsoni*. In chapter 5, a spatial structure is also added to the generalised model in order to find the minimum predator free area required for the survival of kiwi in a larger forest block.

2.5 Conclusions

Estimates of productivity and survival have been derived from a mathematical model of a population of an endangered species with the focus especially on the significance of predation.

An age/gender classified mathematical model with constant predation rates has been developed. The simple linear relationship presumed in the model enabled series solutions to be obtained for the temporal evolution of the population and precisely identified the threshold for survival, i.e. it was possible to predict a threshold value for the predation rate of immature kiwi below which the entire population will survive.

Although kiwi are protected they are subject to extreme predation by introduced mammals and are declining throughout the mainland. The use of the mathematical model for this species showed that the survival threshold would only be reached by considerable human intervention without which extinction would be inevitable. In chapter 3 a component representing predator abundance is added to the model by scaling β, the predation rate for immature kiwi. The refined model is then used to estimate an acceptable predator density for kiwi survival.

Chapter 3

Modelling predation

The decline of northern brown kiwi in mainland forests of New Zealand is caused mainly by stoats, *Mustela erminea*, preying on immature birds ([60]). Predator control is therefore seen as being essential for the survival of kiwi, and indeed for the survival of many other threatened species of animals worldwide. In this chapter the age structured model developed in chapter 2 is extended by incorporating a factor that represents predator density ([7]). The refined model is then used to estimate a critical stoat density above which immature kiwi recruitment falls below the minimum 19% identified for species survival in chapter 2.

Stoats evolved in the northern hemisphere with an unreliable food source. They generally kill any vulnerable prey they encounter and save surplus animals for future use ([43]). They were first introduced to New Zealand in 1885 as the natural predator of rabbits, *Oryctolagus cuniculus cuniculus*, in order to quell burgeoning rabbit populations (see chapter 7). Despite protests by ornithologists, stoats were "liberated in sufficient numbers, and in so many places, that they could well have spread throughout both main islands by or soon after the turn of the century" ([43]). It was not until 1936 that their importation became illegal. Nowadays, stoats and kiwis co-exist in all mainland forests. Kiwis lack defences for mammalian predators because they evolved in the absence of ground dwelling mammals. Kiwis chicks are especially vulnerable because they are small and become independent at an early age. Consequently, over the last century, kiwis have declined (in most mainland forests) from densities of around 40 to 100 adults per km^2 ([13],[14]) to less than four adults per km^2 ([58]).

In beech forests following heavy seeding, [57] estimated stoat densities are around nine animals per km^2. This estimate was based on intensive kill-trapping on a 750 ha peninsula with restricted opportunities for immigration (65 animals removed over a three month period). Natural fluctuations in stoat density appear to be within the range of between two and ten animals per km^2 ([42],[63]) depending on the beech seeding cycle. It is therefore assumed that stoat densities in New Zealand forests reach a maximum of $S = 10$ animals per km^2.

3.1 Refining the age structured model

To incorporate predation into the age structured model from chapter 2, the predation rates of chicks, juveniles and immature (combined chicks and juveniles) kiwi (β_1, β_2 and β respectively) are redefined. Since stoats are the dominant predators of immature kiwis in large

forest tracts of both the North and South Islands, ([60]), it is assumed that the effect of other predators, besides stoats, on immature kiwi is negligible. The annual predation rate of immature kiwi is defined as $\beta\frac{s}{S}$ where s is the stoat density per km^2 at time t years, and S is the maximum density of stoats per km^2. In practical terms, S is the maximum carrying capacity of stoats in any New Zealand forest. The fraction $\frac{s}{S}$ is a number between 0 and 1 and $\beta\frac{s}{S}$ represents a predation rate that ranges between 0 (when there are no stoats i.e. $s = 0$) and β (when $s = S$, that is, when stoats are at maximum density.) The scaling factor, $\frac{s}{S}$, is important (as opposed to having a single parameter to represent mortality) because the aim is to identify the critical density s_c at which $\beta\frac{s_c}{S}$, the linear combination of the predation rates for chicks and juveniles, is low enough to allow kiwi to survive.

Without loss of generality, the population is divided into three compartments, immature kiwi, adult females and adult males as depicted in Figure 3.1.

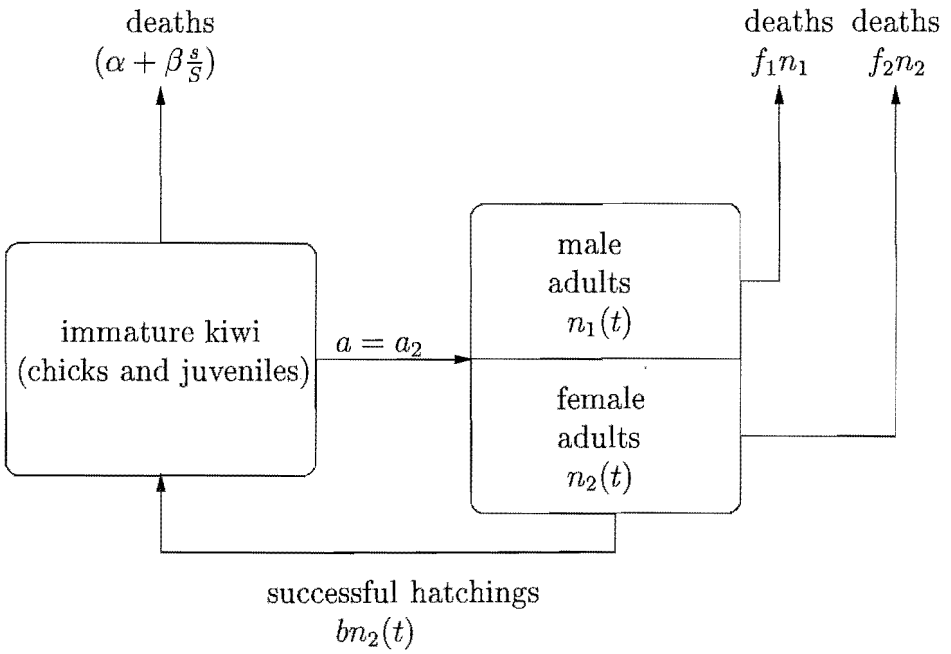

Figure 3.1: Schematic diagram showing the age compartments of the population.

3.2 The critical stoat density

With β redefined as $\beta\frac{s}{S}$, inequality (2.13) becomes

$$\left(\frac{1}{f_2}\right)\frac{b}{2}e^{-(\alpha+\beta\frac{s}{S})a_2} \geq 1 \tag{3.1}$$

where

$$\alpha = \frac{1}{a_2}\left(a_1\alpha_1 + (a_2 - a_1)\alpha_2\right)$$

per year and

$$\beta\frac{s}{S} = \frac{1}{a_2}\left(a_1\beta_1\frac{s}{S} + (a_2 - a_1)\beta_2\frac{s}{S}\right)$$

per year. This is rearranged as before,

$$\begin{aligned}\beta\frac{s}{S} &< \frac{1}{a_2}\ln(\frac{b}{2f_2}) - \alpha \\ &= \frac{1}{1.5}\ln(\frac{0.85}{2\times 0.082}) - 0.5 \\ &= 0.6 \quad \text{per year.}\end{aligned}$$

This gives a critical value for the annual predation rate of immature kiwi of $\beta\frac{s_c}{S} = 0.6$ per year. Assuming data was collected during maximum stoat densities (i.e. $\frac{s}{S} = 1$), the actual value of $\beta\frac{s}{S}$ derived from field measurements is the same as the value of β in chapter 2, i.e. $\beta\frac{s}{S} = 3.1$.

It has been assumed that stoats are the main predator of young kiwi and reducing the stoat population is the only way of reducing the predation rate. It can also be assumed that predation losses change in direct proportion to stoat abundance. Thus, stoat populations have to be reduced by 80% in order to reduce predation losses by 80%. Curve a. in Figure 3.2 suggests that the survival threshold (19% recruitment) is reached when stoats decline to a density of 1.94 animals per km^2. However, this critical density estimate is conservative because it assumes that stoats were at maximum density when the survival rates of immature kiwi were measured in the field. In fact, the data were collected over a range of sites and years, and so reflect average losses over an unknown range of stoat densities. If, at the time of the measurements stoats were at an average density of six rather than ten animals per km^2, (see curve b. in Figure 3.2) then the critical density for kiwi survival would be calculated as 1.16 animals per km^2 rather than 1.94 per km^2. The exact value for the critical stoat density cannot be found but it is between zero and two animals per km^2. Thus, to ensure kiwi survival, stoat populations have to be reduced by at least 80% in years when they are abundant. These management targets are tentative estimates based on limited measurements of stoat density in New Zealand forests and the assumption that predation losses of young kiwi are directly proportional to stoat abundance and independent of kiwi density. Nevertheless, two predictions of the analysis appear to be realistic: (1) that stoat populations have to be reduced substantially in order to produce any measurable benefits,

and (2) that in most habitats, stoat densities seldom if ever decline naturally to levels which allow adequate recruitment in kiwi.

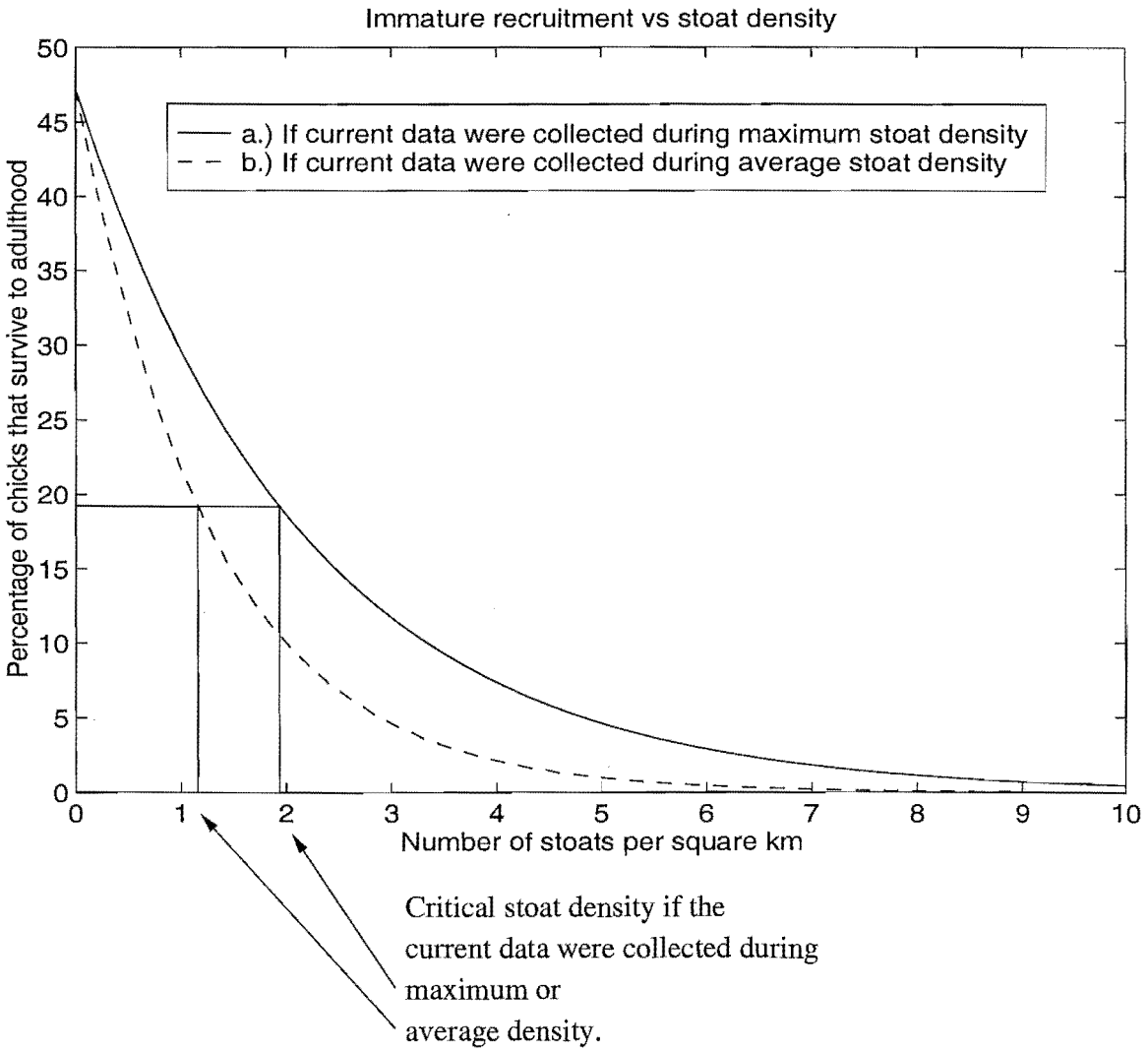

Figure 3.2: Immature recruitment versus stoat density.

The shape of each recruitment curve in Figure 3.2 is such that small changes in stoat density between zero and five animals per km^2 greatly effect survival rates of juvenile kiwi. Once stoat densities reach five animals per km^2, further increases are largely irrelevant, because by then chick survival rates are already close to zero. In 'plague' years, for example, the removal of 50% of the animals would have no significant effect on juvenile survival. The analysis therefore predicts that predation rates will not necessarily decline following the removal of large numbers of predators - the outcome of many mustelid (stoat, ferret and weasel) control operations in New Zealand (for example see [76]). Indeed, if trapping operations generally remove only about 50% of the stoats present, as [44] suggests, most will

fail to markedly reduce predation rates on young kiwi.

3.3 Sensitivity analysis of the threshold condition

The critical value for the annual predation rate of immature kiwi is

$$\beta\frac{s_c}{S} = \frac{1}{1.5}\ln(\frac{b}{2f_2}) - \alpha.$$

It is interesting to see how this critical value changes with small changes in either b or f_2. It should be noted that α is just a linear term so $\beta\frac{s_c}{S}$ changes linearly with changes in α. Since all parameters must be non-negative, the feasible region for b and f_2 is $b \geq 2f_2e^{1.5\alpha}$. If b is close to zero then the critical value is extremely sensitive to small changes in b but $b = 0$ is not in the feasible region. Figures 3.3 and 3.4 show graphically $\beta\frac{s_c}{S}$ as a one and two dimensional function of b and f_2 respectively. The figures show that when productivity rates increase and adult mortality rates decrease, the critical predation rate increases implying that in this situation the cohort can withstand higher predation of immature birds.

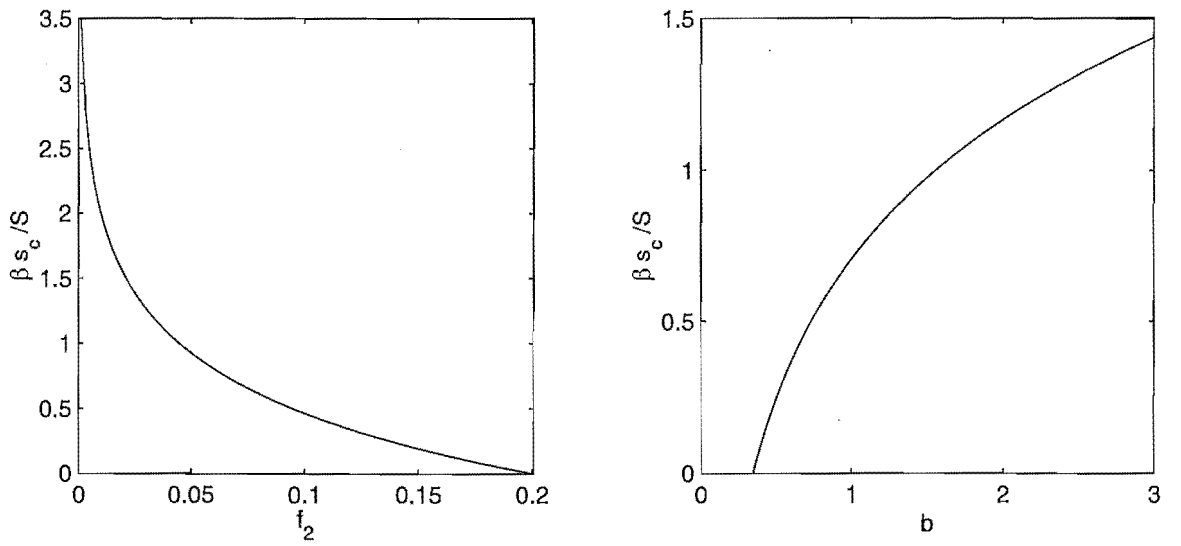

Figure 3.3: Sensitivity analysis of $\beta\frac{s_c}{S} = \frac{1}{1.5}\ln(\frac{b}{2f_2}) - \alpha$ with $\alpha = 0.5$ plotted as a one dimensional function of f_2 (with $b = 0.85$) and b (with $f_2 = 0.082$) respectively.

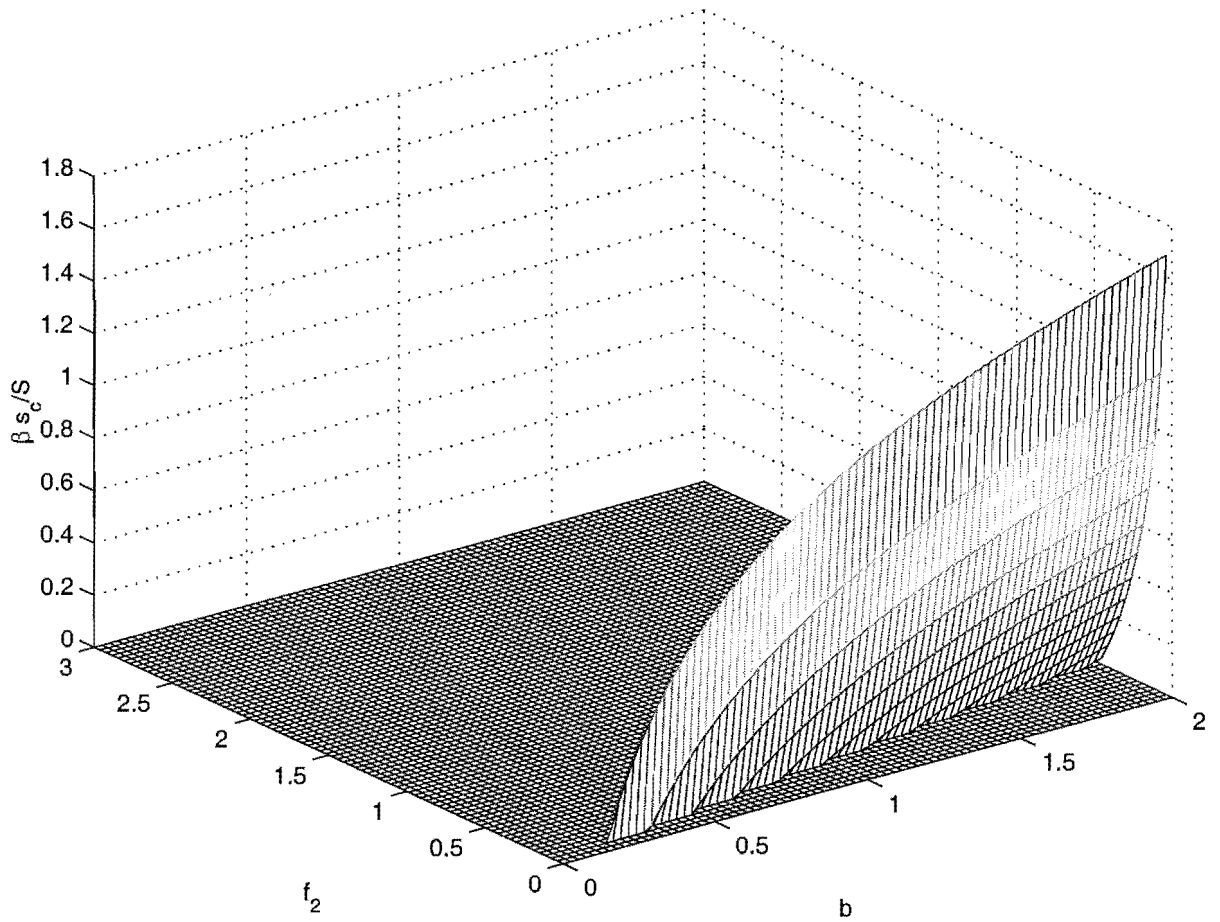

Figure 3.4: $\beta\frac{s_c}{S} = \frac{1}{1.5}\ln(\frac{b}{2f_2}) - \alpha$ with $\alpha = 0.5$ is plotted as a two dimensional function (with only positive function values plotted) of f_2 and b.

3.4 Future of kiwi in mainland forests

In this chapter, the age structured population model, developed in chapter 2, was re-classified into three compartments by age and gender and was then used to obtain estimates of the critical density that stoats should be reduced to in order to sufficiently increase chick and juvenile recruitment to a suitable level for survival. Assuming the time-scale of any change in the stoat population is far greater than that of its kiwi prey, it was found that the stoat population density needs to be reduced by a massive 80 percent to enable the kiwi population to enter the regime in which survival is likely. The analysis indicates that management intervention needs to be substantial in order to guarantee this and the task of increasing recruitment rates of kiwi in mainland forests to required levels involves the removal of a high proportion of predators from large areas over a long time. Current methods of stoat control

(intensive trapping) are only occasionally effective ([57]) and too expensive and labour-intensive to apply on a large scale (> 1000 ha). Clearly, the persistence of kiwi on mainland New Zealand is now largely dependent on the development of new techniques for controlling stoats. In chapter 4 the existence of an optimal secondary poisoning regime as a possible method of stoat control is investigated and pulsed management options are explored in chapter 6.

Chapter 4

An optimal poisoning regime

Reduction of predators and maintaining a suitable habitat is imperative for the survival of many endangered species. Certainly, juvenile predation is the main cause of decline for northern brown kiwi as has been shown in the previous chapters. In this chapter, the feasibility of implementing a secondary poisoning regime for kiwi predator control in a 500 hectare block is examined. Secondary poisoning, where the main food source of the predator is poisoned, is being considered here because current methods of trapping are expensive and ineffective ([2]). The aim is to find out how and when poison should be administered in the environment in order to maximise its impact on predators and minimise negative environmental impact. Negative environmental risks include primary and secondary poisoning of non-target species ([3]) and prey switching. These factors should be considered before any regime can be implemented. Using a mathematical model to investigate benefits and risks of the situation has clear advantages over field trials. Already, preliminary field studies indicate that secondary poisoning may be the key to controlling predators of endangered species ([3],[65]). They have also revealed some of the pitfalls that may be associated with the implementation of such a scheme ([28]).

A model is developed which can be generalised, but specifically under consideration are beech, *Nothofagus spp.*, forests where the endangered species is the northern brown kiwi, the main predators are stoats and their main food source is mice, *Mus musculus*. Two types of poison are considered. An acute, or fast-acting poison, is modelled and a poison which persists in the environment is briefly discussed in terms of a generalised framework.

The daily intake of mice by stoats depends on the density of mice, thus for both types of poison the aims are:

1. Identify, if possible, the threshold density of mice, above which secondary poisoning will be successful (see Figure 4.1) and

2. specify the optimal poisoning strategy (μ, P_0) where P_0 is the initial amount of poison distributed and μ is the proportion of mice initially poisoned

so that the following objectives are realised:

- Stoats are reduced to an acceptable level;

- use of poison is minimised;

- the mouse population is maintained for subsequent poisoning;

- deaths of non-target species are minimised by poisoning as few mice as possible.

The optimal administration can be specified in terms of the control parameters P_0, the initial amount of poison distributed and μ, the initial proportion of mice poisoned, since each pair, (μ, P_0), corresponds to a different poisoning strategy.

If the threshold density of mice, above which secondary poisoning is successful, is known then the season and type of year that secondary poisoning should be implemented can be advised since the density of mice changes with seasons and during mast and non-mast years. Mast years are when beech seed heavily causing high densities of mice estimated to be around 100 per hectare (or 50,000 in a 500 hectare block). Low densities of mice (i.e. in a non-mast year) are around 4 per hectare (or 2000 in a 500 hectare block). The initial stoat density is $S_0 = 25$ animals in 500 hectares, based on density estimates of one female per 25 hectares and 1 male per 100 hectares.

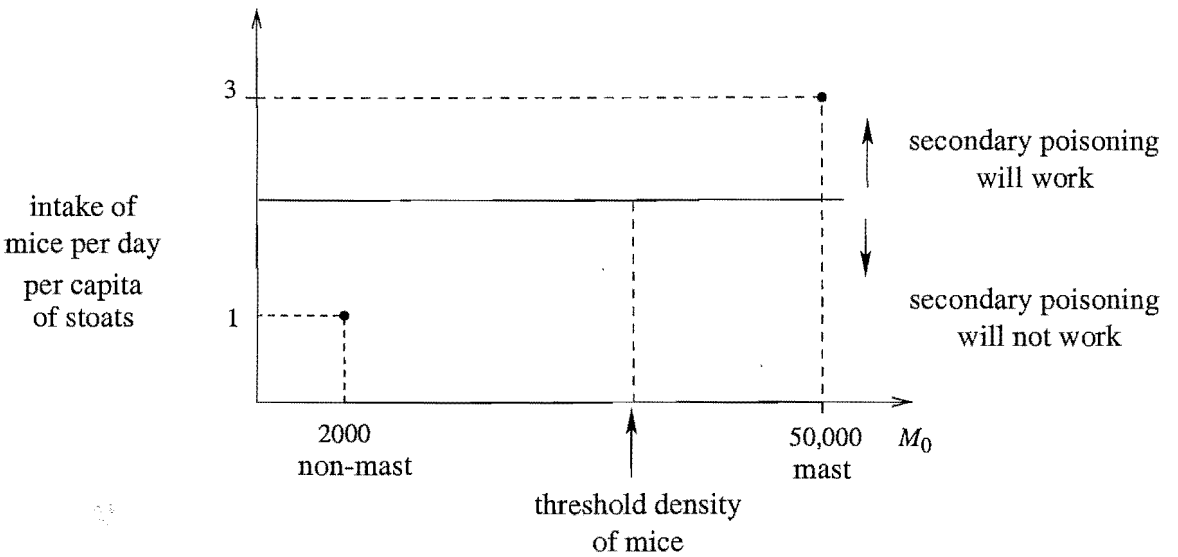

Figure 4.1: An estimate of the stoat per capita daily intake of mice is presumed to depend on M_0, the initial density of mice.

Secondary poisoning will be successful when stoat densities fall to a suitable level. In chapter 3 the critical stoat density for kiwi survival was estimated to be less than two animals per km^2. For the acute poisoning model discussed in this chapter, it is assumed that secondary poisoning is successful when enough poison is consumed by the stoat population to kill approximately 90% of the initial population. In a 500 hectare block, this means that the initial population of 25 animals must be reduced to 2.5 animals or 0.5 animals per square kilometer. This is within the estimated range of the critical threshold density identified in

chapter 3. This criterion was chosen because the toxicity of a poison is usually measured in terms of a 'Lethal Dose rate 50 percent' or a 'Lethal Dose rate 90 percent' which is the amount of poison required to kill 50% or 90%, respectively, of a group of animals. For example, in mice weighing between 18-21 grams, the subcutaneous Lethal Dose 50 percent (or LD_{50}) of mainland tiger snake, *Notechis scutatus*, is 0.118 mg of venom per kg of mice ([85]). An LD_{50} such as this can be experimentally reproduced. Accurate stoat Lethal Dose rates, where the poison is not subcutaneously injected, but instead ingested orally via prey, are not known. For the purposes here, it is assumed that all poison eaten by a mouse remains active and is transferred to the stoat upon consumption. This assumption needs further consideration since the physiological effects of secondary poisoning of stoats are not yet fully understood. Two types of poison are discussed. Tables 4.1 and 4.2 show the acute oral toxicity (primary poisoning) of 1080 poison (sodium monofluroacetate) and brodifacoum (Talon) for stoats and ferrets, *Mustela furo*, respectively.

	LD_{50}	LD_{90}
1080	0.49 mg/kg	0.7 mg/kg
Brodifacoum	unknown	unknown

Table 4.1: The acute oral toxicity rates (mg/kg) of brodifacoum (Talon) and sodium monofluroacetate (1080) for stoats ([83]).

	LD_{50}	LD_{90}
1080	1.2-1.4 mg/kg	unknown
Brodifacoum	unknown	Male: 10 mg/kg Female: 3 mg/kg

Table 4.2: The acute oral toxicity (mg/kg) of brodifacoum (Talon) and sodium monofluroacetate (1080) for ferrets ([28]).

4.1 Acute Poisoning

An acute or fast acting poison, such as sodium monofluoroacetate (1080) has advantages over a more persistent poison such as brodifacoum (Talon) because, after its initial application, it

stays active in the environment for around only 48 hours reducing the effects on non-target species. To model this situation, P_0 mg of poison is distributed at time $t = 0$ over an area of 500 hectares in such a way that the poison is available to μM_0 mice where M_0 is the initial density of mice. Each of the μM_0 poisoned mice eat poison for 24 hours (or until $t_1 = 1$ day) at a rate of $\psi = 2.4$ mg of poison per day ([64]). They then die -assuming they have eaten a lethal dose- but their carcasses are fresh and available to stoats during the following 24 hours or even up to 48 hours in winter. After this time, $t_2 = 2$ days, the carcasses are too decomposed and are no longer scavenged. It is assumed that even if mice consume a sublethal dose, poison is only in the system for $t_2 = 2$ days. Because the time frame is so short, a mathematical model can be greatly simplified to obtain a first approximation of a secondary acute poisoning regime by making the following assumptions:

- Mice are either eaten by stoats or poisoned to death -there are no other causes of death;
- there are no births;
- there is no migration or immigration of mice and stoats;
- there are no other causes of stoat death besides poisoning;
- poison does not decay and is only eaten by mice.

The model is shown in Figure 4.2.

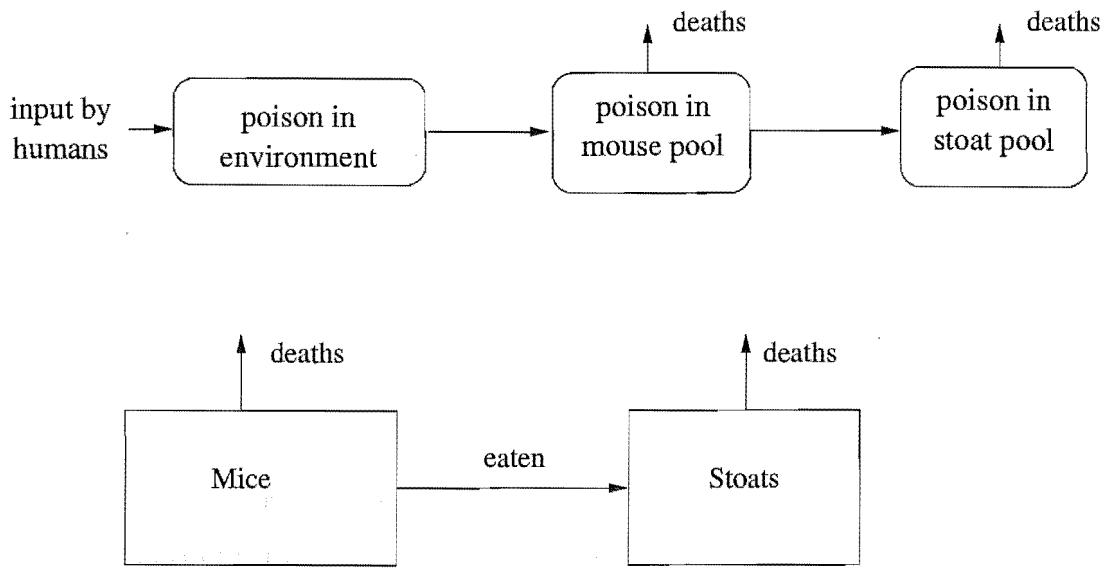

Figure 4.2: The simplest model for acute poisoning over two days.

In the following subsection a continuous model, with discrete mice/stoat deaths at time $t = t_2$ days, is derived.

4.1.1 Finding differential equations for the simplest model

The situation is modelled over the first two days and the amount of poison that is accumulated in the stoat pool is calculated. During the time $0 \leq t < t_2$, it is assumed that the stoat population is constant i.e. $S(t) = S_0$ with all stoat deaths occurring at time $t_2 = 2$ days according to the amount of poison accumulated in the total population. If this amount is greater than or equal to the LD_{90} for the total stoat population, then secondary poisoning is considered successful. The LD_{90} for the total stoat population is $LD_{90} \times S_0$ milligrams per kilogram of stoat body weight or $LD_{90} w_s S_0$ milligrams if the weight of the average stoat is w_s kilograms. The weight, w_s, is taken to be 0.3 kg according to [43].

If $P(t)$ is the amount of poison in the free environment at time t (days), then:

$$\begin{aligned} P(0) &= P_0, \qquad t = 0 \\ \frac{\mathrm{d}P}{\mathrm{d}t} &= -\psi\mu M(t), \qquad 0 < t \leq t_p \\ P(t) &= P(t_p), \qquad t_p < t \leq t_2 \end{aligned}$$

where $M(t)$ is the number of mice available to stoats (i.e. alive or within 24 hours of death) at time t, and μ is the proportion of mice that are poisoned each day, assumed to be essentially constant over two days. ψ is the amount of poison in milligrams consumed daily by each poisoned mouse. If mouse densities are high compared to the initial amount of poison, then the poison supply may be depleted during the first day, thus, $t_p = \min(\min\{t : P(t) = 0\}, 1)$ is the time that poison runs out.

It can immediately be seen that, if poison is not depleted on the first day then, $P(t_1)$ is an amount of poison that is wasted in the system since this is never available to the $(1 - \mu)M_0$ mice not initially poisoned. There may be even more wastage since the poison consumed by mice may be more than enough to reduce stoats to the required level (over poisoning) or may never be consumed by stoats (too many poisoned mice compared to the number of stoats). Thus one way to poison μM_0 mice would be to inject the mice with poison and then distribute these mice so that they are available to all stoats. This would eliminate the effect of non-target species being primarily poisoned by eating baits lying on the ground intended for mice. It would not eliminate non-target species being involuntarily secondarily poisoned

by eating poisoned mice.

All initially poisoned mice that have not been eaten over the first two days become unavailable to stoats at time $t_2 = 2$ days because their carcasses have begun to decompose and are no longer scavenged. The number of stoats at time t is $S(t) = S_0$ where $0 \leq t < 2$. Stoats eat approximately q mice per day and $M(t)$ is the number of living and freshly killed mice. In a mast year $M_0 = 50000$ and $q = 3$. In a non-mast year $M_0 = 2000$ and $q = 1$. The conservation equations for mice are thus:

$$\begin{aligned} M(0) &= M_0, \qquad t = 0 \\ \frac{\mathrm{d}M}{\mathrm{d}t} &= -qS_0, \qquad 0 < t < t_2 \\ M(t_2) &= (1-\mu)M(t_2^-). \end{aligned}$$

At time t where $0 \leq t < 2$, μM mice are poisoned, hence the number of poisoned mice eaten by one stoat is approximately μq per day. If the number of poisoned mice is low compared to the number of stoats it is assumed that stoats eat $\nu\mu q$ poisoned mice per day where $\nu = \nu(x - c_1)$ (and c_1 is a constant), is a contact rate function depending on x, the probability of a stoat encountering at least one poisoned mouse per day. The function $\nu(x - c_1)$ should be chosen so that when there is a small probability of an encounter (for example during low densities of poisoned mice) the contact rate is close to zero and when there is a high chance of an encounter the contact rate is close to one. One such function with these desired properties is

$$\nu(x - c_1) = \begin{cases} 0, & x \leq c_1 \\ \frac{(x-c_1)^2}{c_2^2+(x-c_1)^2}, & c_1 < x \leq 1 \end{cases}$$

where c_1 and c_2 are constants. $\nu(x - c_1)$ becomes non-zero at $x = c_1$. Here the value of c_1 is chosen to be 0.9 so that the contact rate switches on when the probability of a stoat encountering at least one poisoned mouse per day is greater than or equal to 0.9 and c_2 is chosen so that ν goes through the point $(0.99, 0.99)$. As a first approximation, the probability of a stoat encountering at least one poisoned mouse per day out of a total of q encounters is estimated to be from a binomial distribution, thus

$$x = \sum_{i=1}^{q} \binom{q}{i} \mu^i (1-\mu)^{(q-i)}.$$

The contact rate function $\nu(x - c_1)$ is plotted in Figure 4.3. At the scale shown, $v(x)$ appears to 'switch on' sharply at $x = c_1$. In fact the function is differentiable at $x = c_1$. The exclusion

of the contact function gives correct results for laboratory conditions in which it is possible for stoats to eat equal fractions of mice.

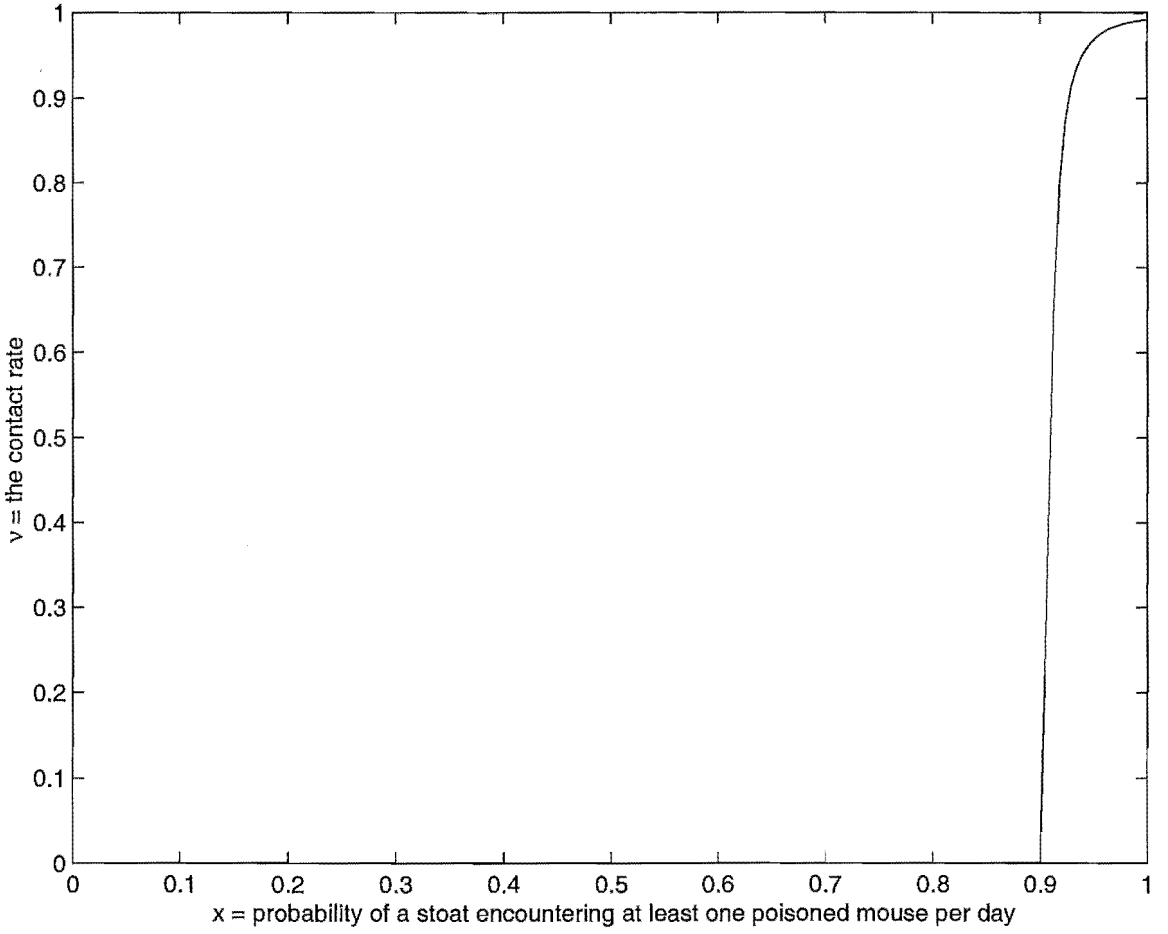

Figure 4.3: Plot of the contact function, $\nu(x - c_1)$, where $q = 3$ mice eaten per stoat per day and x is the probability of a stoat encountering at least one poisoned mouse.

The conservation equations for poison in the mouse pool are:

$$\begin{aligned} P_m(0) &= 0, \qquad t = 0 \\ \frac{\mathrm{d}P_m}{\mathrm{d}t} &= \begin{cases} \psi\mu M - \nu\mu q S_0 \gamma_m, & 0 < t \leq t_p \\ -\nu\mu q S_0 \gamma_m, & t_p < t < t_2 \end{cases} \\ P_m(t_2) &= 0 \end{aligned}$$

showing the influx of poison via μM poisoned mice which are each eating ψ milligrams of poison per day and the outflux due to S_0 stoats eating $\nu\mu q$ poisoned mice per day with the

average mouse containing γ_m milligrams of poison where

$$\gamma_m = \begin{cases} \psi t, & 0 \leq t < t_p \\ \psi t_p, & t_p \leq t < t_2 \\ 0 & t = t_2. \end{cases}$$

Similarly poison in the stoat pool is represented by:

$$\begin{aligned} P_s(0) &= 0, \qquad t = 0 \\ \frac{\mathrm{d}P_s}{\mathrm{d}t} &= \nu\mu q S_0 \gamma_m, \qquad 0 < t < t_2 \\ &= \begin{cases} \nu\mu q S_0 \psi t, & 0 \leq t < t_p \\ \nu\mu q S_0 \psi t_p, & t_p \leq t < t_2 \end{cases} \\ P_s(t_2) &= P_s(t_2^-) - \lambda_s S \gamma_s \end{aligned}$$

where γ_s is the amount of poison in the average stoat at time t and λ_s is the death rate of stoats due to poisoning which will depend on the oral toxicity of the poison used. $P_s(t_2^-)$ is the amount of poison in the stoat pool at a time prior to $t = t_2$.

4.1.2 Solving the simplest model

The equations for $P(t), P_m(t), P_s(t), M(t)$ and $S(t)$ representing milligrams of poison in the free environment, poison in the mouse pool, poison in the stoat pool, mice and stoats densities

respectively for acute secondary poisoning over t_2 days are summarised as:

$$\begin{aligned} P(0) &= P_0, \qquad t = 0 \\ \frac{\mathrm{d}P}{\mathrm{d}t} &= -\psi\mu M, \quad 0 < t \leq t_p \\ P(t) &= P(t_p), \quad t_p < t \leq t_2 \end{aligned}$$

$$\begin{aligned} P_m(0) &= 0, \qquad t = 0 \\ \frac{\mathrm{d}P_m}{\mathrm{d}t} &= \begin{cases} \psi\mu M - \nu\mu q S_0 \psi t, & 0 < t \leq t_p \\ -\nu\mu q S_0 \psi t_p, & t_p < t < t_2 \end{cases} \\ P_m(t_2) &= 0, \end{aligned}$$

$$\begin{aligned} P_s(0) &= 0, \qquad t = 0 \\ \frac{\mathrm{d}P_s}{\mathrm{d}t} &= \begin{cases} \nu\mu q S_0 \psi t, & 0 < t \leq t_p \\ \nu\mu q S_0 \psi t_p, & t_p < t < t_2 \end{cases} \\ P_s(t_2) &= P_s(t_2^-) - \lambda_s S_0 \gamma_s, \end{aligned}$$

$$\begin{aligned} M(0) &= M_0, \qquad t = 0 \\ \frac{\mathrm{d}M}{\mathrm{d}t} &= -qS_0, \quad 0 < t < t_2 \\ M(t_2) &= (1-\mu)M(t_2^-), \end{aligned}$$

$$S(t) = \begin{cases} S_0, & 0 \leq t < t_2 \\ (1-\lambda_s)S_0, & t = t_2. \end{cases}$$

The solution on the interval $0 \leq t < t_2$ is plotted in Figure 4.4 for the parameter values shown. The plots show poison being depleted from the poison pool and consequently being transferred to the mice and stoat pools. Mice numbers are being slowly reduced and stoat

numbers stay constant over the two days. The solution equations are

$$
\begin{aligned}
P(t) &= \begin{cases} \psi\mu q S_0 \frac{t^2}{2} - \psi\mu M_0 t + P_0, & 0 \le t \le t_p \\ P(t_p), & t_p < t < t_2 \end{cases} \\
P_m(t) &= \begin{cases} -\psi(1+\nu)\mu q S_0 \frac{t^2}{2} + \psi\mu M_0 t, & 0 \le t \le t_p \\ -\nu\mu q S_0 \psi t_p (t - t_p) + P_m(t_p), & t_p < t \le t_1 \end{cases} \\
P_s(t) &= \begin{cases} \psi\nu\mu q S_0 \frac{t^2}{2}, & 0 \le t \le t_p \\ \nu\mu q S_0 \psi t_p (t - t_p) + P_s(t_p), & t_p < t < t_2 \end{cases} \\
M(t) &= -q S_0 t + M_0, \quad 0 \le t < t_2 \\
S(t) &= S_0, \quad 0 \le t < t_2.
\end{aligned}
$$

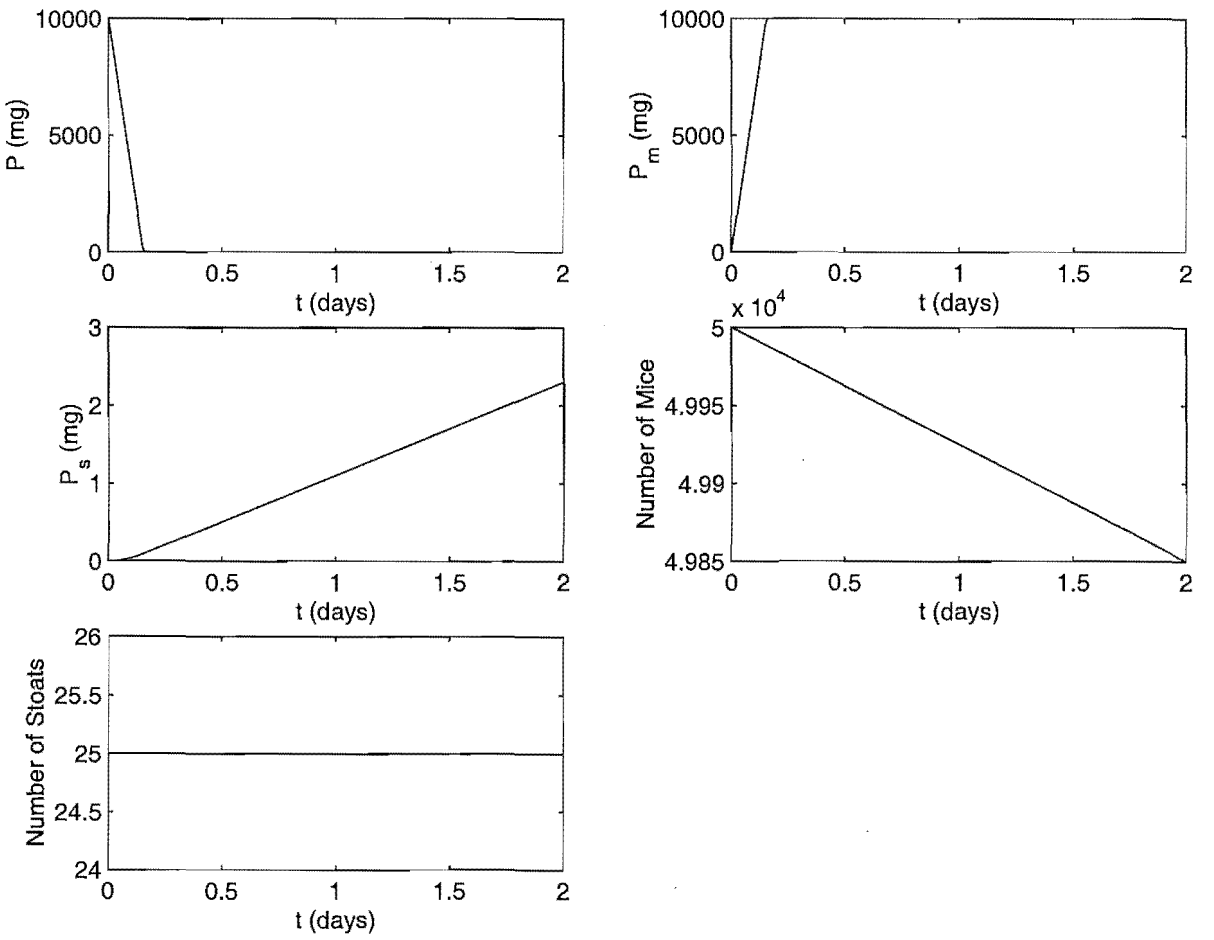

Figure 4.4: The solution of the simplest model for acute poisoning where $P_0 = 10,000$ mg, $M_0 = 50,000$ mice, $S_0 = 25$ stoats, $\mu = .54$, $\psi = 2.4$ mg, $\nu = 0.0798$ and $q = 3$ mice eaten per day per stoat.

4.1.3 Optimal poisoning

To find the minimum amount of poison, P_0, for which secondary poisoning is successful, it is noted that the total amount of poison eaten by S_0 stoats over t_2 days is:

$$\begin{aligned}\int_0^{t_2} \nu\mu q S_0 \gamma_m(t)dt &= \int_0^{t_p} \nu\mu q S_0 \psi t dt + \int_{t_p}^{t_2} \nu\mu q S_0 \psi t_p dt \\ &= \nu\mu q S_0 \psi \frac{t_p^2}{2} + \nu\mu q S_0 \psi t_p t_2 - \nu\mu q S_0 \psi t_p^2 \\ &= \nu\mu q S_0 \psi \left[t_2 t_p - \frac{t_p^2}{2}\right]\end{aligned}$$

where, since $P(t_p) = \psi\mu q S_0 \frac{t_p^2}{2} - \psi\mu M_0 t_p + P_0 = 0$, the time that it takes for poison to run out of the system is given by the expression

$$\begin{aligned}t_p &= \min\left(\min\{t : P(t) = 0\}, 1\right) \\ &= \min\left(\frac{\psi\mu M_0 - \sqrt{(\psi\mu M_0)^2 - 2\psi\mu q S_0 P_0}}{\psi\mu q S_0}, 1\right),\end{aligned} \tag{4.1}$$

realising that the case $t_p = 1$ implies that there is poison wastage in the system. Although $P(t)$ has two zeros, only the smallest positive zero was considered in expression 4.1 because t_p is the first time after $t = 0$ that the graph of $P(t)$ crosses the horizontal axis. It is easily seen that t_p is always non-negative and t_p is non-complex when $P_0 \leq \frac{\psi\mu M_0^2}{2qS_0}$. It is also required that $t_p \leq t_1 = 1$ since poison can only ever be depleted during the first day, thus solving $t_p \leq 1$ and noting that mice densities greatly exceed stoat densities, even in non-mast years, $\Rightarrow$

$$\begin{aligned}\psi\mu M_0 - \sqrt{(\psi\mu M_0)^2 - 2\psi\mu q S_0 P_0} &\leq \psi\mu q S_0 \\ (\psi\mu M_0)^2 - 2\psi\mu q S_0 P_0 &\geq (\psi\mu M_0 - \psi\mu q S_0)^2 \\ -2\psi\mu q S_0 P_0 &\geq \psi\mu q S_0(-2\psi\mu M_0 + \psi\mu q S_0) \\ \Rightarrow P_0 &\leq \psi\mu\left(M_0 - \frac{qS_0}{2}\right).\end{aligned} \tag{4.2}$$

The boundary of inequality (4.2), $P_{01} = \psi\mu\left(M_0 - \frac{qS_0}{2}\right)$, is plotted in Figure 4.5 as a one dimensional function of μ.

For secondary poisoning to work, the total amount of poison eaten is required to be greater than or equal to the LD_{90} for the combined initial number of stoats S_0, that is:

$$\nu\mu q S_0 \psi \left[t_2 t_p - \frac{t_p^2}{2}\right] \geq \mathrm{LD}_{90} w_s S_0.$$

Solving for t_p (noting that $t_2 > 1$ and that t_p must be less than or equal to one) gives,

$$t_p \geq \left(t_2 - \sqrt{t_2^2 - \frac{\mathrm{LD}_{90} w_s 2}{\nu \mu q \psi}} \right). \tag{4.3}$$

Now substituting equation (4.1) into inequality (4.3), solving for P_0 and once again noting that mice densities greatly exceed stoat densities, an expression for successful secondary poisoning is obtained:

$$\begin{aligned}
\frac{\psi\mu M_0 - \sqrt{(\psi\mu M_0)^2 - 2\psi\mu q S_0 P_0}}{\psi\mu q S_0} &\geq \left(t_2 - \sqrt{t_2^2 - \frac{\mathrm{LD}_{90} w_s 2}{\nu \mu q \psi}} \right) \\
\Rightarrow -\sqrt{(\psi\mu M_0)^2 - 2\psi\mu q S_0 P_0} &\geq \left(t_2 - \sqrt{t_2^2 - \frac{\mathrm{LD}_{90} w_s 2}{\nu \mu q \psi}} \right) \psi\mu q S_0 - \psi\mu M_0 \\
\Rightarrow (\psi\mu M_0)^2 - 2\psi\mu q S_0 P_0 &\leq \left[\psi\mu M_0 - \left(t_2 - \sqrt{t_2^2 - \frac{\mathrm{LD}_{90} w_s 2}{\nu \mu q \psi}} \right) \psi\mu q S_0 \right]^2 \\
\Rightarrow P_0 \geq \frac{(\psi\mu M_0)^2 - \left[\psi\mu M_0 - \left(t_2 - \sqrt{t_2^2 - \frac{\mathrm{LD}_{90} w_s 2}{\nu \mu q \psi}} \right) \psi\mu q S_0 \right]^2}{2\psi\mu q S_0}.
\end{aligned}$$

Letting

$$P_{02} = \frac{(\psi\mu M_0)^2 - \left[\psi\mu M_0 - \left(t_2 - \sqrt{t_2^2 - \frac{\mathrm{LD}_{90} w_s 2}{\nu \mu q \psi}} \right) \psi\mu q S_0 \right]^2}{2\psi\mu q S_0}$$

gives the boundary of successful secondary poisoning which is plotted as a function of μ, the proportion of mice initially poisoned, in Figure 4.5.

The condition that

$$t_2^2 - \frac{\mathrm{LD}_{90} w_s 2}{\nu \mu q \psi} \geq 0$$

ensures P_{02} is non-complex. The minimum proportion of mice that can be poisoned for successful secondary poisoning is the solution of

$$\mu\nu - \frac{2\mathrm{LD}_{90} w_s}{3q\psi} = 0$$

which is the intersection of the two functions P_{01} and P_{02}, found by substituting $t_p = 1$ and $t_2 = 2$ into inequality (4.3). Figure 4.6 shows a clearer picture of the lower boundary of Figure 4.5 and the intersection of P_{01} (mg) and P_{02} (mg).

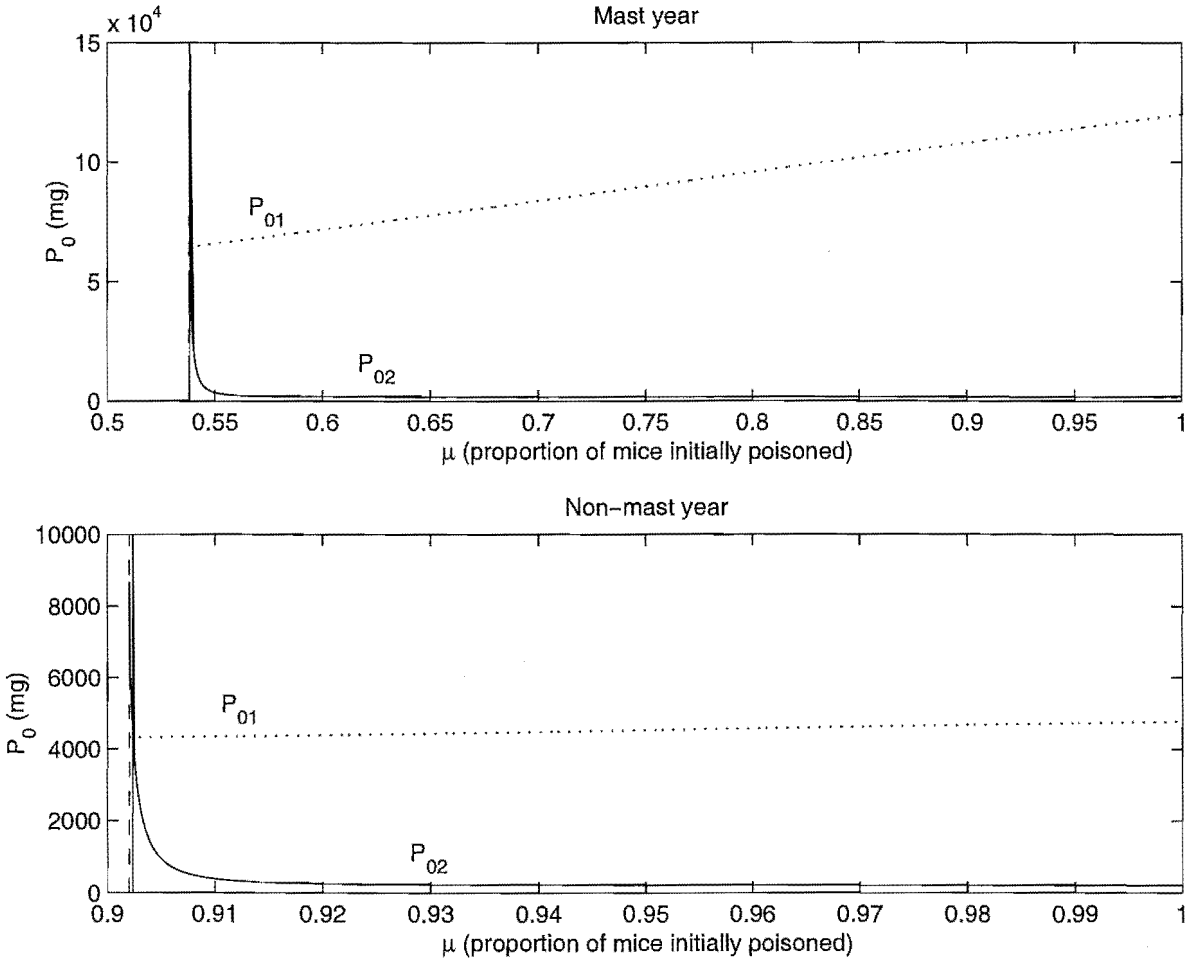

Figure 4.5: P_{01} (mg) (dotted line) and P_{02} (mg) plotted as functions of μ (the proportion of mice initially poisoned) in mast years ($M_0 = 50000$ mice, $q = 3$ mice eaten per stoat per day) and non-mast years ($M_0 = 2000$ mice, $q = 1$ mouse eaten per stoat per day).

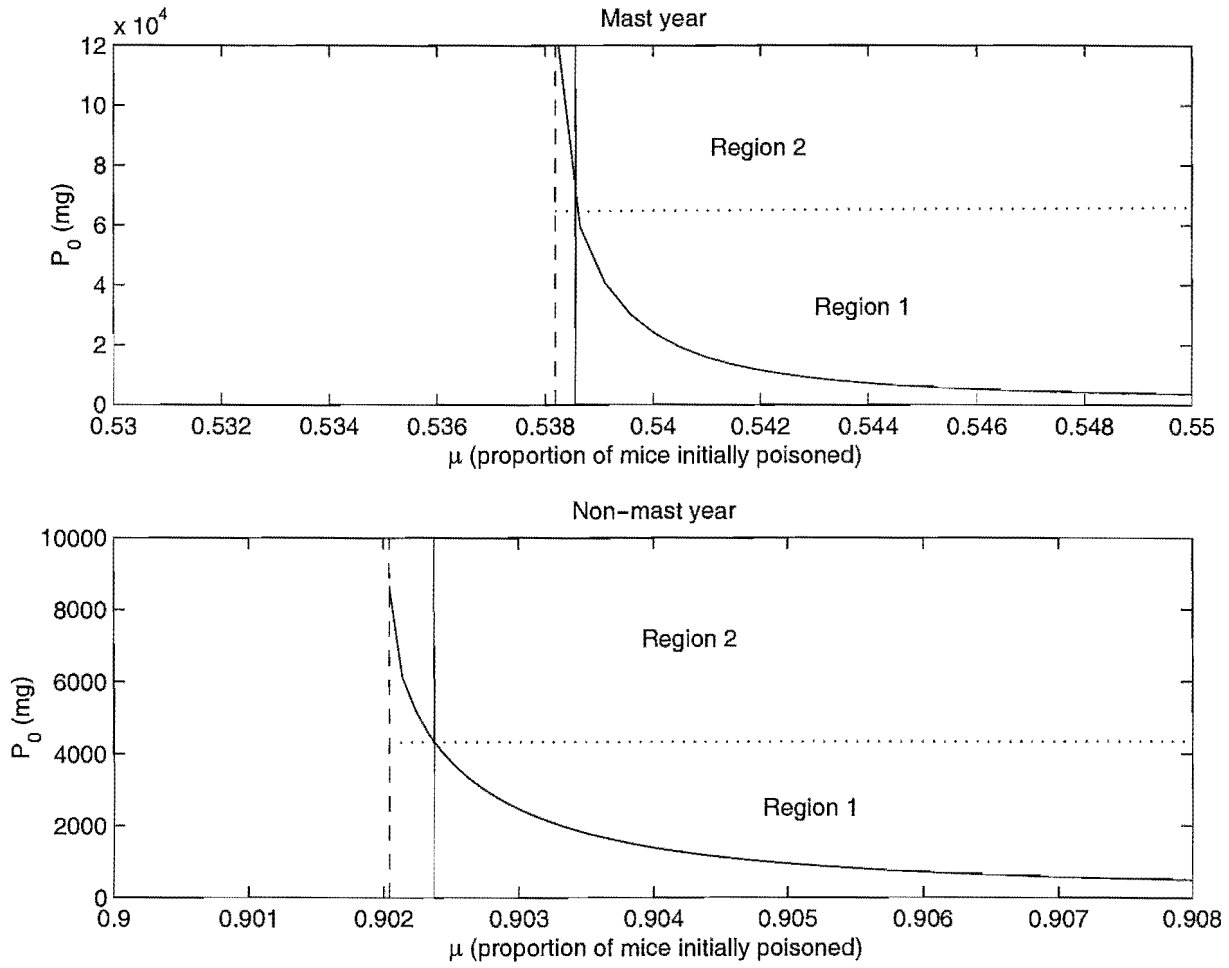

Figure 4.6: An enlargement of the function P_{02} (mg) depicted in Figure 4.5 with P_{01} (mg) (dotted line) and P_{02} (mg) plotted as functions of μ (the initial proportion of mice poisoned) in mast years ($M_0 = 50000$ mice, $q = 3$ mice eaten per stoat per day) and non-mast years ($M_0 = 2000$ mice, $q = 1$ mouse eaten per stoat per day).

As $\mu \to 1$ the value of t_p, the time it takes for all poison to be consumed, becomes small. Figure 4.7 shows t_p as a one dimensional function of P_0 along the line P_{02} for mast and non-mast years.

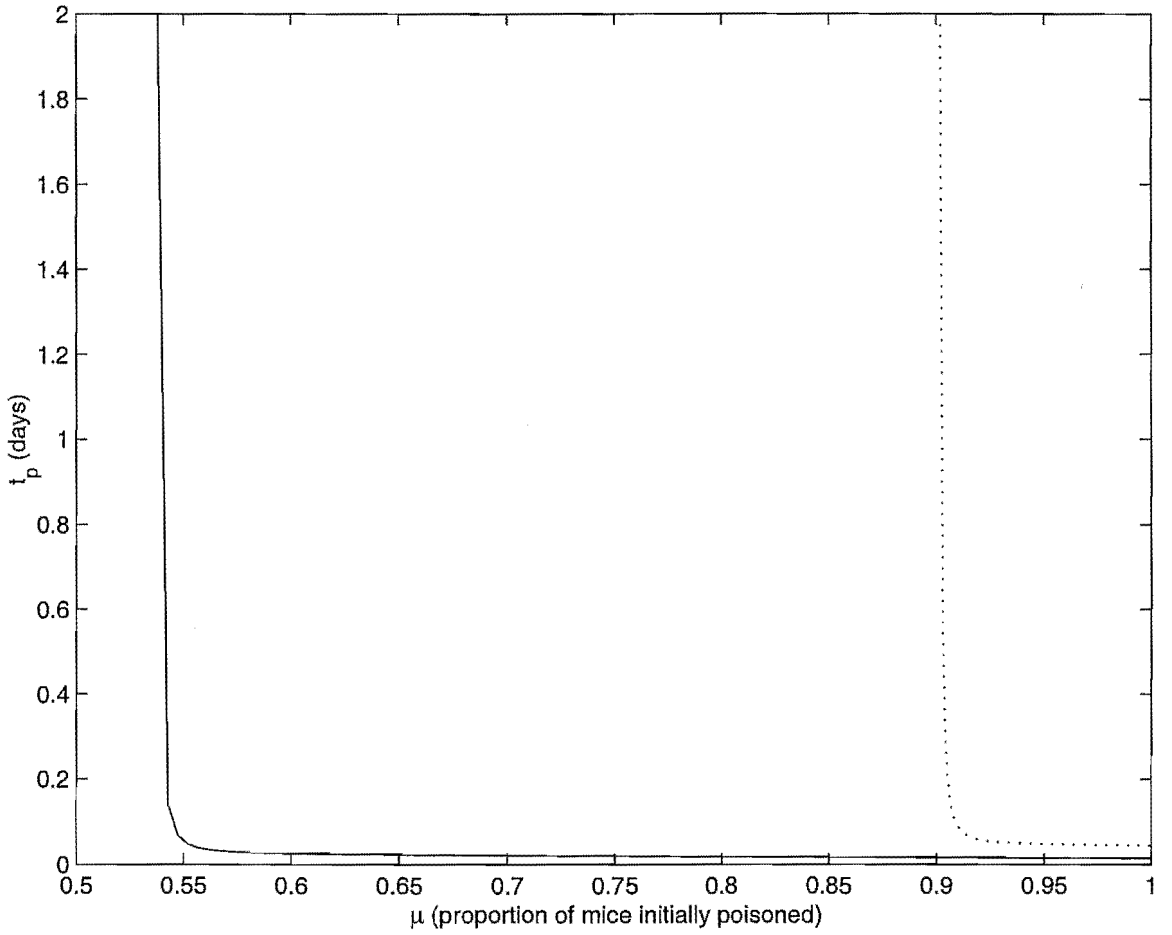

Figure 4.7: Plot of t_p (days) along the line $P_0 = P_{02}$ (mg) for a mast year (solid line, $q = 3$ mice eaten per stoat per day, $M_0 = 50,000$ mice) and a non-mast year (dashed line, $q = 1$ mouse eaten per stoat per day , $M_0 = 2000$ mice.)

4.1.4 Interpretation of Figures 4.5 and 4.6

The main region of interest is P_0 values where $P_0 \geq P_{02}$. This area can be divided into two regions as shown in Figure 4.6.

1. If a poisoning strategy, (μ, P_0), is chosen in Region 1, specified by the constraints

$$\begin{aligned} P_0 &\leq P_{01} \\ P_0 &\geq P_{02}, \end{aligned}$$

as depicted in Figure 4.6, then secondary poisoning will be successful and all poison will be eaten by mice, i.e. there will be no poison pellets left lying on the ground

(although there may still be wastage in the system since not all poison eaten by mice may be transferred to stoats).

2. If a poisoning strategy, (μ, P_0), is chosen in Region 2, specified by the constraints

$$\begin{aligned} P_0 &\geq P_{01} \\ \mu\nu - \frac{2\text{LD}_{90}w_s}{3q\psi} &\geq 0, \end{aligned}$$

as depicted in Figure 4.6, then secondary poisoning will be successful but not all poison will be eaten by mice, i.e. there will be poison still lying on the ground uneaten by mice.

3. If a poisoning strategy, (μ, P_0), is in the region specified by the constraints

$$\begin{aligned} P_0 &\geq P_{02} \\ \mu\nu - \frac{2\text{LD}_{90}w_s}{3q\psi} &< 0, \end{aligned}$$

then secondary poisoning will not be successful because in this region $P_0 > P_{01}$ therefore $t_p > 1$ and mice will die before they have consumed a sufficient amount of poison for successful secondary poisoning.

4.1.5 Results

The model assumes that P_0 mg of poison is distributed so that it is available to μM_0 mice and shows that there are an infinite number of poisoning strategies or pairs, (μ, P_0), where secondary poisoning would be successful. It should be noted that not all poisoning strategies are obtainable in the field. For example, the values along the horizontal axis in Figure 4.6 show minute increments in the values of μ. In practise it would not be possible to implement a regime that could poison a proportion of mice to such precision.

The feasible regions, regions 1 and 2, for successful secondary poisoning are depicted in Figure 4.6 (for mast and non-mast years) and specified by the constraints

1.
$$\mu\nu - \frac{2\text{LD}_{90}w_s}{3q\psi} \geq 0$$

2.
$$P_0 \geq \frac{(\psi\mu M_0)^2 - \left[\psi\mu M_0 - \left(t_2 - \sqrt{t_2^2 - \frac{\text{LD}_{90}w_s 2}{\nu\mu q\psi}}\right)\psi\mu q S_0\right]^2}{2\psi\mu q S_0}.$$

If, in addition, $P_0 \leq \psi\mu\left(M_0 - \frac{qS_0}{2}\right)$, then all poison initially distributed will be consumed by mice and there will be no wastage in the environment.

The model gives

$$P_0 = \frac{(\psi\mu M_0)^2 - \left[\psi\mu M_0 - \left(t_2 - \sqrt{t_2^2 - \frac{\mathrm{LD}_{90} w_s 2}{\nu\mu q\psi}}\right)\psi\mu q S_0\right]^2}{2\psi\mu q S_0}$$

as the bare minimum of poison required for successful secondary poisoning.

The model shows that less poison is needed for successful secondary poisoning in a non-mast year than in a mast year (see Figure 4.5 and Tables 4.3 and 4.4). In both cases, the amount of poison is minimised when all mice are poisoned ($\mu = 1$), so it is better to distribute a smaller amount of poison amongst many mice than it is to distribute larger amounts of poison amongst fewer mice. However, if $\mu = 1$ then the mouse population will not be maintained for subsequent poisoning and non-target species may be adversely affected, especially in a mast year when many poisoned mice will not be eaten by stoats.

4.1.6 Sensitivity analysis of the LD_{90}

It is important to consider the effect of changing the value of the LD_{90} on the outcomes of the model since LD_{90}'s are rough estimates.

The value of

$$\mu_{\min} = \left\{\mu : \mu\nu - \frac{2\mathrm{LD}_{90} w_s}{3q\psi} = 0\right\}$$

is dependent on the LD_{90}. Figure 4.8 shows that as the LD_{90} increases there is only a slight increase in the minimum number of poisoned mice required for successful secondary poisoning. Further analysis shows that this is because the ratio of the LD_{90} to the contact rate ν is virtually constant. The LD_{90} and ν are increasing at the same rate causing $\mu_{\min}$ to stay essentially constant.

Figure 4.9 indicates that P_{02}, the minimum amount of poison required for successful secondary poisoning, increases as the value of the LD_{90} increases, however the increase in P_{02} is not extreme.

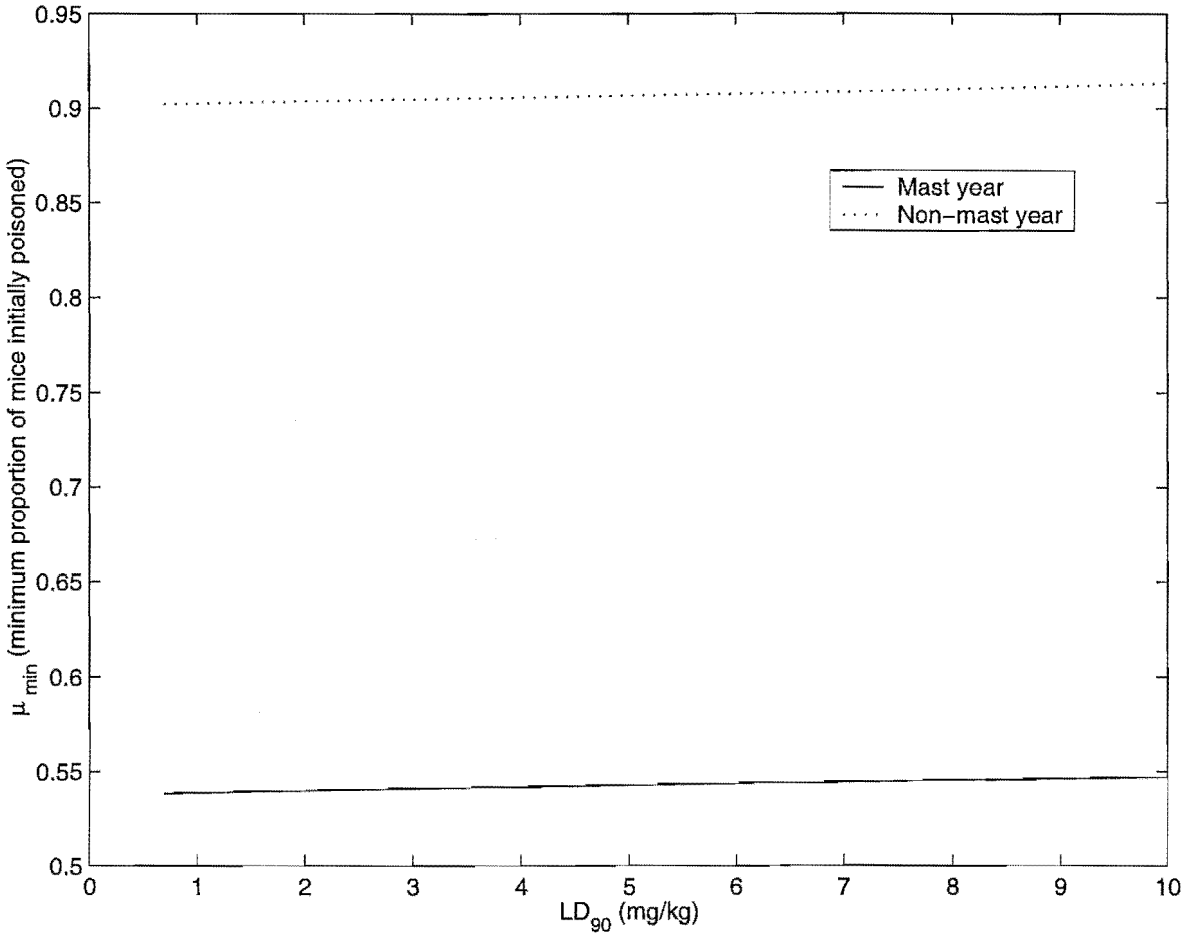

Figure 4.8: Sensitivity analysis of the LD_{90} (mg/kg) on $\mu_{\min}$, the minimum number of poisoned mice required for successful secondary poisoning.

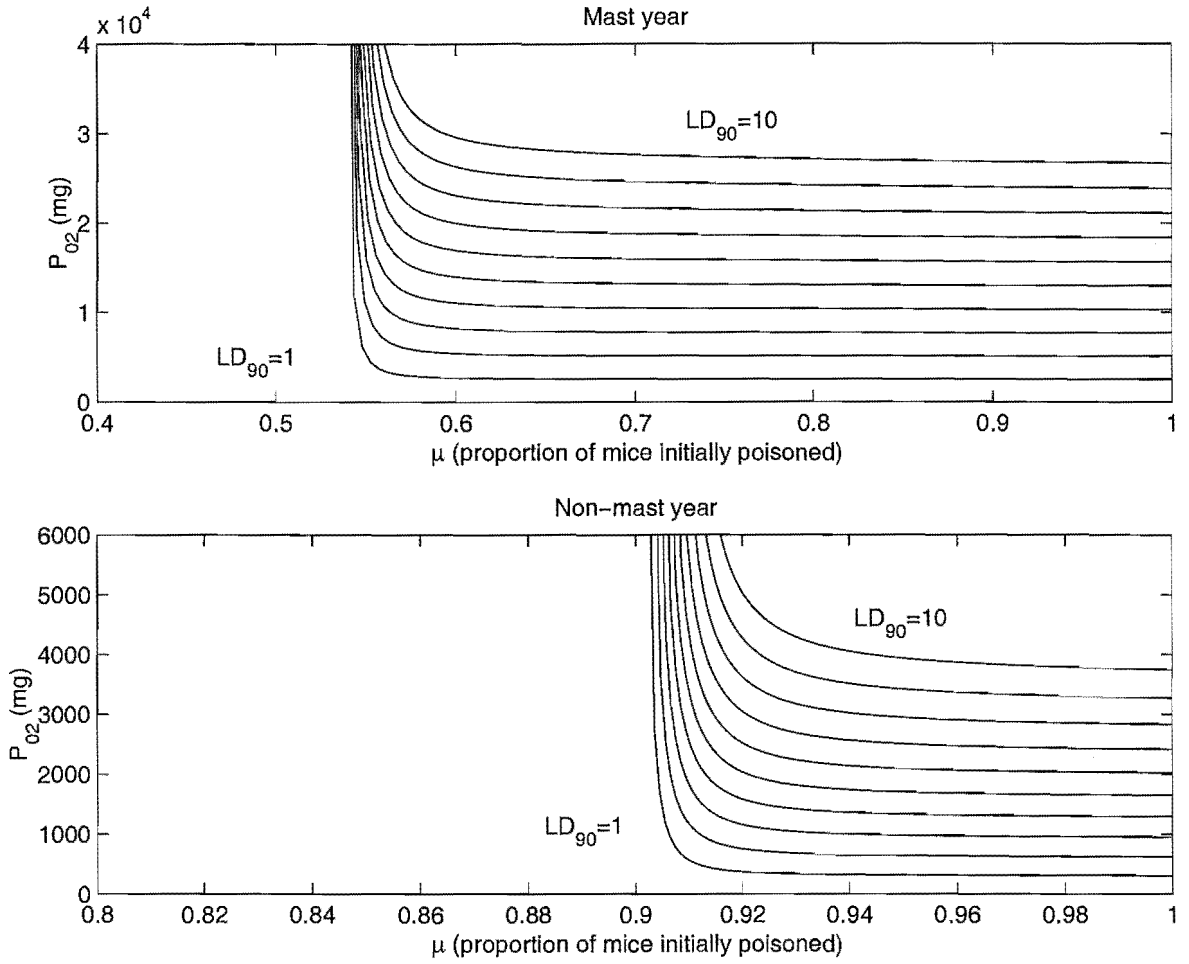

Figure 4.9: P_{02} (mg) vs μ (initial proportion of mice poisoned) for different values of the LD_{90} (mg/kg) in both mast and non-mast years indicate that the minimum amount of poison required for successful secondary poisoning increases as the LD_{90} increases, for example as the poison becomes less toxic.

Both Figures 4.8 and 4.9 indicate that the results are not sensitive to small changes in the LD_{90}. For different LD_{90} values, the conclusion that non-mast years require overall less poison than mast years remains unchanged.

4.1.7 Conclusions: The optimal poisoning regime

Recall the objectives for successful secondary poisoning:

- stoats are reduced to an acceptable level
- use of poison is minimised

- the mouse population is maintained for subsequent poisoning

- deaths of non-target species are minimised by poisoning as few mice as possible

Which is the optimal poisoning strategy satisfying all the requirements? Firstly, the model predicts that non-mast years should be preferred for operations because less poison is needed then than in mast years. Secondly, if possible, poisoned mice, rather than poison pellets, should be released into the environment to reduce the risk of non-target species eating baits. One needs to be sure that stoats will continue to eat poisoned mice in the same manner as if poison pellets had been distributed. Another way to reduce the risk of non-target species eating baits is to put poison baits into containers that only mice have access to. Finally, in order to minimise deaths of non-target species by poisoning as few mice as possible, μ, the proportion of mice to be poisoned, should be chosen to be as small as possible. In a non-mast year, if the $LD_{90} = 0.7$ mg/kg then $\mu_{\min} = .9024$ (Table 4.3), leaving only approximately 10% of mice for subsequent poisoning. Thus the initial number of poisoned mice should be $\mu M_0 = .9024 \times 2000 \approx 1800$. The initial amount of poison, P_0, distributed amongst the $\mu M_0 \approx 1800$ mice should be greater than or equal to $P_{02}(\mu = .9024, LD_{90} = 0.7) = 4304.3$ mg which is of course 2.4 mg of poison for each mouse.

$\mu = \mu_{\min}$		
	Mast	Non-mast
$\mu_{\min}$	0.5386	.9024
M_0	50,000 ($q = 3$)	2000 ($q = 1$)
μM_0	26,930	1804.8
P_0	64,579 mg	4304.3 mg

Table 4.3: Minimum amount of poison required if the minimum amount of mice are poisoned ($\mu = \mu_{\min}$).

$\mu = 1$		
	Mast	Non-mast
M_0	50,000 ($q = 3$)	2000 ($q = 1$)
P_0	1770.8 mg	214.05 mg

Table 4.4: Minimum amount of poison required if all mice are poisoned ($\mu = 1$).

Recall that the aims were to identify the threshold density of mice, above which secondary poisoning will be successful and specify the optimal administration of poison. The latter has been achieved, however the former still needs consideration because it has been shown that secondary poisoning can be successful even at what were assumed the lowest densities of mice. As soon as the number of mice eaten per stoat per day, $q \leq 1$, the contact rate, ν, becomes 0 implying that $q = 1$ is the threshold density for successful secondary poisoning.

4.2 Persistent poisoning

The model can be further generalised by incorporating certain demographic parameters in order to represent secondary poisoning using a persistent poison that stays in the environment for longer than an acute poison.

Brodifacoum (Talon) is an anticoagulant poison which is slowly eliminated from the liver. Animals can obtain a lethal dose over time, simply by consuming a series of sublethal doses. Unfortunately the same applies to non-target species. Many of the indigenous birds of New Zealand are susceptible to both primary poisoning, by eating baits, and secondary poisoning, by eating poisoned prey. Many examples of non-target species being poisoned after field use of brodifacoum (Talon) are given by [28]. It can be argued that the adverse effects depend more on how and where baits are used, with primary poisoning being the main cause of poisoning in non-target species and the potential to successfully reduce stoat numbers needs further consideration. Examples where pest control using brodifacoum (Talon) has been successful with no long term detrimental effects to non-target species are also listed by [28].

Figure 4.10 shows a pictorial representation of a general secondary poisoning model where there is a delay of T days from when poison is ingested by a rodent until the time of death. Rodents could be divided into specific species and/or gender if required.

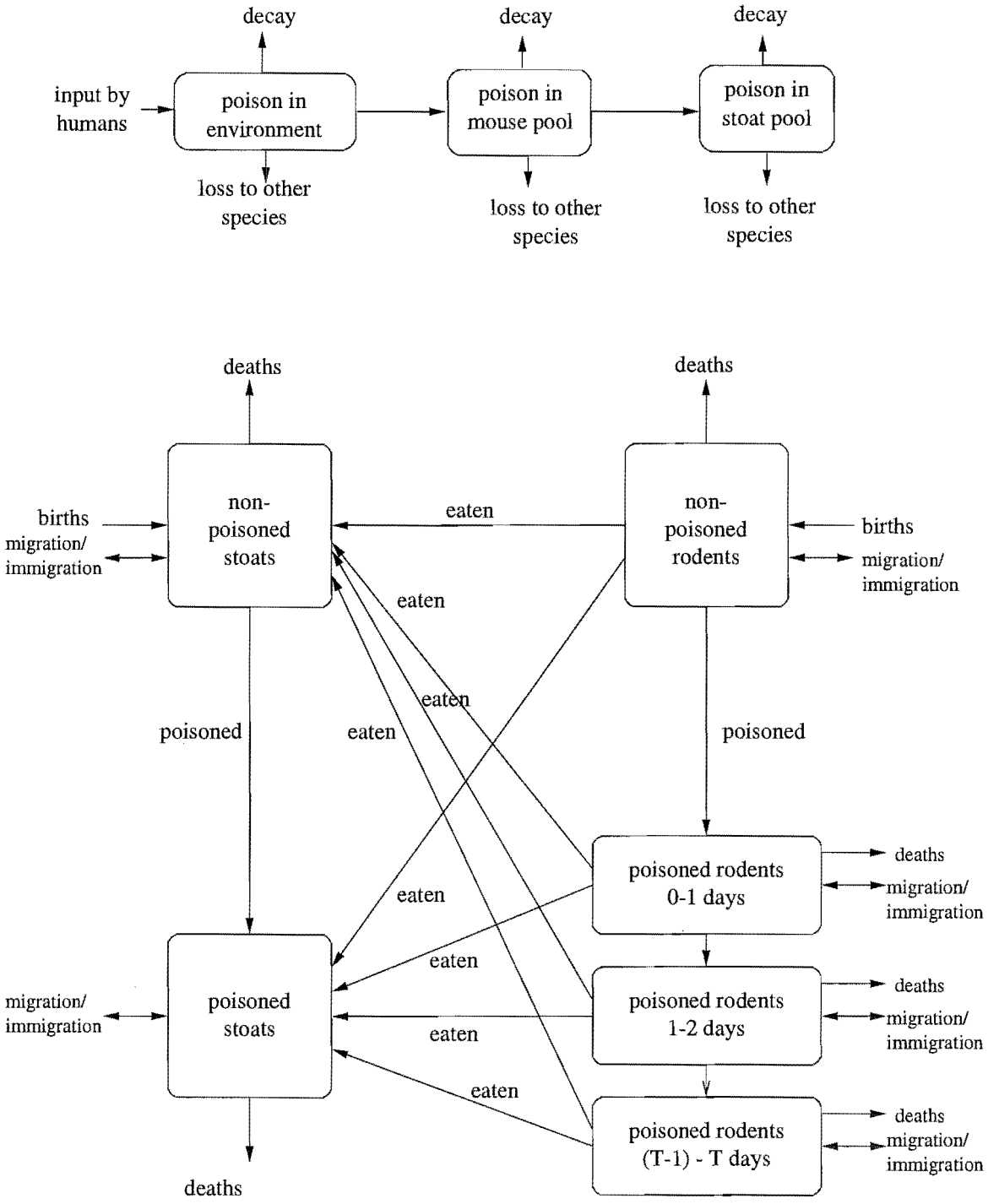

Figure 4.10: A general secondary poisoning model.

A mathematical model representing Figure 4.10 would require delay terms and other non-linearities. An analytical analysis would no longer be possible, however the results of the simplified model and the analytical solution depicted in this chapter give an indication of the dynamics of the more general model.

In this chapter a 500 hectare block for pest eradication was considered. Different areas

would alter the values of the initial densities of mice and stoats, M_0 and S_0, respectively, but all other parameters would remain unchanged. In the next chapter, the minimum critical area required for pest eradication is estimated by simulating different sub-adult dispersal scenarios.

Chapter 5

Critical/minimum areas for pest eradication

The design, selection and management of nature reserves and national parks are some of the challenges facing conservationists worldwide. In this chapter, management strategies for stoat control in Te Urewera National Park in the North Island of New Zealand are investigated. Stoats are the main predator of the endangered indigenous northern brown kiwi whose hatchling to adult recruitment rate is currently well below that required for survival. Stoat reduction or eradication is therefore essential for kiwi survival. In chapter 3, a critical stoat density required for kiwi survival was estimated and it was suggested that current methods of stoat removal often do not achieve this threshold. In chapter 4, an optimal poisoning regime for larger scale stoat removal was examined. Because stoat eradication throughout the entire park is not economically viable, managers need to know the minimum area that needs to be eradicated of pests in order to achieve kiwi survival. Identification of this minimum area is the aim of this chapter.

In chapter 2, an age structured model, representing the population dynamics of northern brown kiwi, was constructed to estimate critical predation and recruitment rates of immature kiwi. Here the model is discretised and a spatial structure is incorporated representing sub-adult dispersal between a treatment block (a managed area eradicated of pests) and a control (unmanaged area). The spatial and temporal dynamics of the population are simulated using MATLAB. Different dispersal scenarios are compared, and for each scenario, a minimum treatment block area that ensures population persistence is estimated.

Results indicate that i.) dispersal scenarios which suppress outward movement result in a smaller critical treatment area and ii.) the current treatment block size in the field is well below the area of the critical treatment block.

5.1 Discretisation

Although in chapter 7 a continuous spatial model is investigated, in this chapter spatial dynamics are incorporated into the age structured model developed in chapter 2 by discretising both the time and space domains. In chapter 2, the population was partitioned into three age classes, chicks (0-3 weeks), juveniles (3 weeks - 1.5 years) and adults (older than 1.5 years), which were chosen due to an approximately constant predation rate in each class. Here the cohort is partitioned into juveniles (0-9 months), sub-adults (10-13 months) and adults (14 months-40 years) because the consideration is now the sub-adults as a dispersing

group of birds who are leaving the natal area and establishing their own territories.

If r_1 is the recruitment rate of juveniles to sub-adults and r_2 is the recruitment rate of sub-adults to adults then the discretised form of equation (2.10), the equation representing $n(t)$, the (discrete) number of adults in the population at time t, is

$$n(t+1) = n(t) + \frac{b}{2} n(t-a_2) r_1 r_2 - f_2 n(t). \tag{5.1}$$

Equation (5.1) is further extended in section 5.5 to incorporate sub-adult dispersal and different demographic rates between treatment and control areas. Analytically, the model becomes difficult to deal with once spatial structure is incorporated (see section 5.5 and chapter 7). For simplicity the dynamics of the model have been simulated by computer and this tool of analysis is used to compare minimum treatment areas for different sub-adult movement scenarios. The simulation is developed in the following sections.

5.2 The simulation

Using a simulation program written in MATLAB (see Appendix), adult densities over a time horizon ([16]) of 50 years were examined for treatment block areas ranging from a starting treatment block area to a final treatment block area with a step-size of block length 0.1 km. A square treatment block, centred inside a 10 km $\times$ 10 km (10,000 ha) control block (see Figure 5.1) is considered. It is assumed that sub-adult birds can disperse between the treatment and control blocks and they can disperse between the control block and the 16 km $\times$ 16 km outer region, but no birds can disperse beyond the outer region and no birds can enter from outside the outer region. This structure represents an area eradicated of pests (the treatment block) inside a reserve or national park (the whole block) which itself is surrounded by land where birds may live but is outside the realms of management (the outer region). Unsuitable habitat, for example pasture or urbanisation, lies beyond the outer region.

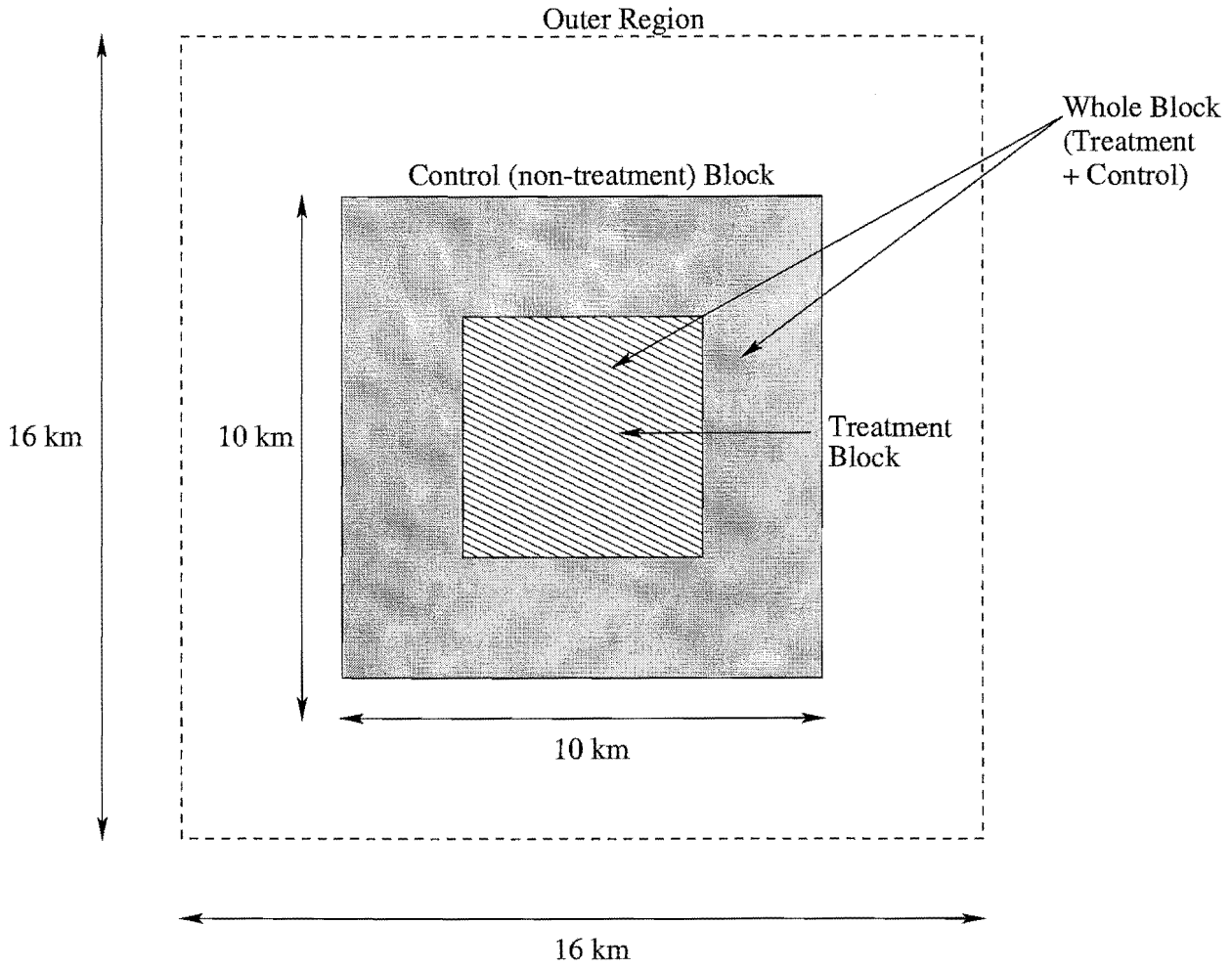

Figure 5.1: The whole block (control and treatment blocks) plus the outer region.

Stochasticity is built into the model via the movement of sub-adults. The birds move once each month from the age of 10 months to 13 months. They thus make four jumps each with a distance and angle assigned according to one of five different movement scenarios. The movement scenarios, which assign angle and distance from uniform distributions, are summarised in section 5.3. The aim is to find the minimum treatment block area, which ensures a high probability of adult population persistence and hence a low probability of extinction, for each movement scenario. The critical treatment block sizes for each movement scenario can then be compared.

The probability of extinction is defined in terms of Population Viability Analysis (PVA) as the probability that the population drops below a critical population threshold at least once in the next t years ([16]). For the analysis here, it is preferable to calculate the probability of quasi-extinction, a term that can refer to any sort of population decline over t years and not necessarily a population decline below a certain threshold value ([16]). In this case, actual

values are not of great interest but rather the slope of the time series line over 50 years for adult densities and the comparison between different movement scenarios. The probability of quasi-extinction is calculated by simulating 50 times the adult time series in the whole block over 50 years for a particular treatment block area and counting the number with approximately negative slope over the final 10 years. That is, the number where the adult population density in the final year was less than the adult population density in the 10th year previous were counted. This gave an, albeit crude, estimate as to whether the slope was decreasing or not. This viability criterion for the whole block will be referred to as 'viability criterion 1' throughout the remainder of the chapter. It is possible that the whole block is viable under criterion 1 when in fact most of the birds lie within the treatment block and virtually none reside in the control. Taking this into account, 'viability criterion 2' compares the adult population in the control in the final (50th) year to that in the first year. This criterion is conservative because it depends on the initial age distribution of kiwi. Less conservative than criterion 2 but more conservative than criterion 1, 'viability criterion 3' compares the adult population in the control over the last 20 years. Viability criterion 2 and 3 are discussed in greater detail in section 5.6.

The model can be expressed as a matrix (see section 5.5) where the long term age distribution of the population is either 0 in each age class, ∞ in each age class or a steady state depending on whether the dominant eigenvalue of the matrix is $< 1, > 1$ or $= 1$ respectively ([18]). This is independent of the initial age distribution which in the simulation is chosen to have no sub-adults or juveniles and adult ages uniformly distributed between 14 months and 40 years. Such an initial age density distribution is unrealistic because it biases the population towards older birds. This results in a higher than normal adult death rate in the first few years and a lower than normal recruitment rate of young birds. However, the long term changes in population density are unaffected by this choice of initial age distribution so it was not necessary to start with something that closely reflected natural populations. In section 5.6 when different viability criteria are discussed a negative exponential distribution is considered as an initial age distribution.

The rate of convergence of the initial age distribution to the eigenvector of the matrix depends on both the initial distribution and the ratio between the two largest (in magnitude) eigenvalues of the matrix ([32]). In the simulation here it has been assumed that 50 years is enough time to know whether the age distribution will eventually converge to either 0 or

∞. Section 5.5 illustrates how the problem can be solved using a matrix approach and how the spatial structure adds to the complexity in finding a solution.

The starting and final treatment block areas in the simulation program were chosen so that the probability of quasi-extinction for the starting treatment block area was 1 (Figure 5.2) and the probability of quasi-extinction for the final treatment block area was 0 (Figure 5.3). The critical (minimum) treatment block area is the smallest treatment block area which gives a greater than 99% probability of adult population persistence or a less than or equal to 1% probability of adult quasi-extinction over 50 years (Figure 5.4).

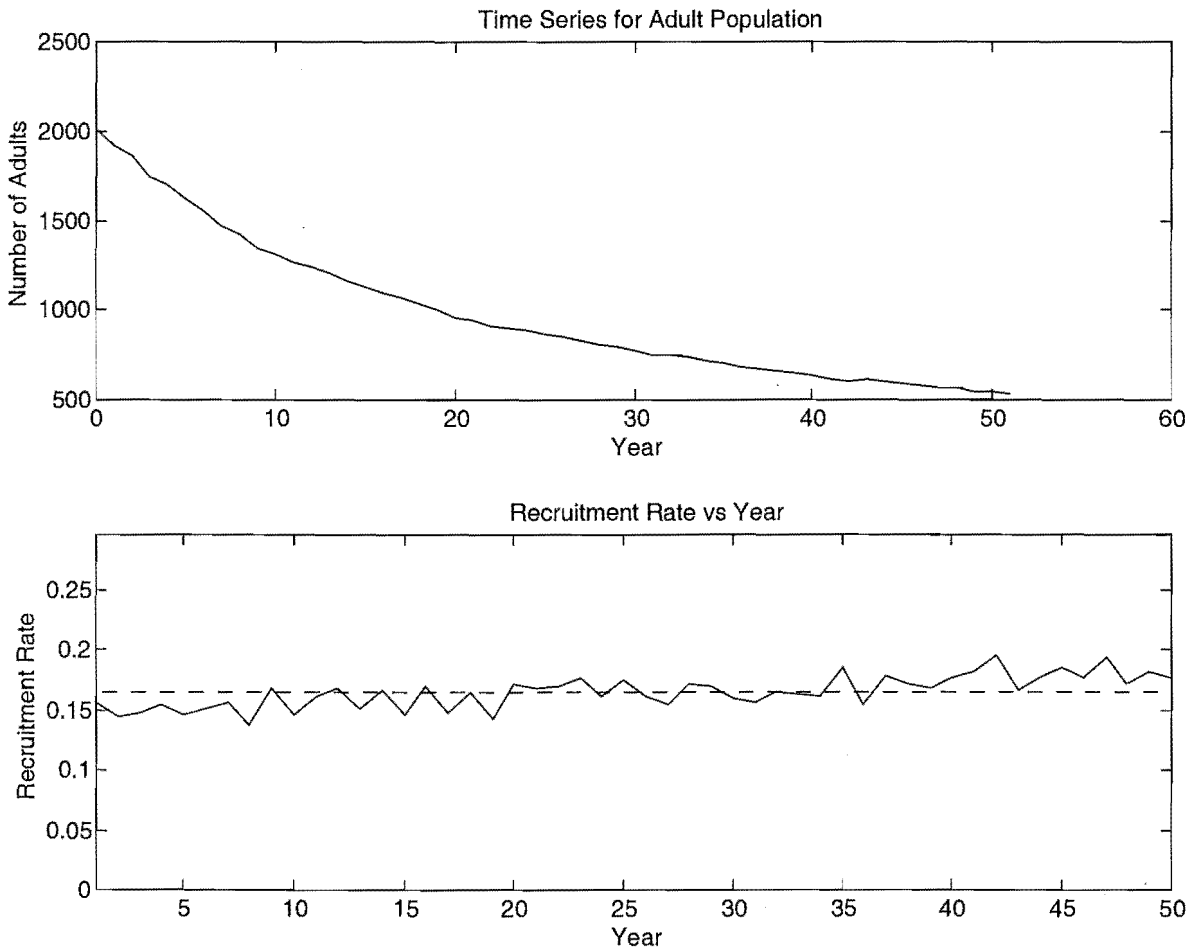

Figure 5.2: Time series for adults and recruitment rates over 50 years. For the starting treatment block size, the adult time series decreases over 50 years in all 50 simulations. Therefore the probability of extinction is unity.

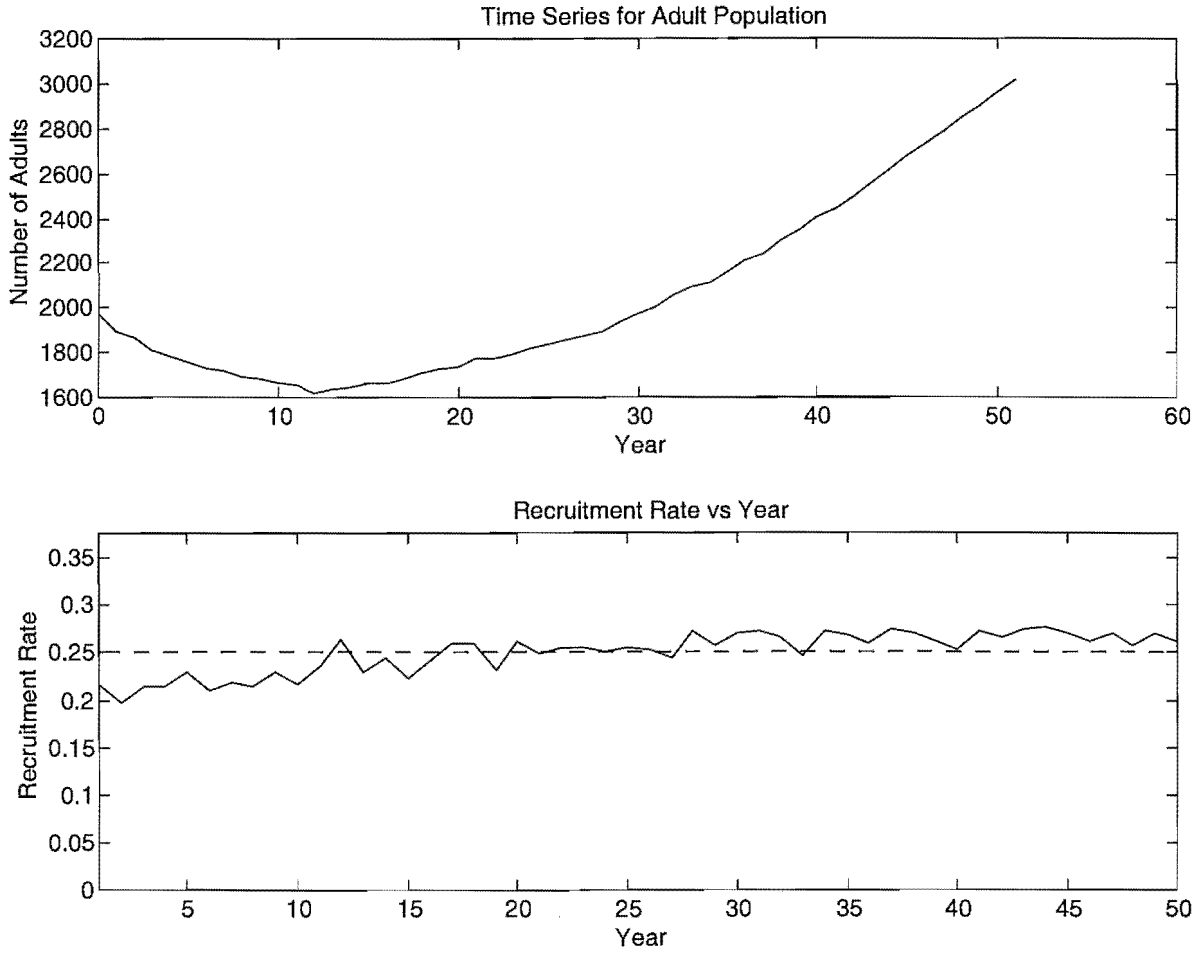

Figure 5.3: Time series for adults and recruitment rates over 50 years. For the final treatment block size, by the 50th year the time series for the adults has increased in all 50 simulations. Therefore the probability of extinction is zero.

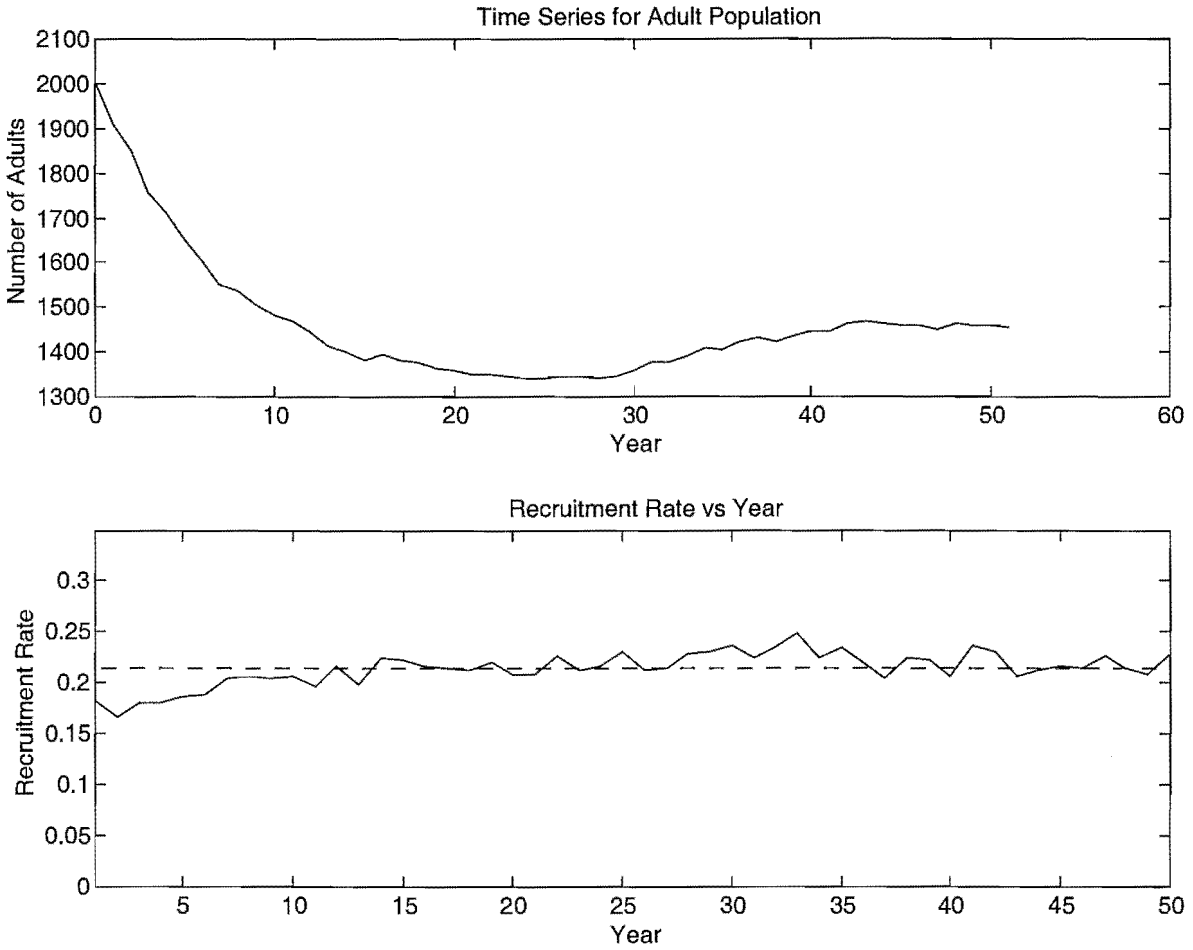

Figure 5.4: Time series for adults and recruitment rates over 50 years. For the critical (minimum) treatment block size. After 50 years the time series appears to level out. This is the smallest treatment block area that ensures population persistence.

Although the main aim is to find a critical treatment block size, the corresponding critical recruitment rate can also be evaluated. The critical recruitment rate is just the averaged (over 50 years and 50 simulations) recruitment rate from that particular critical treatment block size.

A flow chart, showing the month by month demographic and dispersal processes of the simulation, is given in Figure 5.5.

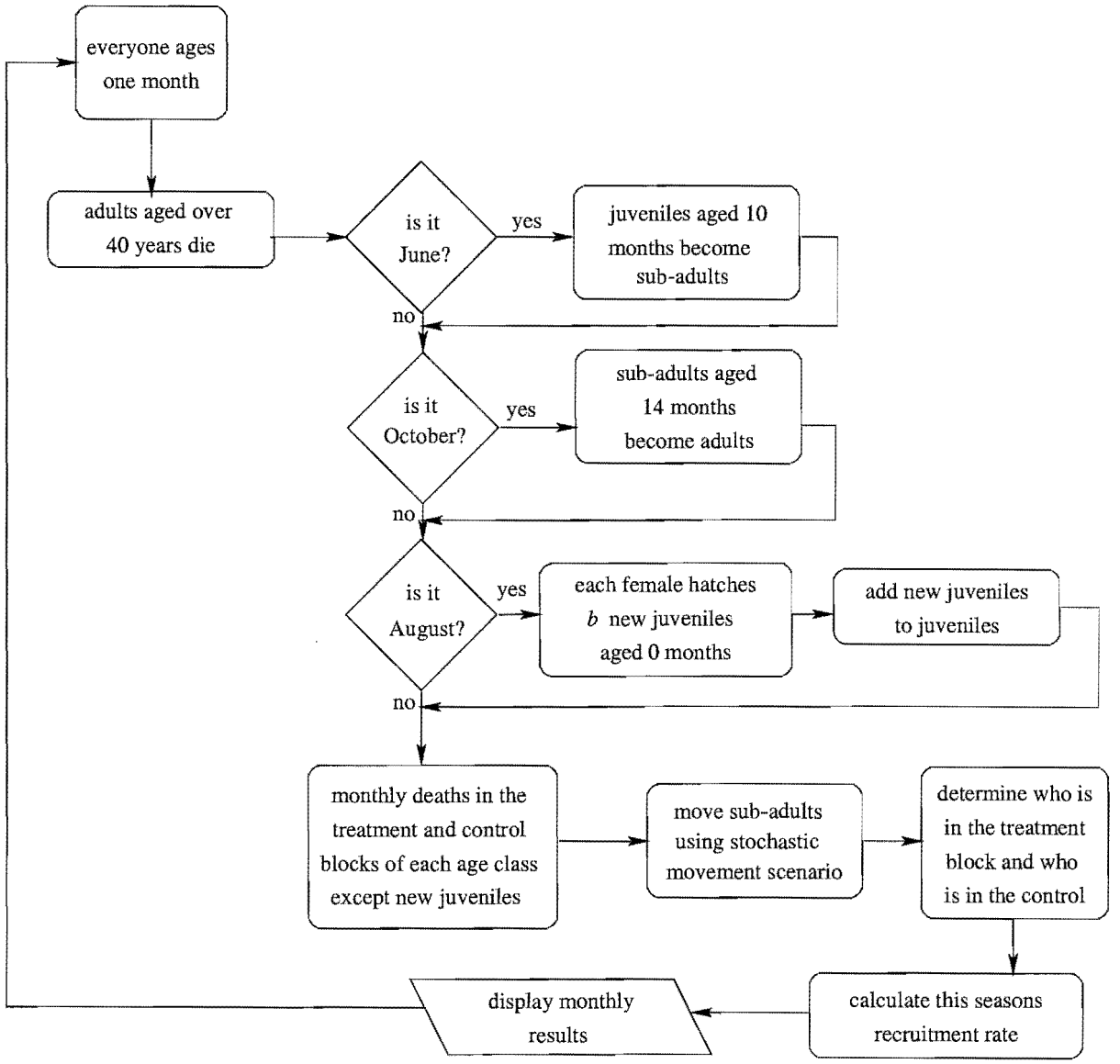

Figure 5.5: Flow chart of the month by month processes in the simulation.

The demographic rates are all density independent. In many simulations stochasticity is built into the model via sampling demographic rates (at each time step) from some distribution ([10]). Adding demographic uncertainty in PVA can change estimates of the probability of extinction ([53]). Density independent stochasticity has been built into the model here via different movement scenarios of sub-adults. A discussion of the demographic parameters used in the model follows. All parameter values are based on field observations.

Recruitment rates: Without dispersal, Figure 5.6 shows how the hatchling to adult recruitment rates are calculated in each of the treatment and control blocks. In the treatment block, 50% of hatchlings survive to become sub-adults. Of those sub-adults, 90% become adults. This gives a hatchling to adult recruitment rate of 45%. Similarly in the control

block, 5% of hatchlings survive to become sub-adults. Of those, 90% become adults. This gives a hatchling to adult recruitment rate of 4.5% in the control block. The outer region has the same hatchling to adult recruitment rate as the control. To incorporate dispersal, monthly death rates are calculated (Table 5.1) and sub-adults make monthly jumps (see section 5.3).

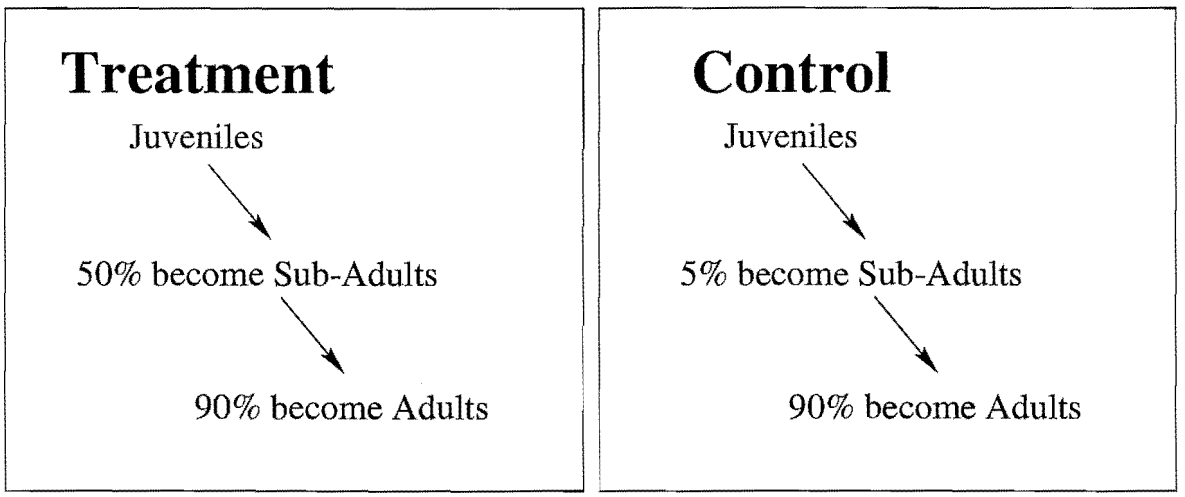

(a) In the treatment block $r_T = 50\% \times 90\% = 0.45$

(b) In the control block $r_C = 5\% \times 90\% = 0.045$

Figure 5.6: Without dispersal, in the treatment block 50% of hatchlings become sub-adults and of those 90% become adults. In the control 5% of hatchlings become adults and 90% of those become adults.

Age structure and death rates: Table 5.1 shows the age classes and monthly death rates (since the simulation runs month by month) in treatment and non-treatment areas. New juveniles (hatchlings) are 0 months, new sub-adults are 10 months, new adults are 14 months. In chapter 2 it was found that there is an 8.2% loss of adults per year. Here, it has also been assumed that any adult over 40 years dies. With the initial age distribution being uniform, these combine to give an overall adult death rate of around 8.95% per year on average, still well within the range observed in wild populations.

Reproduction: All adults breed and produce 0.85 chicks (of age 0 months) per female in August of each year.

Gender ratios: It has been shown ([59]) that there is no significant difference between death rates of adult males and females thus the gender ratio is taken as 1:1.

Initial age and position distribution of the adults: At the start of the simulation the

adults are distributed uniformly over the entire block (this assumes a uniform habitat) and the ages of these adults are between 14 and 480 months, sampled from a uniform distribution and then rounded to the nearest month (see Figure 5.7).

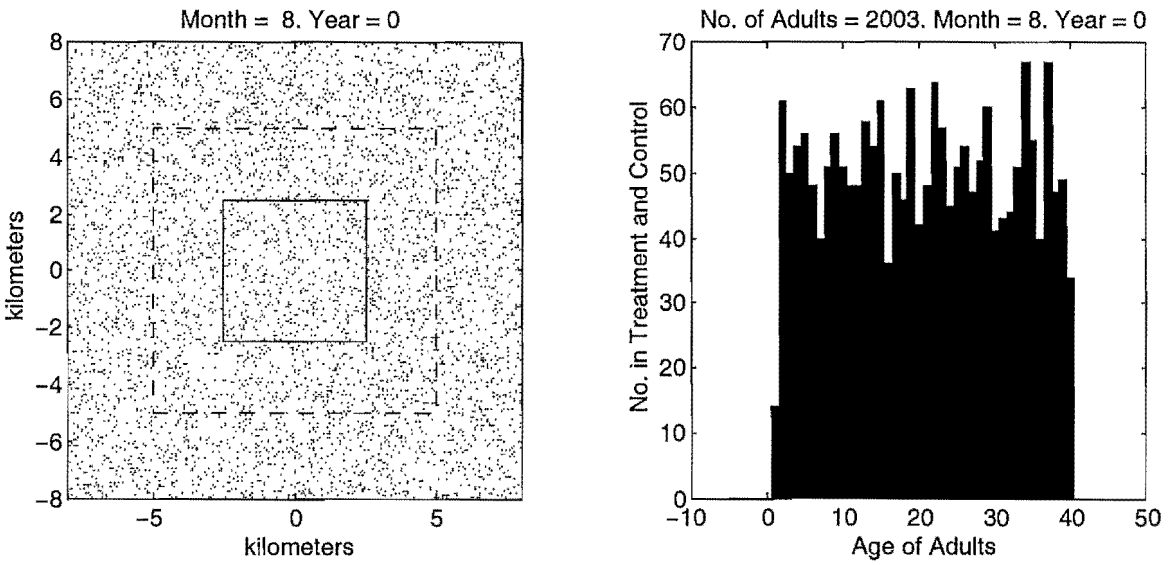

Figure 5.7: Initial uniform position and age distributions of adults. The treatment block size is 5 km $\times$ 5 km.

Initial densities of adults and carrying capacity: The initial density of adults was taken as 20 birds per km^2. This is higher than is normally observed in the field but is necessary in order to avoid rounding errors when population sizes become small ([10]) since bird numbers are discretised. Once again, it is not actual numbers in the distribution that are of interest but whether densities are decreasing from year to year, what the long term distributions are and how different movement scenarios affect distributions. Because of this, carrying capacity has not been considered (see section 5.6).

Sub-adult dispersal: Kiwis are sub-adults for four months from the age of 10 months to 13 months inclusive. They thus make four jumps. Five possible movement scenarios have been considered. These are summarised in section 5.3.

	Treatment	Control
Juveniles 0-9 months	$1-(1-0.5)^{\frac{1}{9}}=0.0741$ (50% over 9 months)	$1-(1-0.95)^{\frac{1}{9}}=0.2831$ (95% over 9 months)
Sub-adults 10-13 months	$1-(1-0.1)^{\frac{1}{4}}=0.0260$ (10% over 4 months)	$1-(1-0.1)^{\frac{1}{4}}=0.0260$ (10% over 4 months)
Adults 14 months - 40 years	$1-(1-0.082)^{\frac{1}{12}}=0.0071$ (8.2% per annum)	$1-(1-0.082)^{\frac{1}{12}}=0.0071$ (8.2% per annum)

Table 5.1: Monthly deaths rates.

5.3 Results

Five different sub-adult movement scenarios are investigated. Simulations were run and a resulting minimum treatment block area and critical recruitment rate were found. The movement scenarios and results are as follows:

5.3.1 Movement scenario 1: Directional movement

This scenario reflects sub-adult dispersal outward from the nest site as seen in the field. Sub-adults make four moves (one jump per month). Each jump has a distance uniformly distributed between 0 and 1.5 km per month. The direction of movement at each jump is an angle uniformly distributed between $\theta_0 \pm \frac{\pi}{8}$, where θ_0 is set at the beginning of the four jumps. This means that movement is directional. The overall distance travelled is 2.95 km (2dp) on average.

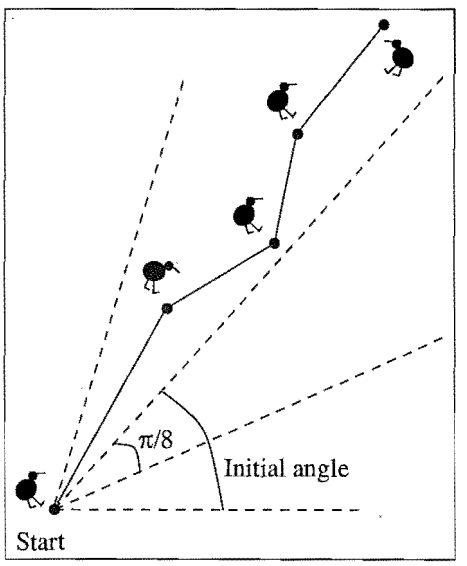

Figure 5.8: Movement scenario 1.

50 simulations were run over a time horizon of 50 years. The smallest treatment block area to give a probability of quasi-extinction less than or equal to 1% was 6.2 km × 6.2 km (3844 ha). The corresponding critical recruitment rate was 0.22 (2dp) that is, 22% of chicks are required to reach adulthood for survival of the species.

5.3.2 Movement scenario 2: First month directional

This scenario reflects outward dispersal to a lesser extent than that described in movement scenario 1. Sub-adults make four moves (one jump per month). The first jump is directional of length 1.5 km but the remaining three jumps are at a random angle, uniformly distributed between 0 and 2π, with the length being uniformly distributed between 0 and 1.5 km. The overall distance travelled is 1.9 km (1dp) on average.

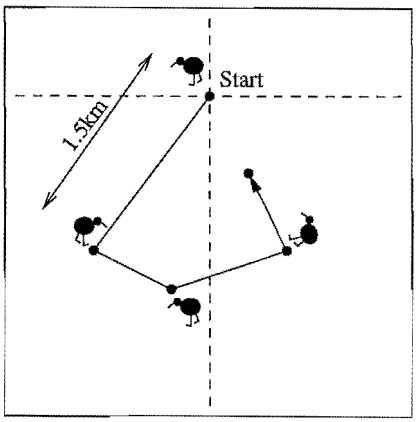

Figure 5.9: Movement scenario 2.

50 simulations were run over a time horizon of 50 years. The smallest treatment block area to give a probability of quasi-extinction less than or equal to 1% was 4.2 km $\times$ 4.2 km (1764 ha). The corresponding critical recruitment rate was 0.20 (2dp), that is, 20% of chicks are required to reach adulthood for survival of the species.

5.3.3 Movement scenario 3: Sub-adults settle after one month

Sub-adults only move in the first month and then settle. This reflects birds who are able to find new territories easily. There is one jump of length 1.5 km with an angle uniformly distributed between 0 and 2π.

50 simulations were run over a time horizon of 50 years. The smallest treatment block area to give a probability of quasi-extinction less than or equal to 1% was 3.5 km $\times$ 3.5 km (1225 ha). The corresponding critical recruitment rate was 0.21, that is, 21% of chicks are required to reach adulthood for survival of the species.

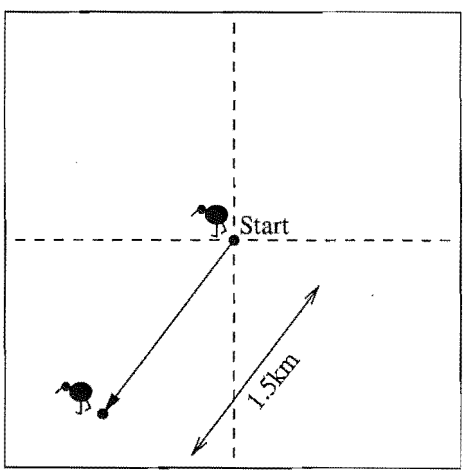

Figure 5.10: Movement scenario 3.

5.3.4 Movement scenario 4: Monthly random movement, distance 1.5 km

This movement scenario assumes sub-adults make one jump per month. Each monthly jump is of length 1.5 km and the angle is randomly chosen (from a uniform distribution) between 0 and 2π. This scenario reflects the possibility of random movement as opposed to outward movement. The overall distance travelled is 2.7 km (1dp) on average.

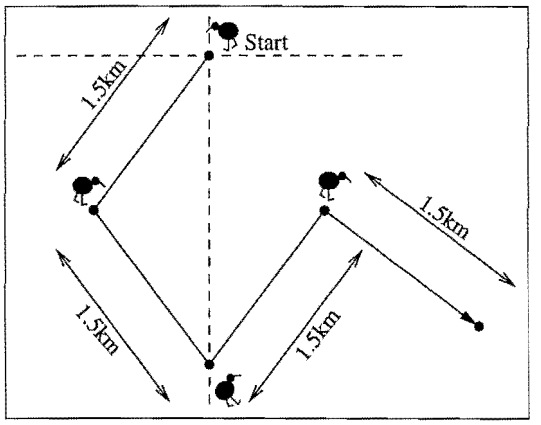

Figure 5.11: Movement scenario 4.

50 simulations were run over a time horizon of 50 years. The smallest treatment block area to give a probability of quasi-extinction less than or equal to 1% was 5.7 km $\times$ 5.7 km (3249 ha). The corresponding critical recruitment rate was 0.21, that is, 21% of chicks are required to reach adulthood for survival of the species.

5.3.5 Movement scenario 5: Monthly random movement, distance uniformly distributed

This movement scenario is equivalent to movement scenario 4 except the jump length is uniformly distributed between 0 and 1.5 km. The overall distance travelled is 1.52 km (2dp) on average.

50 simulations were run over a time horizon of 50 years. The smallest treatment block area to give a probability of quasi-extinction less than or equal to 1% was 3.5 km $\times$ 3.5 km (1225 ha). The corresponding critical recruitment rate was 0.20, that is, 20% of chicks are required to reach adulthood for survival of the species.

5.3.6 Sensitivity analysis of parameters

The results from the previous section are summarised in Table 5.2.

Movement scenario	CRR	CTBS	ADT
1	0.2195	6.2 km × 6.2 km (3844 ha)	2.9516 km
2	0.2018	4.2 km × 4.2 km (1764 ha)	1.9357 km
3	0.2060	3.5 km × 3.5 km (1225 ha)	1.5 km
4	0.2129	5.7 km × 5.7 km (3249 ha)	2.7178 km
5	0.1960	3.5 km × 3.5 km (1225 ha)	1.5239 km

Table 5.2: Critical treatment block sizes (CTBS), critical recruitment rates (CRR) and average distances travelled over four jumps (ADT) for different sub-adult dispersal scenarios.

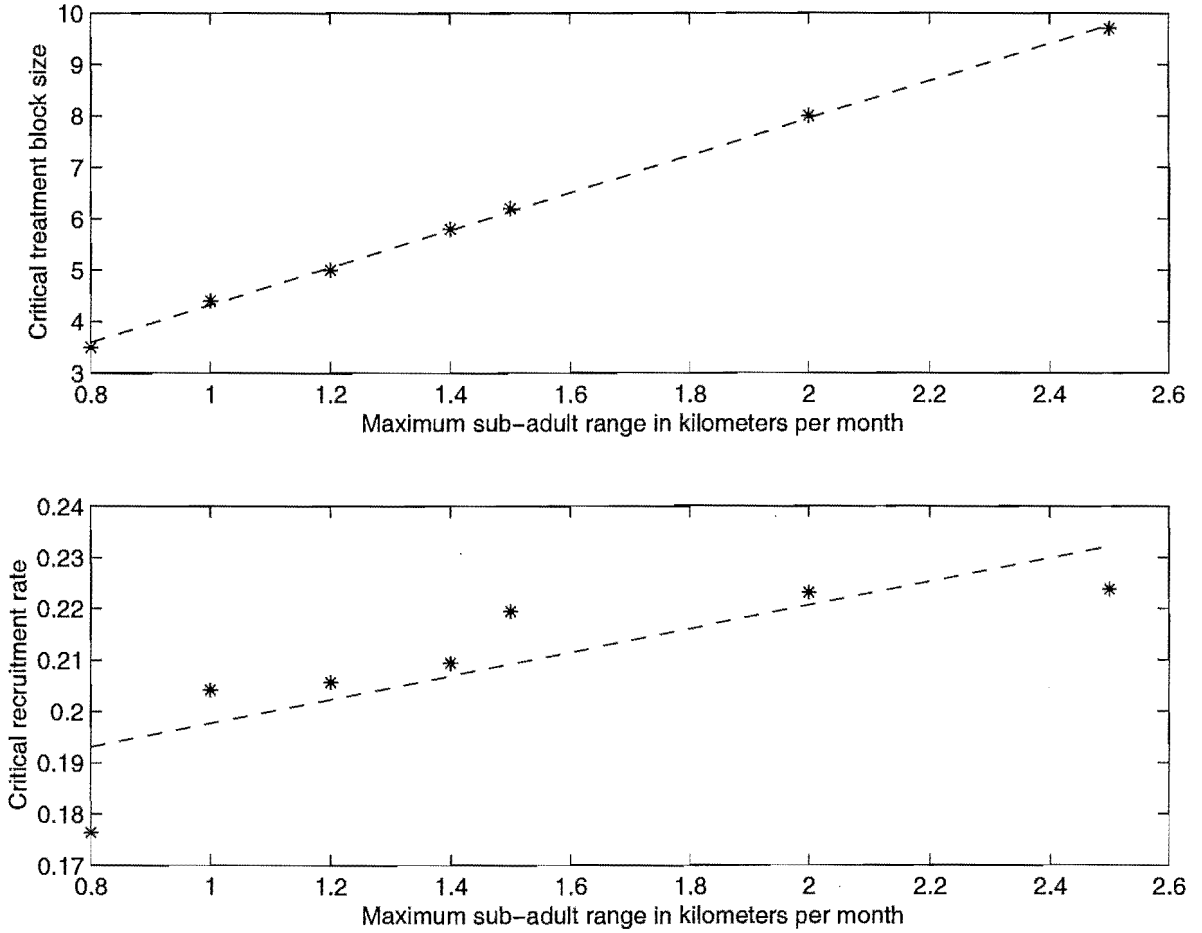

Figure 5.12: Sensitivity analysis of the maximum sub-adult range (km). The dotted line in each graph is the linear least squares fit.

Movement scenario 1 was taken and separately both the maximum length of the jump distance and the annual productivity rate for females were perturbed. The plot of critical treatment block size versus maximum jump length shows that the analysis is not mathemat-

ically sensitive to small changes in the maximum jump length. Practically this may not be the case. Changing a treatment block length from 4 to 5 km for example, may substantially increase costs of managing such an area. Figure 5.12 shows a linear relationship between the maximum sub-adult range and the critical treatment block length (and the critical recruitment rate). Note that a maximum distance of 3 km per month means that the critical treatment area is bigger that the whole block.

The plot of critical treatment block size versus the productivity rate shows that the analysis is not mathematically sensitive to small changes in the productivity rate. Once again the biological interpretation may be different but this needs further analysis of productivity rates and their variability. Figure 5.13 shows a quadratic relationship between the productivity rate and the critical treatment block length (and the critical recruitment rate). Note that as the productivity rate becomes smaller the critical treatment area is bigger than the whole block.

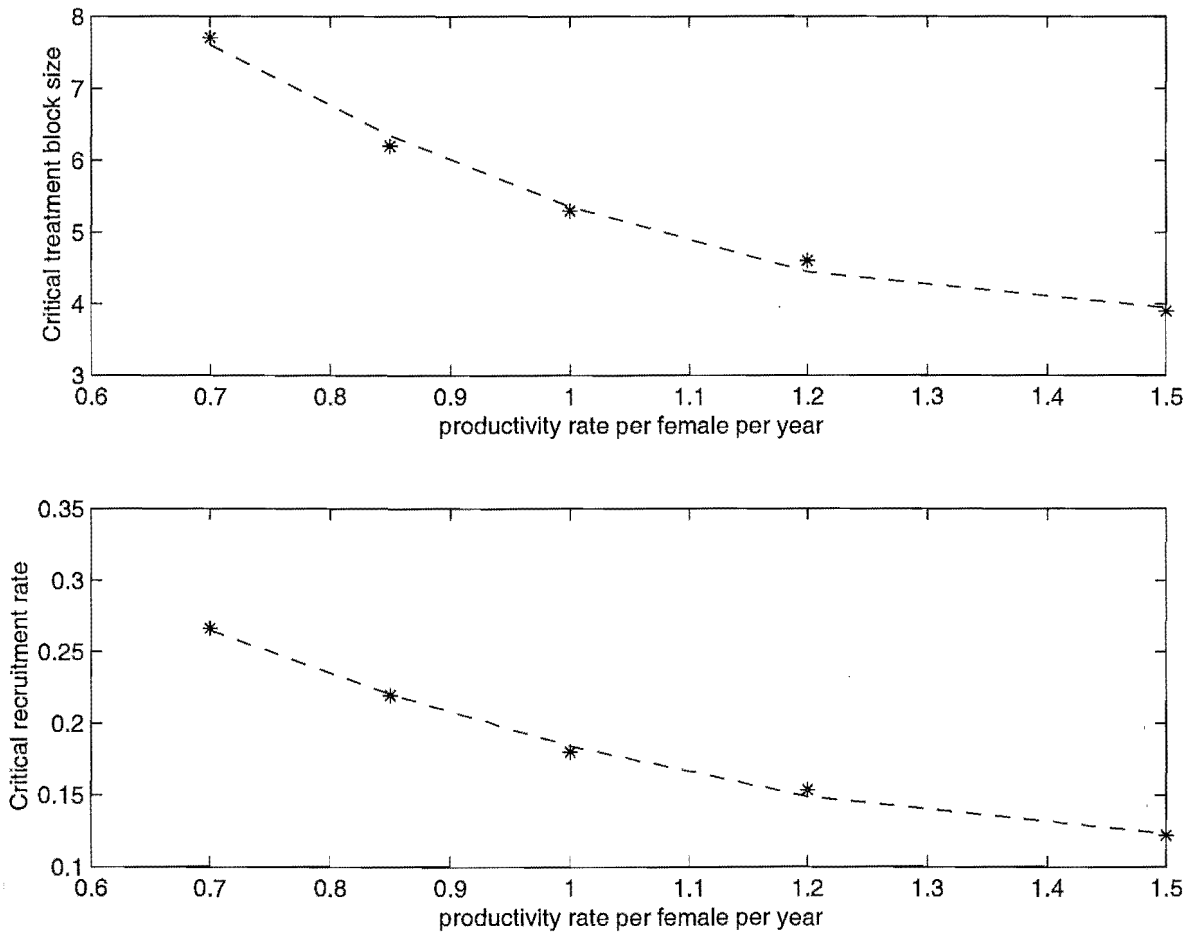

Figure 5.13: Sensitivity analysis of the productivity rate per female per year. The dotted line in each graph is the quadratic least squares fit.

5.4 Simulation conclusions

The results of the simulation indicate that the outward dispersal by sub-adult kiwi increases the required critical/minimum treatment area.

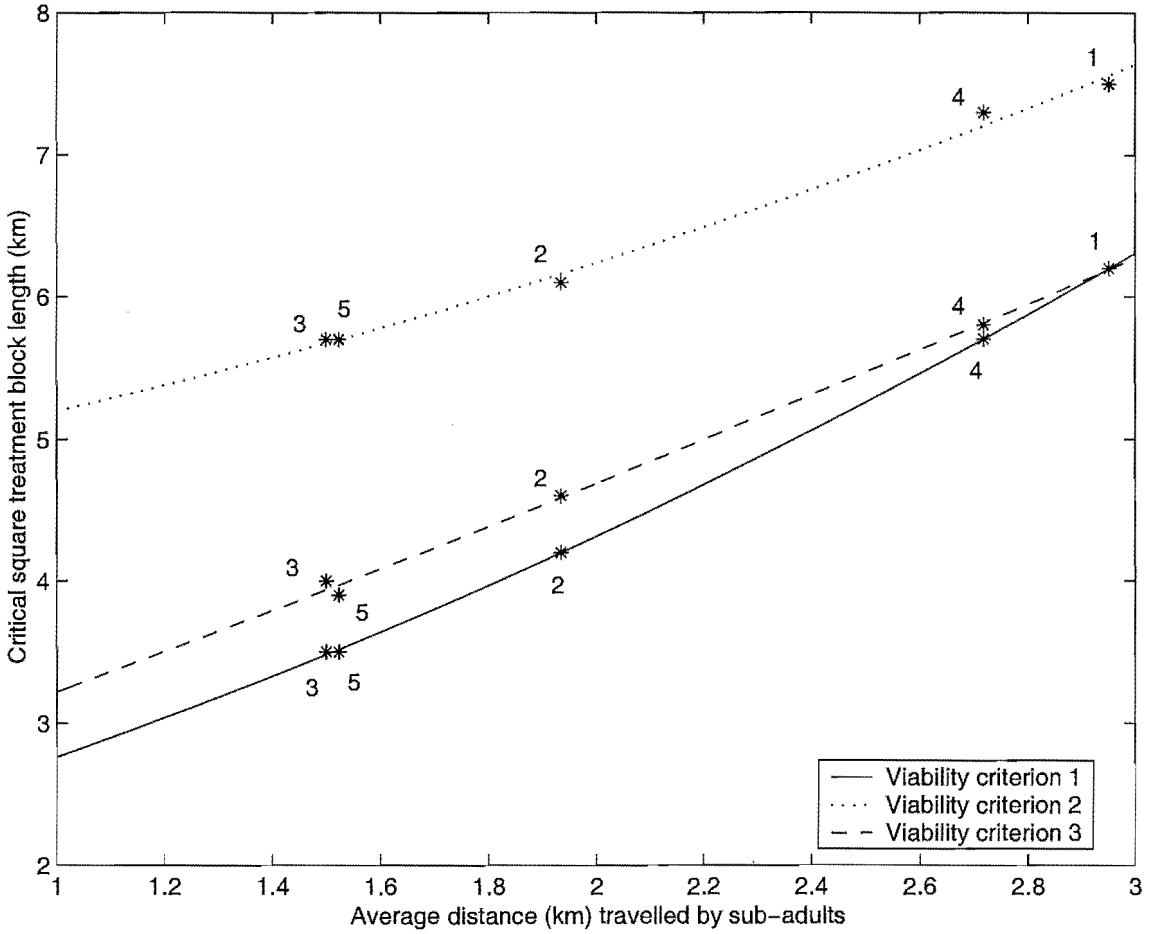

Figure 5.14: Critical square treatment block length (km) versus average distance travelled by sub-adults (km) over four months for viability criterion 1 (whole block viable over last 10 years), viability criterion 2 (control viable over 50 years) and viability criterion 3 (control viable over last 20 years). Numbers indicate the movement scenarios.

Movement scenarios 3 (birds settle after one month) and 5 (monthly random movement with the distance travelled per month uniformly distributed between 0 and 1.5 km) resulted in a smaller minimum treatment block area compared to movement scenarios 1 (directional movement), 2 (first month directional, remaining jumps random) and 4 (random movement with the jump distance exactly 1.5 km per month). Movement scenario 1, which corresponded to the greatest outward dispersal of sub-adults, resulted in the largest required minimum treatment area. It is evident that if sub-adults can be persuaded to settle in the

treatment area then in turn, their chicks will have a better survival chance thus increasing the recruitment of the whole block. Management options to achieve this could include choosing a treatment area that makes use of existing natural boundaries such as lakes and bluffs for example ([6]) or even fencing an area or exit route in order to inhibit sub-adult dispersal. Figure 5.14 indicates that there is a quadratic relationship between the critical treatment block area and the average distance travelled by sub-adults over the four jumps.

Most 'predator free' reserves on the New Zealand mainland are less than 2000 ha in area. The simulation indicates that these reserves are too small to support viable populations of kiwi if dispersal cannot be prevented.

The simulation results were not mathematically sensitive to the productivity rate b or the jump distance of sub-adults. Note however that this may not be the case biologically since a small change in the calculation of the productivity rate, for example, means an increase in critical treatment block size that may be significantly more difficult to implement in practise. Since the cost of setting up a treatment block has not been considered here, such effects are difficult to quantify.

5.5 Matrix approach

Rather than using simulations to find a minimum treatment area, it is possible to use a matrix approach. The spatial nature of the model, however, gives rise to reasonable complexity, so although this line of solution was considered it was not completely followed through and simulation was considered the better approach at least in the first instance. In chapter 7 continuous diffusion equations are employed in order to model spatial dynamics. In this section an outline of the matrix (discrete spatial dynamics) approach is given.

Let the hatchling to sub-adult and sub-adult to adult recruitment rates in the treatment, control and the outer region be defined as in Table 5.3.

Area	hatchling to sub-adult	sub-adult to adult	hatchling to adult
Treatment	$(r_1)_T$	$(r_2)_T$	$(r_1r_2)_T$
Control	$(r_1)_C$	$(r_2)_C$	$(r_1r_2)_C$
Outer Region	$(r_1)_C$	$(r_2)_C$	$(r_1r_2)_C$

Table 5.3: Recruitment rates in the treatment and control blocks and the outer region.

Let b be the annual per capita productivity rate of adult females and assume that half of the adult population are female. Let f be the annual death rate of adults. Each block can be analysed separately and allowances can be made for dispersal of sub-adults between appropriate blocks. The notation that JT, SAT and AT are the juveniles, sub-adults and adults in the treatment respectively is used. Similarly JC, SAC and AC are juveniles, sub-adults and adults in the control block and JO, SAO and AO are the juveniles, sub-adults and adults in the outer region. Thus:

1. In the treatment block:

$$\begin{aligned} \mathrm{JT}_{t+1} &= \frac{b}{2}\mathrm{AT}_t \\ \mathrm{SAT}_{t+1} &= (r_1)_T\mathrm{JT}_t - p_1\mathrm{SAT}_t + p_2\mathrm{SAC}_t - p_3\mathrm{SAT}_t + p_4\mathrm{SAO}_t \\ \mathrm{AT}_{t+1} &= (r_2)_T\mathrm{SAT}_{t+1} + (1-f)\mathrm{AT}_t, \end{aligned}$$

   where

   - p_1 is the probability that a sub-adult in the treatment block will disperse to the control block.
   - p_2 is the probability that a sub-adult in the control block will disperse to the treatment block.
   - p_3 is the probability that a sub-adult in the treatment block will disperse to the outer region.
   - p_4 is the probability that a sub-adult in the outer region will disperse to the treatment block.

2. In the control block:

$$\begin{aligned} \mathrm{JC}_{t+1} &= \frac{b}{2}\mathrm{AC}_t \\ \mathrm{SAC}_{t+1} &= (r_1)_C\mathrm{JC}_t + p_1\mathrm{SAT}_t - p_2\mathrm{SAC}_t - p_5\mathrm{SAC}_t + p_6\mathrm{SAO}_t \\ \mathrm{AC}_{t+1} &= (r_2)_C\mathrm{SAC}_{t+1} + (1-f)\mathrm{AC}_t, \end{aligned}$$

   where

   - p_5 is the probability that a sub-adult in the control block will disperse to the outer region.

- p_6 is the probability that a sub-adult in the outer region will disperse to the control block.

3. In the outer region:

$$\begin{aligned} \mathrm{JO}_{t+1} &= \frac{b}{2}\mathrm{AO}_t \\ \mathrm{SO}_{t+1} &= (r_1)_C\mathrm{JO}_t + p_3\mathrm{SAT}_t - p_4\mathrm{SAO}_t + p_5\mathrm{SAC}_t - p_6\mathrm{SAO}_t \\ \mathrm{AO}_{t+1} &= (r_2)_C\mathrm{SAO}_{t+1} + (1-f)\mathrm{AO}_t. \end{aligned}$$

$$\text{If } X_{t+1} = \begin{bmatrix} \mathrm{JT} \\ \mathrm{SAT} \\ \mathrm{AT} \\ \mathrm{JC} \\ \mathrm{SAC} \\ \mathrm{AC} \\ \mathrm{JO} \\ \mathrm{SAO} \\ \mathrm{AO} \end{bmatrix}_{t+1} \quad \text{and } A =$$

$$\left[\begin{array}{ccc|ccc|ccc} 0 & 0 & \frac{b}{2} & 0 & 0 & 0 & 0 & 0 & 0 \\ (r_1)_T & -p_1-p_3 & 0 & 0 & p_2 & 0 & 0 & p_4 & 0 \\ 0 & r_{2T} & 1-f & 0 & 0 & 0 & 0 & 0 & 0 \\ \hline 0 & 0 & 0 & 0 & 0 & \frac{b}{2} & 0 & 0 & 0 \\ 0 & p_1 & 0 & (r_1)_C & -p_2-p_5 & 0 & 0 & p_6 & 0 \\ 0 & 0 & 0 & 0 & r_{2C} & 1-f & 0 & 0 & 0 \\ \hline 0 & 0 & 0 & 0 & 0 & 0 & 0 & 0 & \frac{b}{2} \\ 0 & p_3 & 0 & 0 & p_5 & 0 & (r_1)_C & -p_4-p_6 & 0 \\ 0 & 0 & 0 & 0 & 0 & 0 & 0 & r_{2C} & 1-f \end{array}\right]$$

then $X_{t+1} = AX_t$ which can be written as $X_{t+1} = A^tX_0$ where X_0 is the initial age distribution of the population. Assuming all parameters are constant, the Perron-Frobenius

theorem ([18]) says that X_t will eventually converge to a vector proportional to the eigenvector, w, of A (chosen so that $\sum w_i = 1$) that is associated with λ, the largest positive real eigenvalue of A. The proportion in each age class is irrespective of the (non-zero) initial distribution X_0. Asymptotically, (i.e. as $t \to \infty$),

$$\begin{aligned} \lambda < 1 &\Rightarrow X_t \to 0 \quad \text{(a stable solution)}, \\ \lambda > 1 &\Rightarrow X_t \to \infty \quad \text{(an unstable solution)}, \\ \lambda = 1 &\Rightarrow X_t \quad \text{(a stable solution)}. \end{aligned}$$

Calculating λ depends on the calculation of the probabilities of sub-adults moving between blocks. These probabilities will depend on the initial position of the sub-adult before it takes a step, the movement strategy (which depends on the direction and the length of the step) and the sizes of the treatment and control blocks in relation to each other and the outer region. For example, suppose the starting position of an individual is $(r_0 \cos\theta_0, r_0 \sin\theta_0)$ and the individual makes four moves where each move has a distance, r, uniformly distributed between $r_{\min}$ and $r_{\max}$ and an angle, θ, uniformly distributed between $\theta_{\min}$ and $\theta_{\max}$. The final destination is then $\sum_{i=0}^{4}(r_i \cos\theta_i, r_i \sin\theta_i)$. The probability density function for each step, i, is the probability density function of the two dimensional uniform distribution given by

$$f_i(r,\theta) = \frac{1}{(r_{i\max} - r_{i\min})(\theta_{i\max} - \theta_{i\min})}$$

where $r_{i\min} \leq r \leq r_{i\max}$ and $\theta_{i\min} \leq \theta \leq \theta_{i\max}$. In Cartesian co-ordinates $f_i(x,y) = \frac{1}{r} f(r,\theta)$ where $r^2 = x^2 + y^2$ and $\tan(\theta) = \frac{y}{x}$. The probability that the final destination of a sub-adult is outside a rectangular region $A = \{(x,y) : a \leq x \leq b, c \leq y \leq d\}$ is calculated as

$$1 - \int_a^b \int_c^d ((f_1 * f_2) * f_3) * f_4 \quad dydx \tag{5.2}$$

where $((f_1 * f_2) * f_3) * f_4$ is the convolution of the functions $f_i(x,y)$ ([93]). Recall that the convolution of two functions $h(x,y)$ and $g(x,y)$ is

$$h * g = \int\int_{\mathrm{R}^2} h(x-u, y-v) g(u,v) du dv.$$

The integral in expression (5.2) would have to be calculated numerically and does not take into account the way that individuals react to the boundaries of the outer regions. For this reason, the approach outlined in this section was not investigated further.

5.6 Limitations of the model and future work

In a study on gray wolf ([33]), it has been suggested that PVA has created unnecessary dilemmas by overstating the minimum population size required for persistence. With the model discussed in this chapter, population sizes have not been the focus but there is always the possibility that the minimum treatment areas calculated by the simulation are over or under conservative. Overstating a minimum area could be economically costly while understating will lead to population failure. From a conservation perspective, errors of overstatement are of little importance. The additional cost of maintaining a reserve that is larger than required is small compared to the economic and biological cost of maintaining a reserve that fails to achieve its purpose.

Different viability criteria can give different results. In criterion 1, the adult population in the whole block could be viable, despite there being almost no birds in the control block. This was possible because densities in the treatment area were not capped, so could eventually exceed the total number of birds present in the whole block at the beginning of a simulation. A more conservative approach is viability criterion 2 where the adult density in the control block in the final year is compared to that in the first year (Table 5.4 and Figure 5.14). Because the first year is involved in the comparison, the initial age distribution has an affect on the results rendering them more conservative than viability criteria 1 and 3. The latter criterion compares the adult density in the control over the last 20 years (see Table 5.5 and Figure 5.14). An alternative and perhaps better initial age distribution is the negative exponential with the average life expectancy at $\frac{1}{0.082} = 12.2$ (1dp) years. This initial distribution was used for movement scenario 1 and both of viability criteria 2 and 3. It showed less conservative estimates of the critical treatment block area for viability criterion 2 (7.2 km $\times$ 7.2 km compared to 7.5 km $\times$ 7.5 km) and the same estimates for viability criterion 3.

The minimum self sustainable treatment block was calculated for movement scenarios 1 and 3 (chosen as the two extremes of average sub-adult distance) and the results are shown in Table 5.6 for viability criteria 2 and 3 applied to the treatment block alone. Once again criterion 2 is more conservative than criterion 3.

There is plenty of room for the modification and expansion of the model. Many factors have not been considered but could be easily included. Examples include inbreeding depression, catastrophes that may decrease a population significantly in a short period of

Scenario	CRR	CTBS	ADT
1	0.2418	7.5 km × 7.5 km (5625 ha)	2.95 km (2dp)
(initial exp. age dist.)	0.2319	7.2 km × 7.2 km (5184 ha)	
2	0.2466	6.1 km × 6.1 km (3721 ha)	1.9 km (1dp)
3	0.2400	5.7 km × 5.7 km (3249 ha)	1.5 km
4	0.244	7.3 km × 7.3 km (5329 ha)	2.7 km (1dp)
5	0.2484	5.7 km × 5.7 km (3249 ha)	1.5 km (1dp)

Table 5.4: Viability criterion 2 (viable control comparing final and first years): Critical treatment block sizes (CTBS), critical recruitment rates in the control (CRR) and average distances travelled over four jumps (ADT) for different sub-adult dispersal scenarios.

Scenario	CRR	CTBS	ADT
1	0.2036	6.2 km × 6.2 km (3844 ha)	2.95 km (2dp)
(initial exp. age dist.)	0.2014	6.2 km × 6.2 km (3844 ha)	
2	0.1924	4.6 km × 4.6 km (2116 ha)	1.9 km (1dp)
3	0.1922	4.0 km × 4.0 km (1600 ha)	1.5 km
4	0.1987	5.8 km × 5.8 km (3364 ha)	2.7 km (1dp)
5	0.1810	3.9 km × 3.9 km (1521 ha)	1.5 km (1dp)

Table 5.5: Viability criterion 3 (viable control comparing last 20 years) Critical treatment block sizes (CTBS), critical recruitment rates in the control (CRR) and average distances travelled over four jumps (ADT) for different sub-adult dispersal scenarios.

Scenario	CRR	CTBS	ADT
1 (viability criterion 2)	0.2375	6.3 km × 6.3 km (3969 ha)	2.95 km (2dp)
3 (viability criterion 2)	0.2528	3.4 km × 3.4 km (1225 ha)	1.5 km
1 (viability criterion 3)	0.2230	5.9 km × 5.9 km (3481 ha)	2.95 km (2dp)
3 (viability criterion 3)	0.2383	3.2 km × 3.2 km (1024 ha)	1.5 km

Table 5.6: Sustainable treatment block sizes for movement scenarios 1 and 3 and viability criteria 2 and 3 applied to the treatment block.

time and territorial behaviour of birds. Carrying capacity has not been considered because starting densities were higher than in the field and even then saturation estimates of around 50 birds per km^2 in the treatment were not reached until around year 50 in most cases. Two ways capacity could be built into the model are to either kill off surplus new adults or else relocate them into the control. With discrete numbers of birds, rounding errors are a problem and must be taken into account as population numbers diminish. Different treatment block landscape patterns, locations and shapes could be considered and there might be more than one treatment block in an attempt to answer the question as to whether fewer larger reserves are better than many small reserves ([4], [12]), although many small reserves may not necessarily be economically viable ([74]).

The simulation number was set at 50 for the convenience of having a faster computer run time and because similar results were produced at 100 simulations. Ideally more simulations are desirable for obtaining a better estimate of the probability of extinction for a particular treatment block size but here a trade off seemed necessary. A program written in a faster language for example C as opposed to MATLAB would enable 1000 simulations over 1000 years, and small treatment block increments, to be computed without running out of memory or becoming slow. It would also be interesting to compare the results with other programs that simulate spatial dynamics of a population such as VORTEX ([46]), ALEX ([73]) and RAMAS-space ([1]).

The need to verify simulation results empirically is discussed by [26]. That is certainly a desired approach for all modelling and one that is not always easily fulfilled as shall be seen in chapter 7.

In this chapter, a discrete spatial and temporal model was developed in order to model sub-adult dispersal. In chapter 7 a continuous spatial and temporal model of the spread of a virus is investigated. But first, chapter 6 uses a modified version of the simulation program here to consider pulsed management for kiwi. A generalised discrete version of equation (2.14) is then used to simulate and compare different pulsed management strategies for another endangered bird, kokako, *Callaeas cinerea wilsoni.*

Chapter 6

Pulsed management

6.1 Pulsed management of kiwi

Pulsed management implies that a particular area undergoes extensive pest control at certain time intervals over a period of years or seasons. In this chapter, the simulation program from chapter 5 was modified to represent different possible pulsed management options for kiwi. The simulations of the model from chapter 5 suggest that, for the northern brown kiwi in mainland forests of New Zealand, pulsed management does not have a linear effect on critical treatment areas. That is, eradicating pests in a treatment block every second year (biennial pulsed management) does not double the size of the critical treatment area. In fact, with all the five movement scenarios, treating the whole block every 2 years wasn't enough for the survival of the cohort when there was no treatment every other year.

Another, possibly more economical, option is to maintain a smaller core area each year and once every n years treat the whole block. For movement scenario 1, and $n = 2$ (i.e. biennial management) the minimum core area size is 5.6 km $\times$ 5.6 km. Future work could include looking at different scenarios and different n values and the cost effectiveness of such schemes.

6.2 Comparison of pulsed management strategies for North Island kokako, *Callaeas cinerea wilsoni*

As another example of the wide applications of a generic model, the comparison of pulsed management strategies for the endangered North Island kokako bird, *Callaeas cinerea wilsoni*, were investigated. Fewer than 400 pairs of kokako currently exist in small, isolated populations in the North Island of New Zealand. The kokako recovery group aims to restore the national population to around 1000 pairs by the year 2020 ([39]). Kokako eggs and nestlings are particularly vulnerable to rats and possums therefore management affects this stage of the life cycle. The mathematical model derived here represents adult females in an area of isolated native forest surrounded by a sea of pasture so there are no possibilities of dispersal from the block. This is the case with the 1400ha Mapara Wildlife Reserve where some of the data used to estimate model parameters comes from ([62]). There is no dispersal in the model because, although the birds fly, they do not fly far. The whole block is treated in management years, thus, birds always re-settle in the managed area.

6.2.1 Model set up and error analysis of the adult female kokako productivity

The number of female adult kokako at the end of season/year $t+1$ is equal to the number of female adults at the beginning of that year minus those that died during the year plus half of all 1 year old recruits plus all 2 year old recruits. The equation representing this is a further generalised and discretised version of equation (2.14):

$$a_f(t+1) = a_f(t) - d_f a_f(t) + r_1 \frac{b(t)}{4} a_f(t) + r_2 \frac{b(t-1)}{2} a_f(t-1). \tag{6.1}$$

Parameters switch depending on whether t is a managed year of an unmanaged year. They are described in Table 6.1. All values used in the model are derived from field data ([40],[38] and pers. comm. John Innes, Landcare Research and Ian Flux, Department of Conservation). It is assumed that the number of adult females at time 0, $a_f(0)$, is 20 and that the number of adult females one year previous is $a_f(-1) = 20$. In any year, the number of new recruits is given by the expression $r_1 \frac{b(t)}{4} a_f(t) + r_2 \frac{b(t-1)}{2} a_f(t-1)$, thus, in any one season, there are $r_1 \frac{b(t)}{4} a_f(t)$ recruits aged 1 year old and $r_2 \frac{b(t-1)}{2} a_f(t-1)$ aged 2 years. Note that the number of 1 year old recruits in any one year is not necessarily equal to the number of 2 year old recruits.

Parameter	Description	Managed	Unmanaged
b	annual productivity	1.93 (sd= 0.65,$n = 70$)	.19 (sd= 0.09, $n = 2$)
r_1	0-1 year recruitment	0.655	0.655
r_2	0-2 year recruitment	0.605	0.605
d_f	annual death rate	0.16	0.15

Table 6.1: Parameter values for female kokako

Six pulsed management strategies were considered. Strategy 1 is continuous management, strategy 2 is biennial management, strategy 3 is three years of pest control five years without. Strategy 4 is three years of pest control followed by ten years without, strategy 5 is one year of pest control followed by ten years without. Finally, strategy 6 is no pest control.

6.2.2 Results after 10 years

Figure 6.1 shows the time series of female adult kokako over 10 years predicted by the model. After ten years it appears that the strategies should be rated according to their

numerical value. Thus, strategy 1 (continuous management) is the best strategy, strategy 2 comes second etc. This may seem a logical ordering but it should be noted that at year 10 both strategies 2 and 3 (biennial and 3 on 5 off respectively) have accumulated 5 years of management in total, however biennial management results in a higher density. It therefore appears that the management strategy should be wisely chosen.

It was decided to vary one parameter and perform an error analysis. The productivity rate, b, was arbitrarily chosen. A 95% confidence interval for b, the annual productivity rate of adult females, is (1.78,2.09) in a managed year (mean 1.93, standard deviation 0.65, sample size 70) and (0,.39) in an unmanaged year (mean 0.19, standard deviation 0.09, sample size 2). The upper and lower limits of each confidence interval where put into the model (equation (6.1)) and corresponding upper and lower limits of the adult time series were calculated. These are depicted in Figures 6.2 to 6.4.

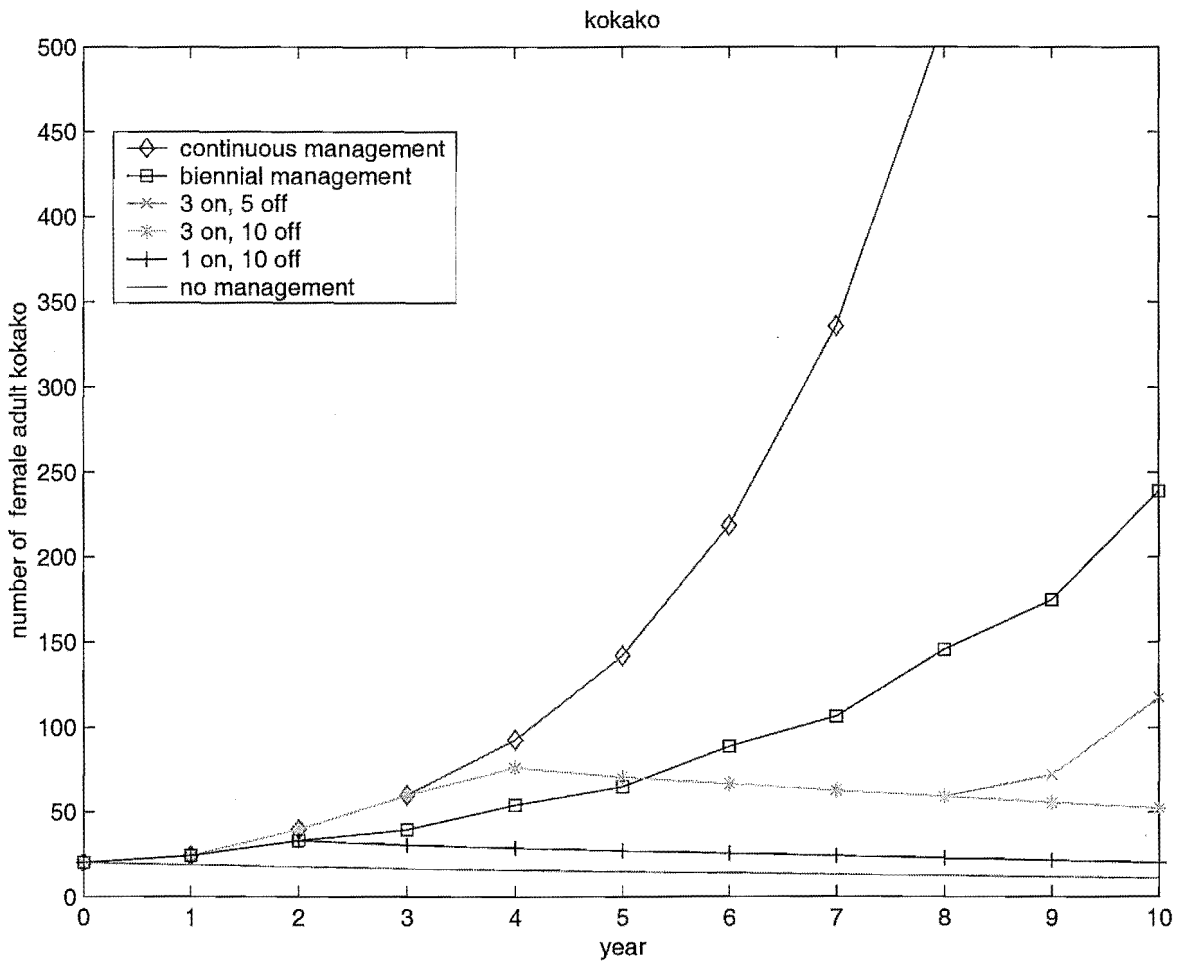

Figure 6.1: Number of adult female kokako over 10 years for different pulsed management strategies.

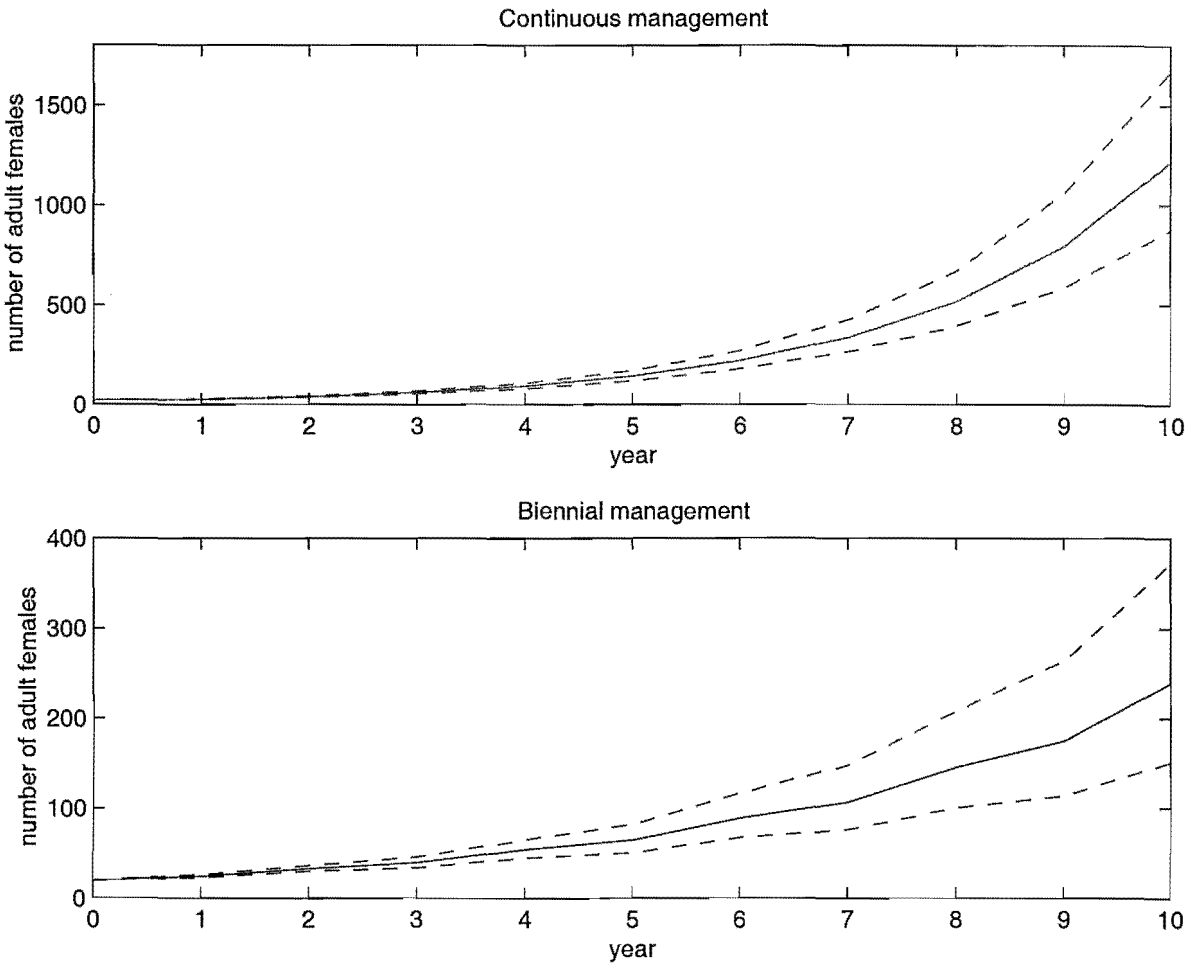

Figure 6.2: Continuous management (strategy 1) and biennial management (strategy 2) showing upper and lower limits (dashed lines) on the time series corresponding to upper and lower limits of 95% confidence intervals for b, the annual female productivity rate.

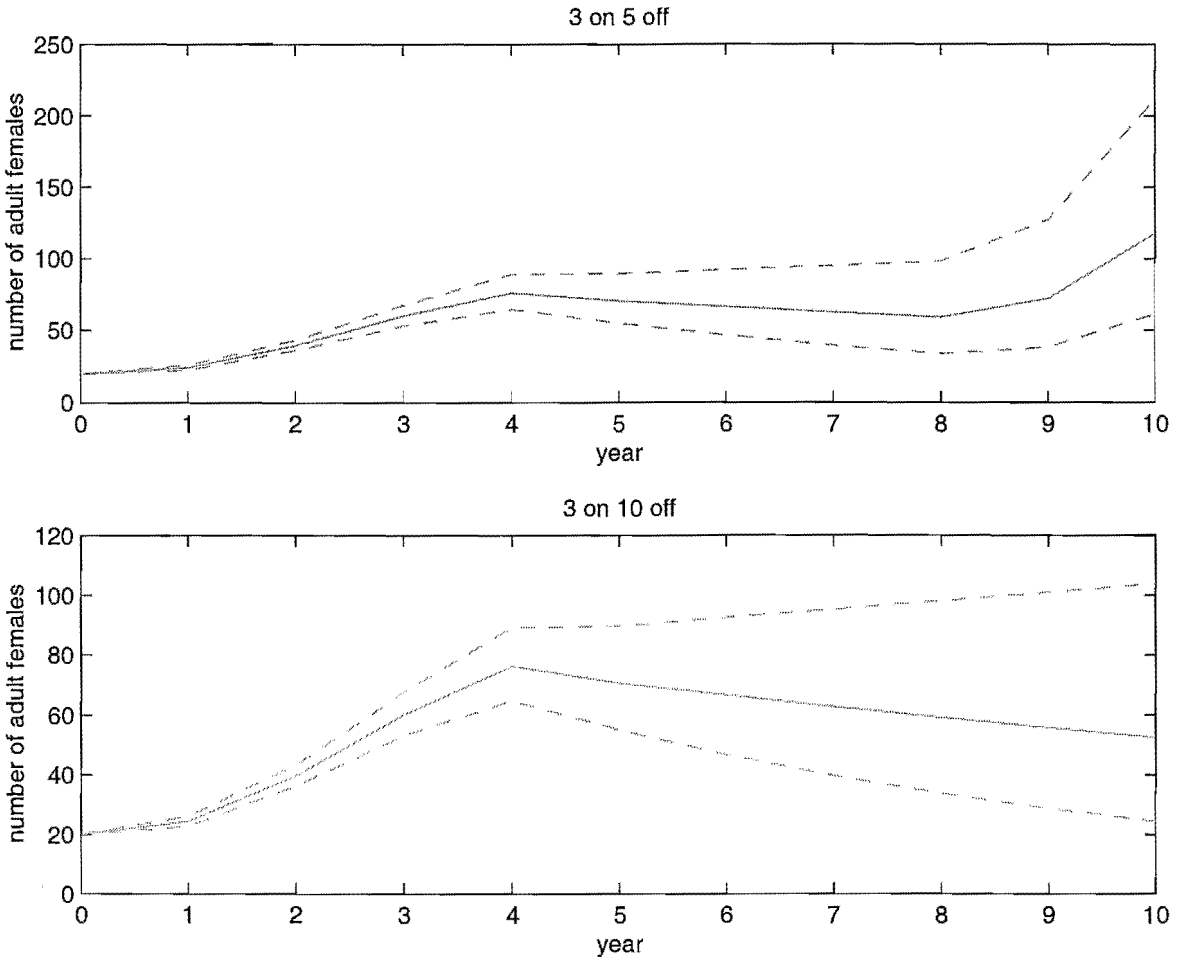

Figure 6.3: Three years on, 5 years off (strategy 3) and 3 years on, 10 years off (strategy 4) showing upper and lower limits (dashed lines) on the time series for adult female kokako corresponding to upper and lower limits of 95% confidence intervals for b, the annual female productivity rate.

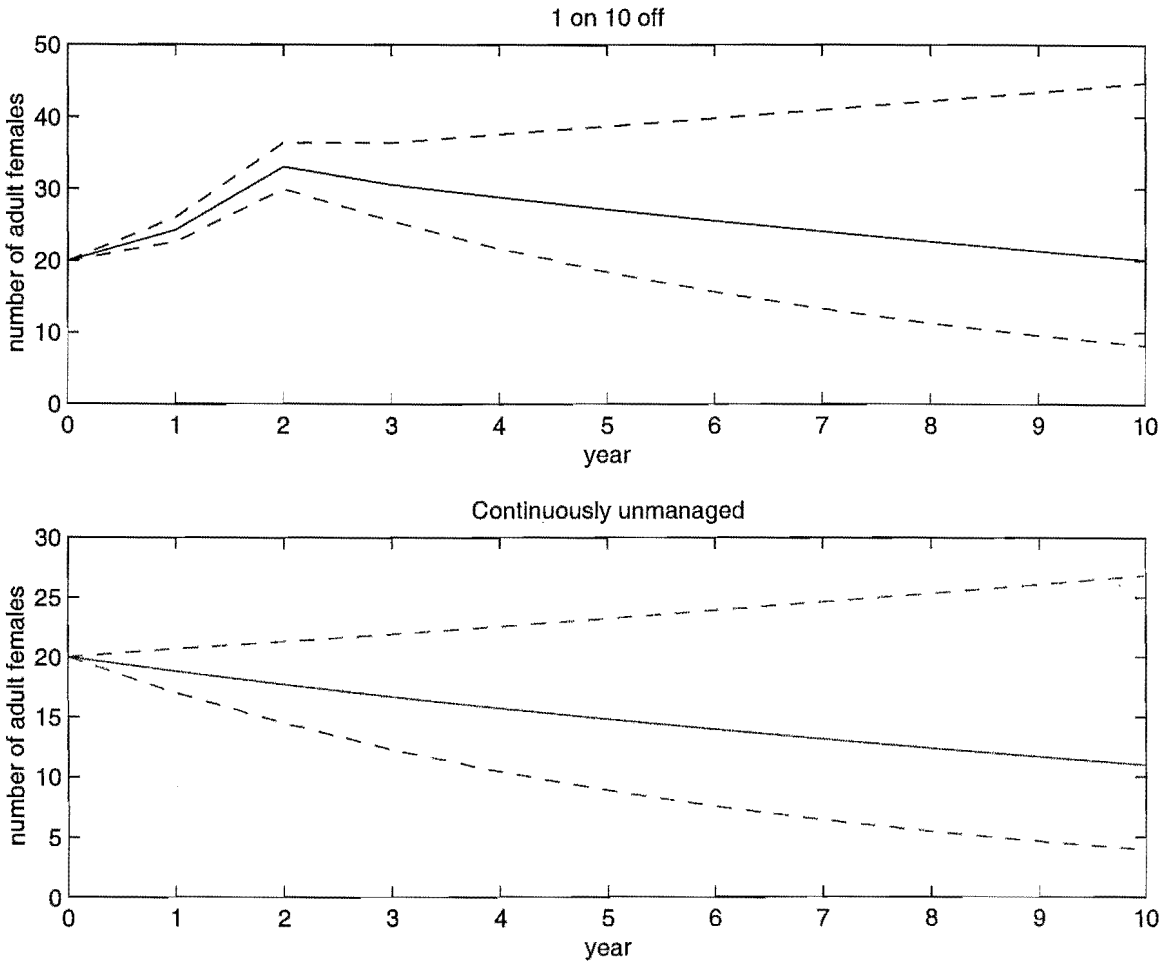

Figure 6.4: 1 year on, 10 years off (strategy 5) and continuously unmanaged (strategy 6) showing upper and lower limits (dashed lines) on the time series corresponding to upper and lower limits of 95% confidence intervals for b, the annual female productivity rate.

A snapshot is taken at time $t = 10$ for each of Figures 6.2 to 6.4. An interval corresponding to the range of values the number of female adults can take is plotted for each management strategy and is depicted in Figure 6.5. It is assumed that if one interval is higher than the other with no overlap, then this management strategy is the more successful management strategy. Table 6.2 gives actual values for the intervals plotted in Figure 6.5. The values are the upper and lower limits of the female adult population density at the end of the 10th year.

Strategy	Description	Lower	Upper
1	continuous management	872	1671
2	biennial management	150	372
3	3 years on 5 years off	61	212
4	3 years on 10 years off	24	104
5	1 year on 10 years off	8	45
6	continuously unmanaged	3	27

Table 6.2: Approximate upper and lower limits for time series of adult female kokako

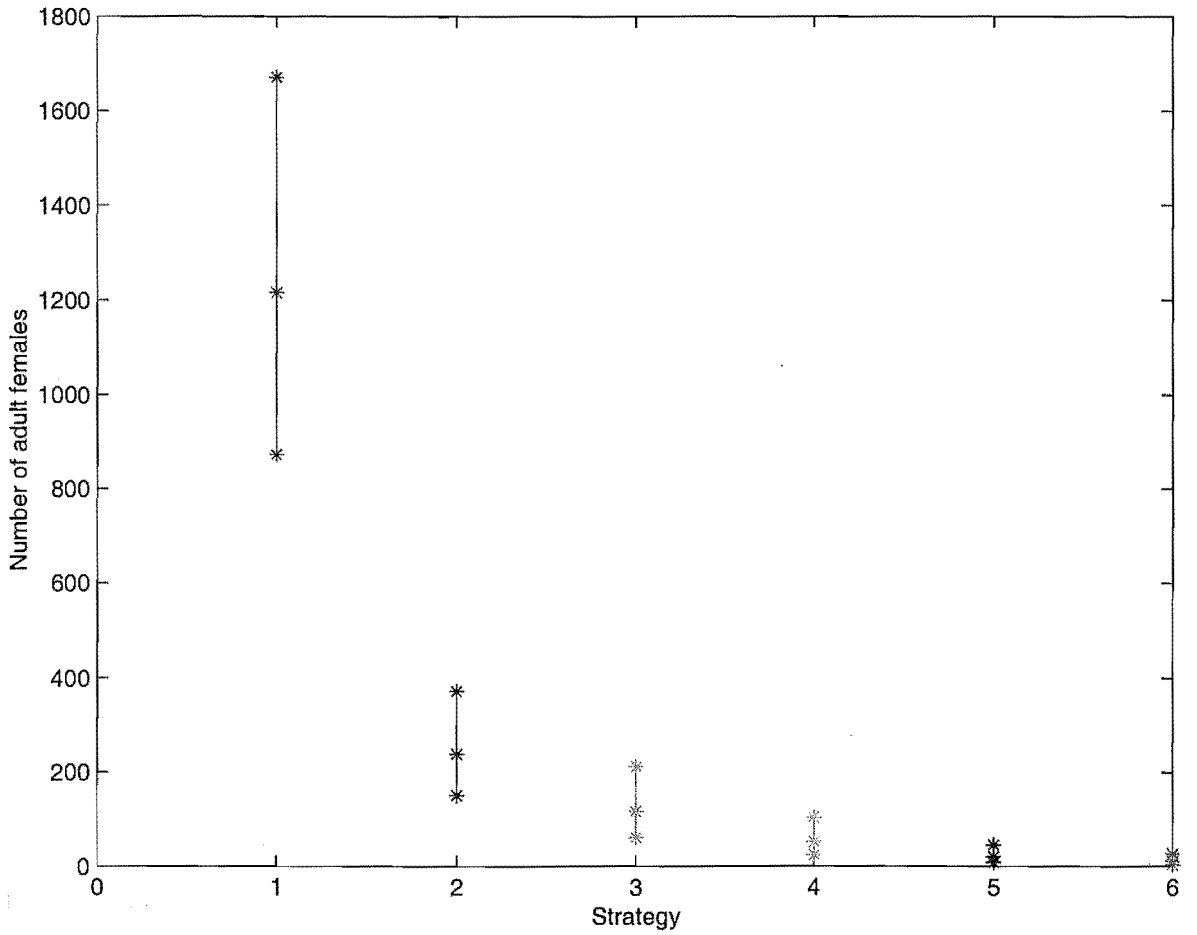

Figure 6.5: Snapshot at the end of the 10th year for the adult female kokako time series. Upper and lower limits of each interval result from upper and lower limits of a 95% confidence interval for b, the female annual productivity rate.

6.2.3 Conclusions

1. Continuous management (strategy 1) results in a higher adult female population density at the end of the 10th year compared to all the other pulsed management strategies (Figure 6.5).

2. Biennial management (strategy 2) does not necessarily result in a higher population density at the end of the 10th year compared to 3 years on 5 years off pulsed management (strategy 3), but it appears to be a more successful management strategy than 3 on 10 off (strategy 4), 1 on 10 off (strategy 5) and continuously unmanaged (strategy 6) (Figure 6.6).

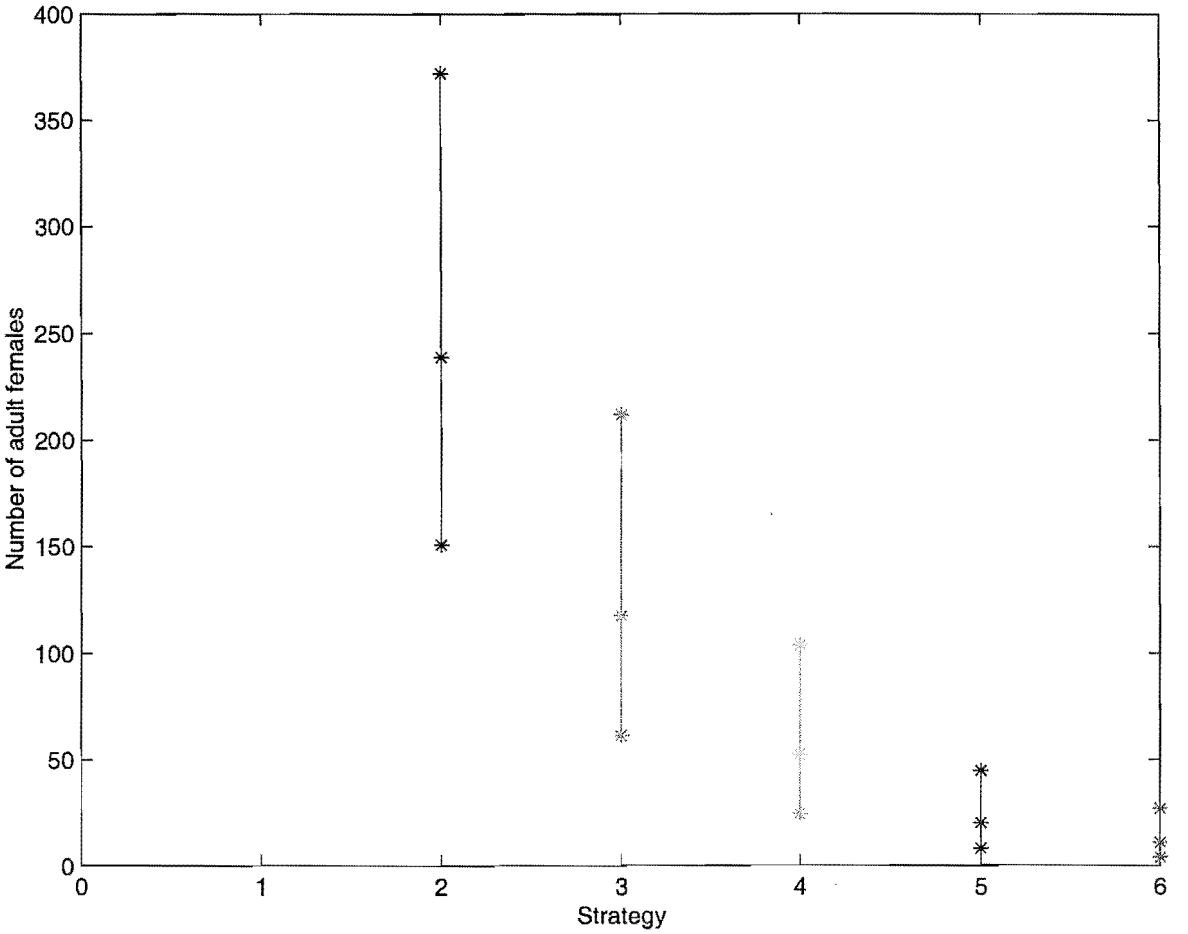

Figure 6.6: Enlargement of Figure 6.5.

3. 3 years on 5 years off pulsed management (strategy 3) results in a higher adult female population density at the end of the 10th year compared to both 1 year on 10 years off (strategy 5) and continuously unmanaged (strategy 6), but it is not necessarily more successful than 3 on 10 off (strategy 4) (Figure 6.6).

4. There is not necessarily any difference between the three strategies 3 on 10 off, 1 on 10 off and continuously unmanaged (strategies 4,5 and 6 respectively).

6.2.4 Results after 20 and 50 years

Time series and snapshots of the female adult density at year 20 and 50 are depicted in Figures 6.7 to 6.10. The range of possible values for adult female density gets wider and wider the further one tries to predict so it was decided to examine model results over 10 years.

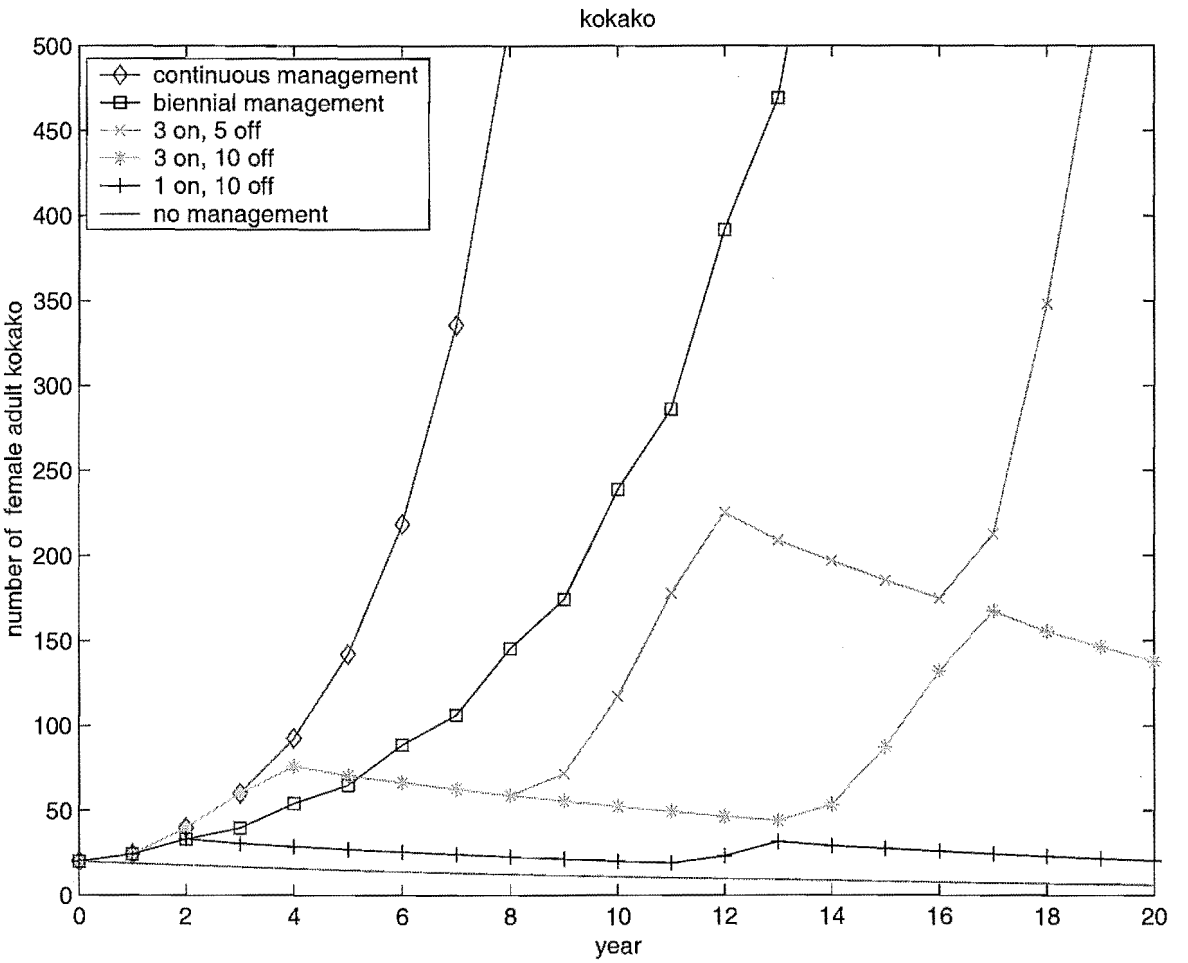

Figure 6.7: Pulsed management strategies over 20 years.

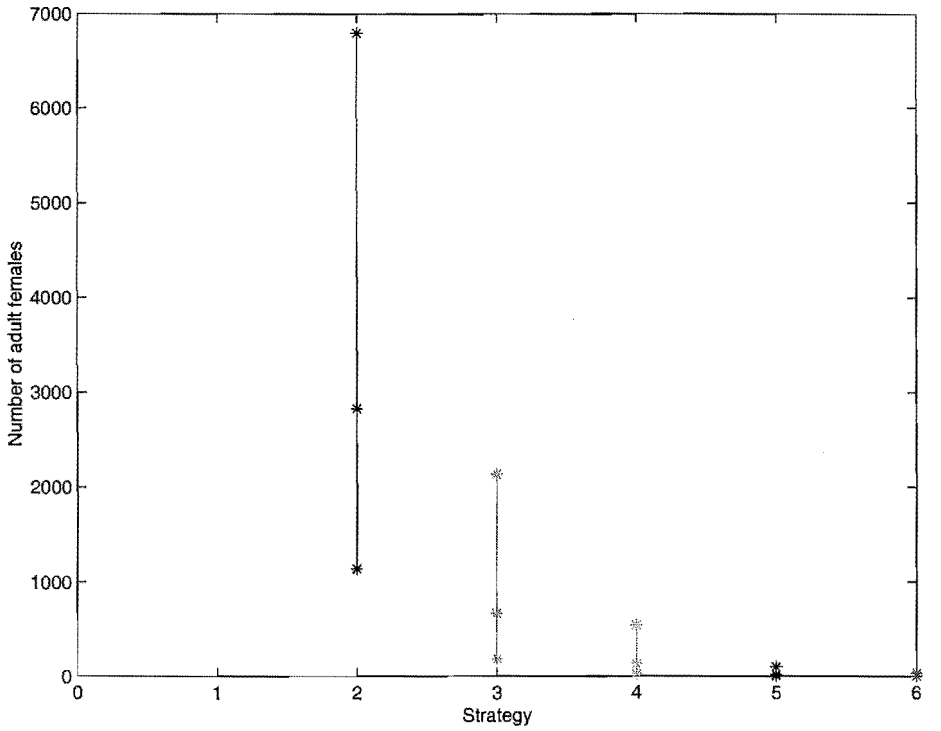

Figure 6.8: Snapshot at the end of the 20th year for the adult female kokako time series. Upper and lower limits of each interval result from upper and lower limits of a 95% confidence interval for b, the female annual productivity rate.

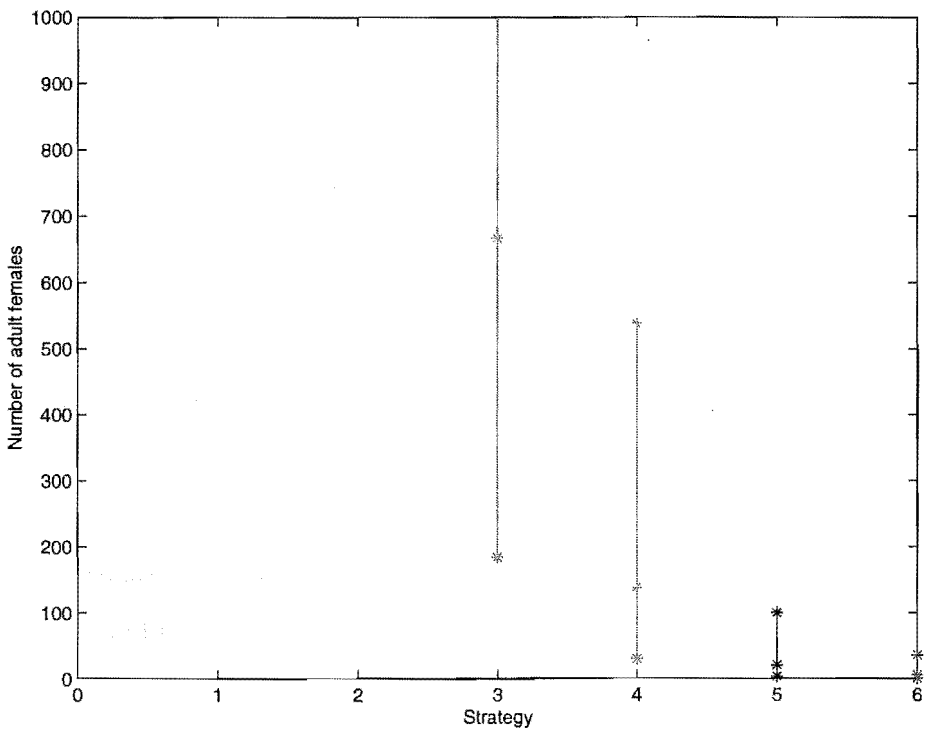

Figure 6.9: Enlargement of Figure 6.8.

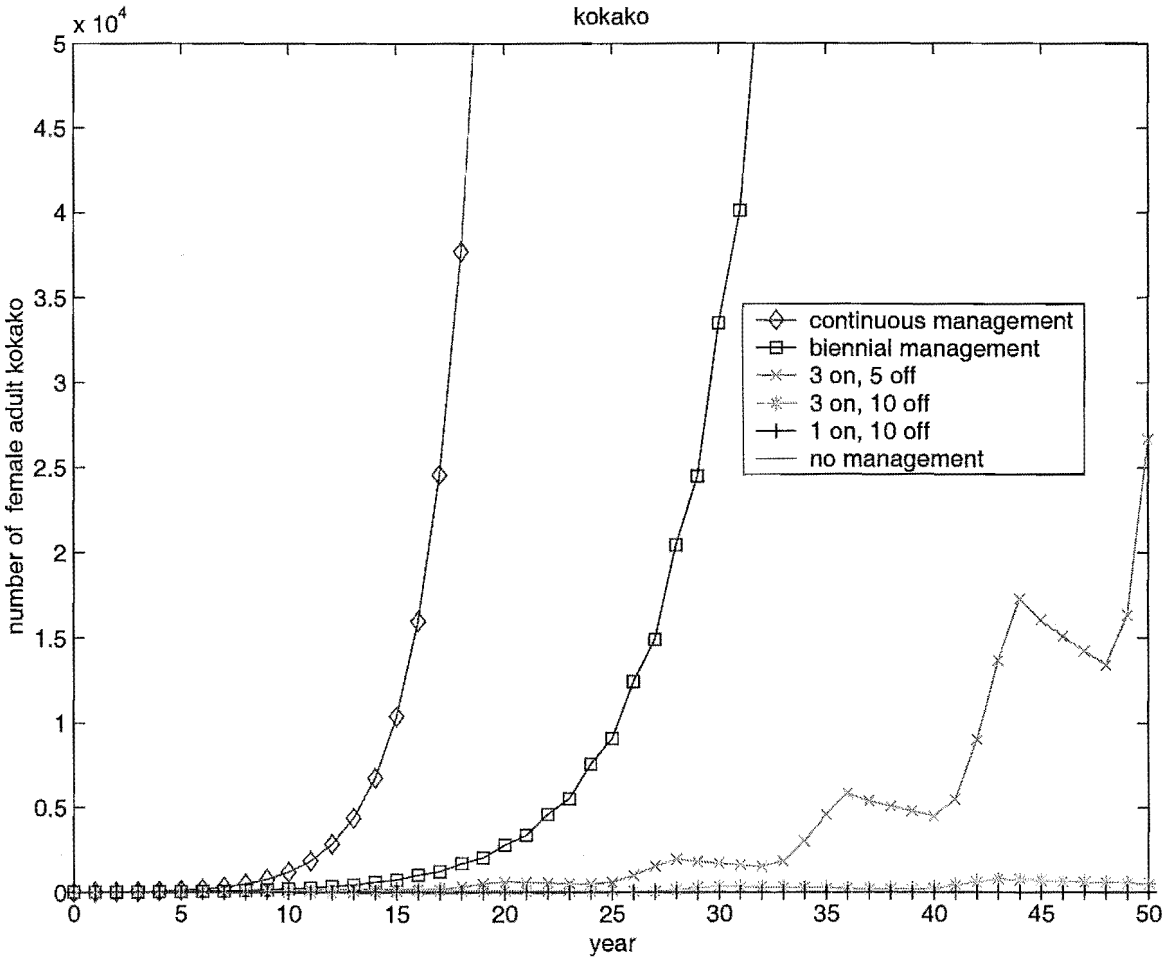

Figure 6.10: Pulsed management strategies over 50 years

6.2.5 Simulations

Multiple simulations of the model (equation (6.1)) for each management strategy, with stochastic allocations of key parameters in any year/run, yield a mean outcome in a particular snapshot year with a distribution around it. In this section, at each time step the productivity rate b was randomly chosen from a normal distribution with mean 1.93 and .19 in managed and unmanaged years respectively and standard deviations .65 and .09 respectively. 1000 simulations were run, and snapshots at year 10 were taken for each simulation. Figures 6.11 to 6.16 represent each management strategy. In these figures, 1000 snapshots are plotted in a histogram, showing that the distribution of the number of female adults in year 10 is close to normal, with a slight skew to the right. Plots of the number of female adults in year 10 versus simulation number in Figures 6.11 to 6.16 show that simulation results are noisy. 95% of observations lie within the upper and lower horizontal lines. These

upper and lower values, means and standard deviations are summarised in Table 6.3 for each management strategy. The upper and lower values are plotted as intervals and are depicted in Figures 6.17 and 6.18. For each management strategy there is a 95% probability that any particular simulation run will result in a population number in year 10 somewhere in between the upper and lower values listed in Table 6.3.

Strategy	Lower	Upper	Mean	Std
1 (continuous management)	647	1942	1219	334
2 (biennial management)	127	406	240	72
3 (3 years on 5 years off)	71	181	119	27
4 (3 years on 10 years off)	34	74	52	10
5 (1 year on 10 years off)	12	27	20	3
6 (continuously unmanaged)	8	14	11	1

Table 6.3: Approximate upper and lower limits, means and standard deviations for the distribution of adult female kokako (1000 simulations) at year 10. There is a 95% probability that a particular simulation will result in a female adult population number in year 10 within the upper and lower values.

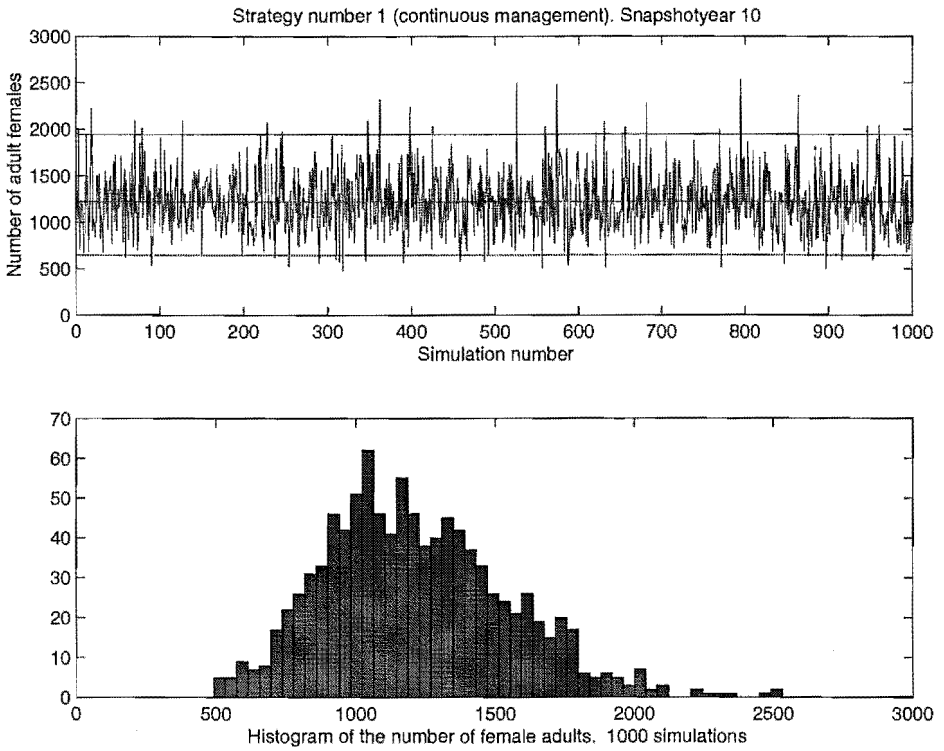

Figure 6.11: The distribution of adult female kokako. Snapshot in year 10 with 1000 simulations. Management strategy 1, continuous management.

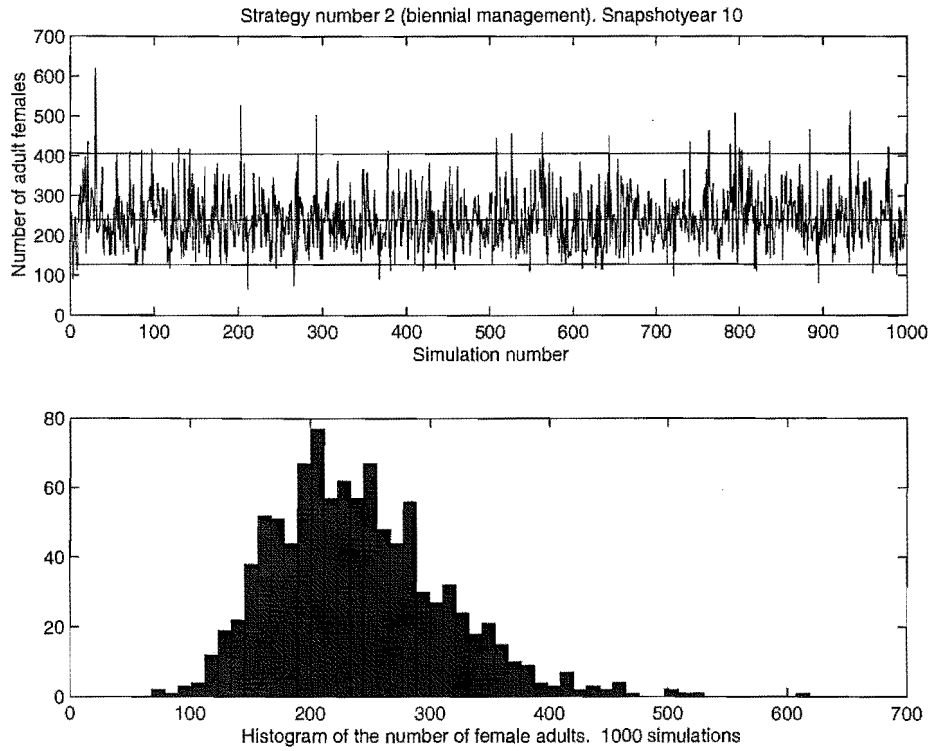

Figure 6.12: The distribution of adult female kokako. Snapshot in year 10 with 1000 simulations. Management strategy 2, biennial management.

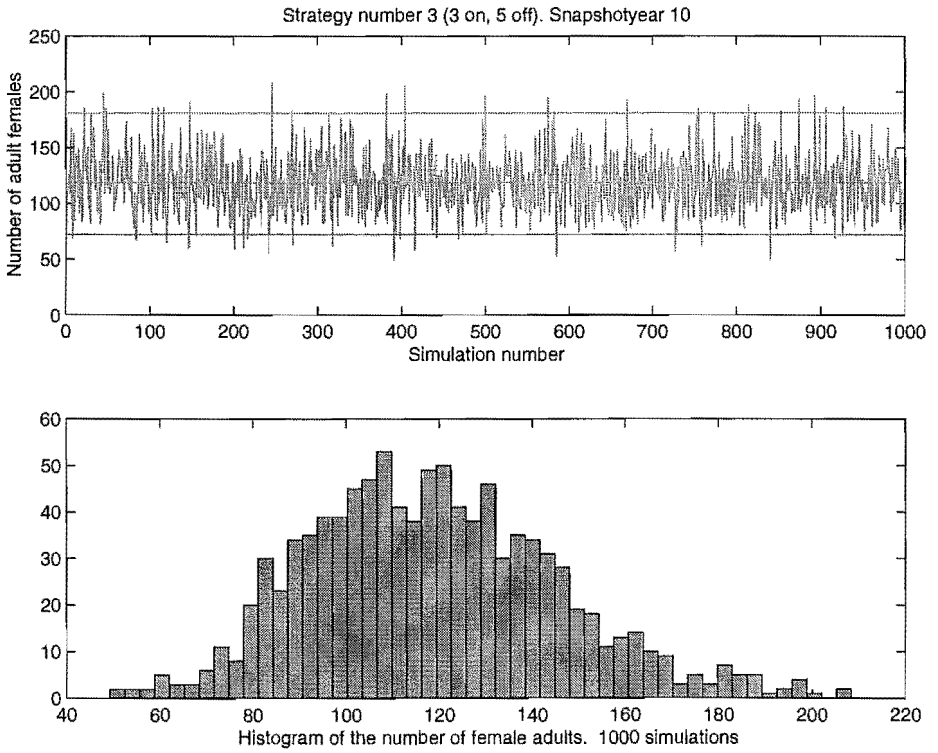

Figure 6.13: The distribution of adult female kokako. Snapshot in year 10 with 1000 simulations. Management strategy 3, 3 years on and 5 years off.

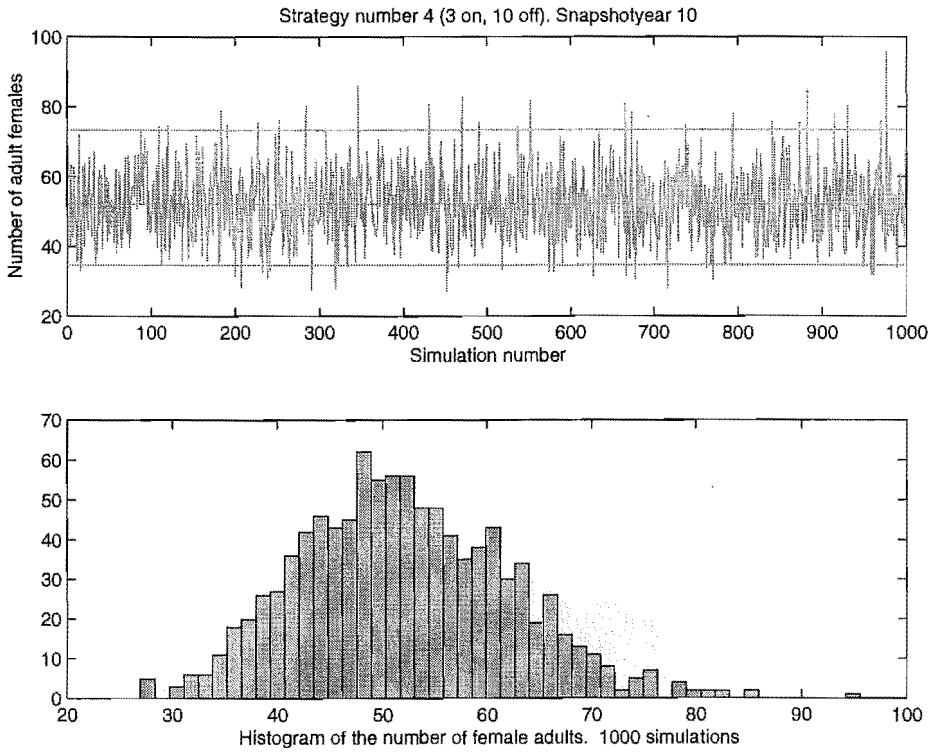

Figure 6.14: The distribution of adult female kokako. Snapshot in year 10 with 1000 simulations. Management strategy 4, 3 years on and 10 years off.

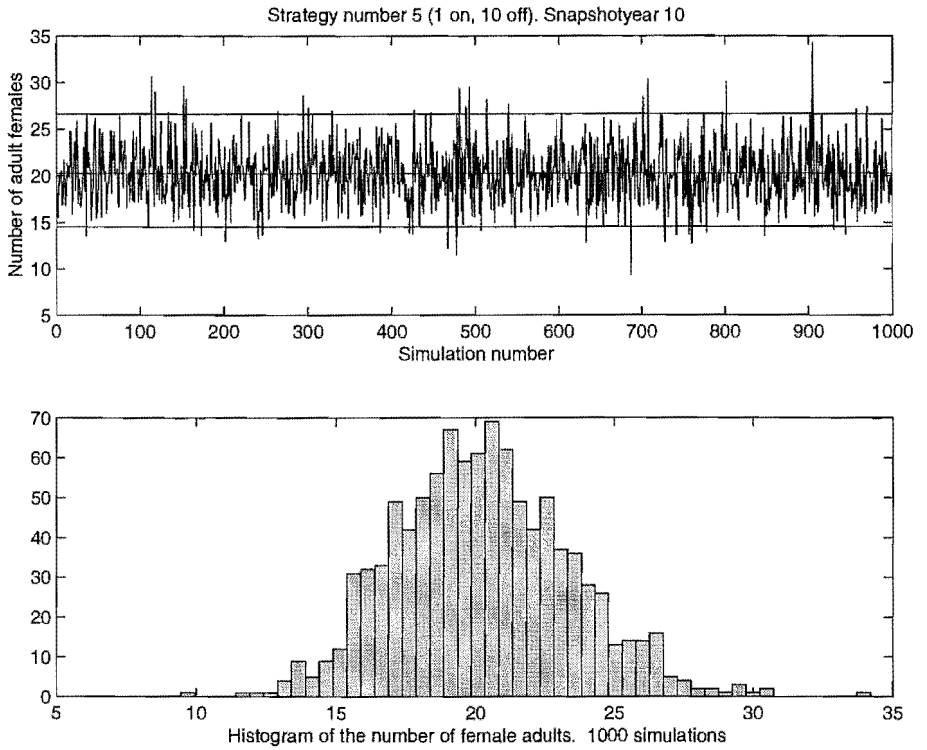

Figure 6.15: The distribution of adult female kokako. Snapshot in year 10 with 1000 simulations. Management strategy 5, 1 year on and 10 years off.

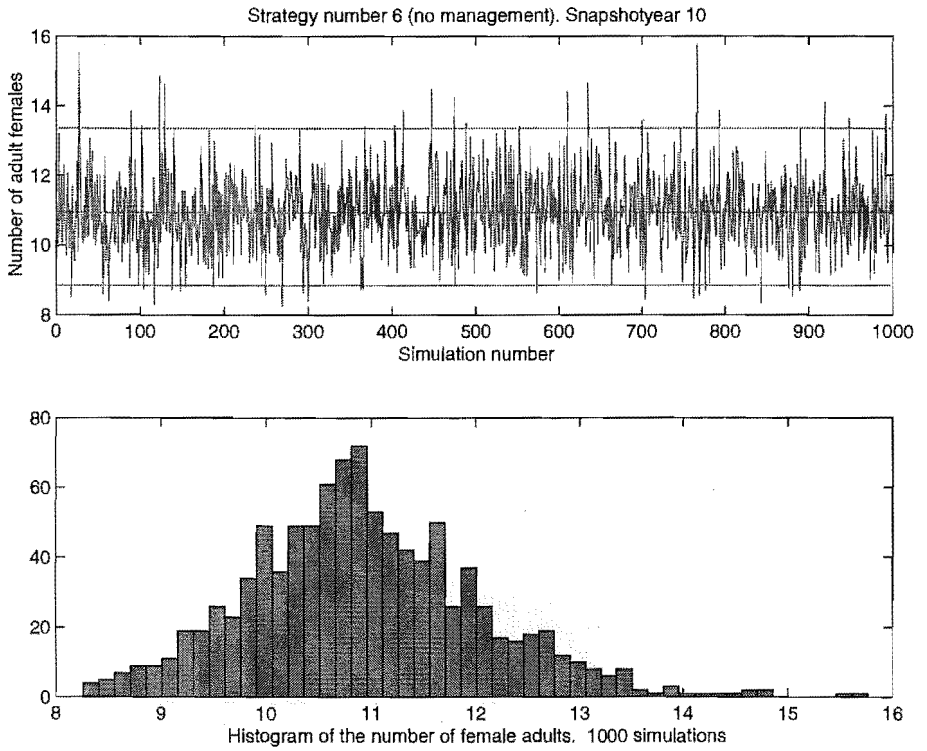

Figure 6.16: The distribution of adult female kokako. Snapshot in year 10 with 1000 simulations. Management strategy 6, continuously unmanaged.

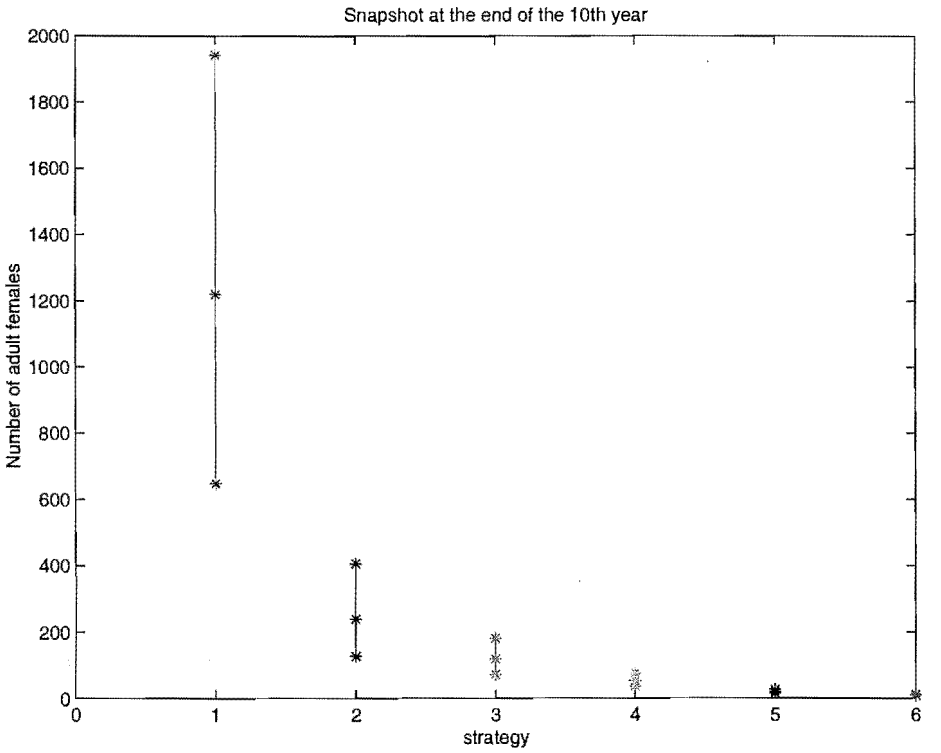

Figure 6.17: Plot of intervals within which 95% of female density observations lie versus management scenario. Snapshot year 10.

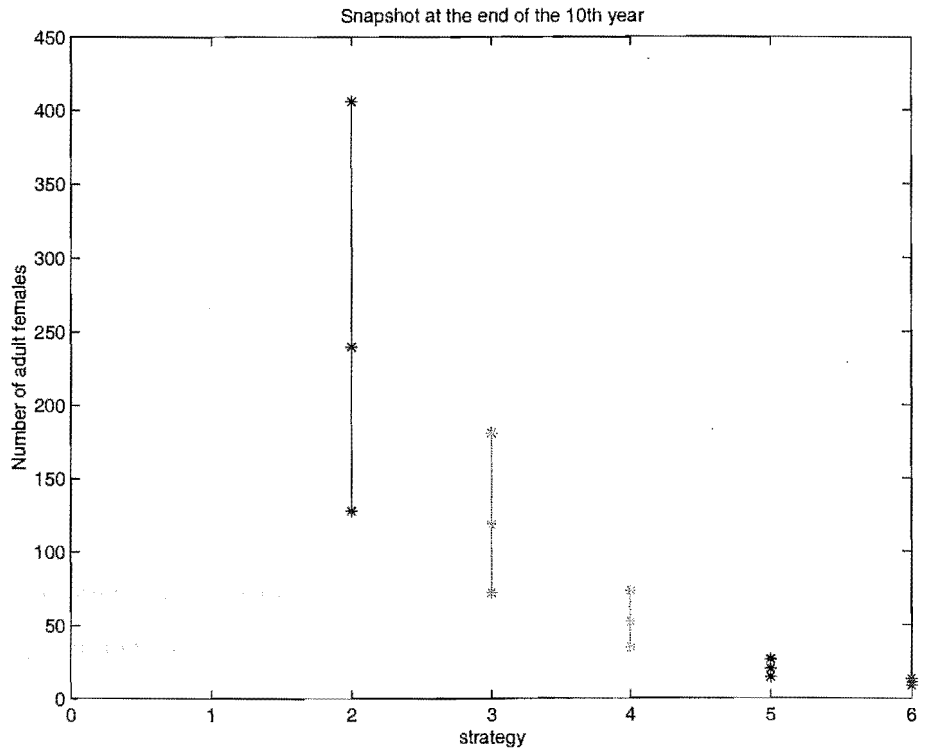

Figure 6.18: Enlargement of Figure 6.17.

It is interesting to compare Figures 6.17, 6.18 and Table 6.3 with Figures 6.5, 6.6 and Table 6.2. Intervals for management strategies 1 and 2 are wider here, whereas intervals for strategies 3-6 are smaller here. Perhaps the difference arises from the resulting distribution not being normal, however this needs further investigation. The conclusions are not quite the same as before, since now the intervals for strategies 4,5 and 6 do not overlap.

A formal test for comparing the distributions for each management strategy is the Wilcoxin rank sum test ([92]). This test was performed on each of the six snapshot data sets from each management strategy and it was concluded that all distributions are significantly different from each other at the 5% level of significance. This concludes that strategy $i \in \{1 \ldots 6\}$ is more likely to result in a higher population density after 10 years than strategy $j \in \{1 \ldots 6\}$, where $i < j$. In practical terms suppose that, for example, strategies 3 and 4 are to be considered. One simulation run of the model is applied to each of these strategies and population densities of adult females in year 10 are compared. There is at least a 95% probability that the population density from strategy 3 will be higher than that of strategy 4.

6.2.6 Further work

- Outcomes where different initial population densities are put into the model should be compared.

- An error analysis, where all parameters are varied, both individually and combined, should be performed.

- This model applies to only one cohort of kokako. Eventually all cohorts, perhaps with dispersal between blocks could be modelled.

In chapter 7, a side step from endangered species is taken. Using similar modelling and methodologies to those seen so far, another conservation issue, the spread of the Rabbit Haemorrhagic Disease (RHD) virus in the rabbit population of New Zealand, is examined. The introduction of such a virus could eventually impact upon indigenous species such as kiwi and kokako because in certain habitats, where lagomorphs play an important part in the diet of stoats, prey switching, as rabbit population densities are lowered, could further decimate bird populations. However prey switching will not be investigated, instead, the

main focus will be to find out under what conditions the virus spreads and the speed of its propagation.

Chapter 7

The spread of Rabbit Haemorrhagic Disease

In the previous chapters, the plight of endangered birds has been discussed and all the models developed have related to issues surrounding these threatened species. It should be emphasised that each model has had a generic framework which can be adapted to a wide range of applications. In this chapter, another conservation issue which has recently become prevalent in New Zealand is tackled. Rabbit Haemorrhagic Disease (RHD) is a viral disease that was illegally introduced into New Zealand at the end of 1997 to control rabbit populations. The importation of such a disease may eventually impact upon native bird species if prey switching occurs due to declining rabbit densities but here the specific interest is to model factors relating to the spread of the disease such as speed and conditions of propagation. In chapter 5 a discrete spatial model was used to simulate sub-adult dispersal of kiwi. In this chapter continuous spatial and temporal dynamics are employed to model the spread of the Rabbit Haemorrhagic Disease (RHD) ([8]).

The analytical tools used in the modelling here are diffusion equations which can be, interestingly, derived from the discrete random walk approach of that used in the simulations of chapter 5. Diffusion equations are widely used in other applications especially fluid dynamics.

7.1 The history of RHD and its introduction into New Zealand

Rabbit Haemorrhagic Disease (RHD) is a viral disease which affects European rabbits ([91]). It first appeared in China in 1984 and has subsequently spread through most of Europe as a result of human trading of rabbits on the domestic market ([86]). Its initial appearance may have been due to the mutation of a benign strain of the virus but this is uncertain, although there is evidence to suggest that a benign strain does exist ([17]). In 1993 the virus was introduced into Australia under quarantine by CSIRO (Commonwealth Scientific and Industrial Research Organisation) for the testing of its capabilities as a biological control of wild rabbits in both Australia and New Zealand ([67]). In 1995 a quarantined experiment began on Wardang Island but despite precautions the virus escaped onto the mainland and spread quickly to many other parts of Australia over the following months ([23]).

Rabbits first arrived in New Zealand with European colonists as early as 1777 ([35]). They were originally carried aboard sailing ships as a food source but by 1866 they were regularly

bred and distributed throughout parts of New Zealand's mainland and offshore islands by acclimatisation societies. They responded favourably to New Zealand's conditions. With an adequate food supply available throughout most of the year, the breeding season was lengthened, and by 1889 rabbits had become a pest.

Although it is not well quantified economically or environmentally, rabbits have a large negative impact on one of New Zealand's main industries, agriculture. Rabbit damage to New Zealand pastures has been an on-going problem over the last century and more than $NZ600 million has been spent by governments since 1950 in a bid to limit rabbit numbers ([77]). Many methods of rabbit control have been investigated over the last century, particularly those involving disease agents. The myxoma virus was introduced in the early 1950's ([35]) but failed to establish. A second application to import the virus in 1987 was rejected. On July 2nd 1997 the application to have RHD legally introduced into New Zealand was refused by P.J. O'Hara, the Deputy Director General of MAF (Ministry of Agriculture and Forestry) ([69]). However by August 25th 1997 there were rumours circulating that the disease was in New Zealand. This was later confirmed when the virus was found on four properties in Cromwell in the southern part of the South Island of New Zealand. After its initial release, RHD was spread mainly through the human vector. Illegally, farmers were instigating spot releases and then taking the livers of infected rabbits, grinding them in a kitchen blender and spraying this mixture over chopped carrots. The carrots were then aerially distributed over large areas. The virus was also released in the North Island and soon it appeared naturally at certain sites. It was suspected that releasing virus in this manner might be actually immunising large numbers of rabbits. It became evident that the virus was becoming established and hopes of containment, or better still, eradication were fading. In an effort to control RHD, the use of the virus as a biological control was legalised.

7.2 Knowns and unknowns of RHD

Despite studies in Australia, Europe and New Zealand, little is known about the spread of RHD. There are two possible modes of transport, the faecal/oral route ([22]) and via a possible wind-bourne vector ([86]). The latter would explain why RHD spreads long distances in a short space of time (i.e. its escape from Wardang Island in Australia ([90])). In many Australian sites, viable RHD virus has been detected in blowflies ([61]).

Spread seems to be radial with a tendency in the prevailing wind direction in some cases ([51]). RHD epidemics occur seasonally ([91]). This is no surprise if the mechanism for the spread of the disease is via a seasonally numerous insect vector, or if the epidemic occurs when population densities are high and there is an increase of rabbit to rabbit contact.

The aim from the farming perspective is to:

- Minimise the adverse effects of RHD and implement management to gain full use of RHD in order to maximise the reduction of rabbit densities. For example, the current percentage of kills after an epidemic of RHD is anywhere between 10% and 90% ([25]). The aim is to have a 90% kill rate in all environments.
- Find out whether RHD should be spread as a biocide (where RHD virus is spread by distribution of baits over an area) or a bio-control (where the virus is initiated at a point source and then allowed to spread naturally).
- Identify when the virus should be released (for example, which season) and under what conditions (temperature, rabbit density etc).
- Ascertain what should be the next move if the virus is not effective.

The aim from the scientific perspective is to:

- Investigate how RHD works and if it is predictable.
- Estimate under what conditions RHD persists and how frequently epidemics occur. For example, persistence might depend on rabbit density, time of year, temperature or different vectors.
- Determine whether flies are the aerial vector.

Such studies are important because they help to identify when and how RHD should be used as a biological control both here in New Zealand and in other countries. Understanding the persistence of a virus is crucial if it is to be used as a biological control.

7.3 The modelling, analytical/numerical

The natural spread of RHD in New Zealand (and elsewhere) from a point source will be modelled in order to find the critical population density threshold below which the disease

will no longer persist. The model can also be used to predict the speed of the wave of infection. A specific question addressed is how the speed of infection depends on the density of the population. A key ingredient is the need of the model outcomes to match the available data. This matching of model outcomes to real data is important because it helps to establish whether the key factors determining the behaviour of the disease have been correctly identified.

Estimates of rabbit densities can be calculated in the field using spotlight counts along a one kilometre transect line. With this in mind, a SIR (susceptibles, infectives, recovereds) model of RHD developed by [5], is extended to incorporate an one dimensional spatial spread of rabbits and diffusion of infection (Figure 7.1). A similar approach was taken by [72] who investigated the spread of foot and mouth disease in feral pigs.

Let $I(x,t)$ be the spatial density of infectives at position x in kilometres at time t in days. It is assumed that the point source release is at the origin x=0, giving an initial condition for infectives $I(x,0) \propto \delta(x)$ where δ is the Dirac-delta function. Similarly, let $S(x,t)$ and $R(x,t)$ be the density of susceptibles and recovereds (who are immune) respectively at position x, in kilometres, at time t, in days. It is assumed that initially there are no rabbits with immunity ($R(x,0) = 0$) and that the density of rabbits is uniform ($S(x,0) = S_{t_0}$).

It is also assumed that susceptible and immune rabbits are essentially stationary but diffusion and advection, with parameters D and v respectively, are incorporated into the equation for the infectives. This allows for the diffusion of the infection by rabbits moving randomly and also the possibility of the infection being spread via a wind vector. Many diffusion models are derived from a random walk approach (for example, [70], [34], [37], [79] and [66]). The diffusion equation using the Fokker-Planck (stochastic) approach is derived by [27]. The random walk derivation of the diffusion equation for infectives is as follows: Assume that the number of infectives at position x at time $t + \triangle t$ (given by $I(x, t + \triangle t)$) is equal to those infectives who moved from position $x + \triangle x$ a distance $\triangle x$ to the left in the time interval from t to $t + \triangle t$ (i.e. $p_1 I(x + \triangle x, t)$ where p_1 is the probability of moving a distance $\triangle x$ to the left) together with those infectives who were at position $x - \triangle x$ at time t and moved a distance $\triangle x$ to the right during the same time interval (i.e. $p_2 I(x - \triangle x, t)$ where p_2 is the probability of moving a distance $\triangle x$ to the right) added to those infectives who did not move at all from position x (i.e. $(1 - (p_1 + p_2))I(x,t)$). That is

$$I(x, t + \triangle t) = p_1 I(x + \triangle x, t) + p_2 I(x - \triangle x, t) + (1 - (p_1 + p_2))I(x,t).$$

Taylor's series expansions in $\triangle x$ and $\triangle t$ of the terms are taken. The equation is then rearranged and higher order terms are ignored. When $\triangle x$ and $\triangle t \to 0$ the equation becomes

$$\frac{\partial I}{\partial t} = D\frac{\partial^2 I}{\partial x^2} - v\frac{\partial I}{\partial x} \tag{7.1}$$

where $D = \lim_{\triangle x, \triangle t \to 0} \left(\frac{p_1+p_2}{2}\right) \frac{\triangle x^2}{\triangle t}$ and $v = \lim_{\triangle x, \triangle t \to 0}(p_2 - p_1)\frac{\triangle x}{\triangle t}$ are the diffusion and advection (constant) coefficients respectively. It should be noted that for these limits to exist, p_1 and p_2 must depend on $\triangle x$ and $\triangle t$. The advection coefficient represents wind speed. The actual calculation of the diffusion and advection coefficients in the field is discussed in section 7.3.3. Equation 7.1 is the standard diffusion/advection equation. Adding spread of infection, mortality due to disease and immunity gives equation (7.3) for infectives below. The model assumes that the rabbits can die by contracting the disease which has a constant mortality rate, d per capita per day. A transmission coefficient, Γ, represents the proportion of susceptibles that can be infected each day by contact with one infected rabbit, thus the spread of infection is proportional to the product of the densities of infectives and susceptibles ([49]). Intuitively, the product of the densities of infectives and susceptibles is the number of possible single contacts between the two parties. A more complicated transmission term, such as may arise from a different mechanism, may replace S with a function $f(S)$ although this is not considered here.

It is possible to ignore the spatial movement of the susceptible population as a first approximation and so equation (7.2) is a conservation equation for susceptibles with the term ΓSI being the loss due to infection. It is assumed that both susceptibles and recovereds can breed. The breeding rate, a, of rabbits depends on pasture biomass available ([20]) but because the duration of infection is of the order of 40-80 days ([71]) it is assumed that the breeding rate is constant over this time.

Similarly equation (7.4) is the conservation equation for the recovereds where the rate of immunity is r per capita per day. Equations (7.5), (7.6) and (7.7) are initial conditions for susceptibles, infectives and recovereds respectively. Thus, the system of equations and

initial conditions governing the above assumptions is:

$$\frac{\partial S}{\partial t} = -\Gamma SI + a(S+R) \tag{7.2}$$

$$\frac{\partial I}{\partial t} = D\frac{\partial^2 I}{\partial x^2} - v\frac{\partial I}{\partial x} + \Gamma SI - dI - rI \tag{7.3}$$

$$\frac{\partial R}{\partial t} = rI \tag{7.4}$$

$$S(x,0) = S_{t_0} \tag{7.5}$$

$$I(x,0) \propto \delta(x) \tag{7.6}$$

$$R(x,0) = 0. \tag{7.7}$$

See Figure 7.1 for descriptions of individual terms and Table 7.1 for the units of the parameters used in the model.

parameter	units	description
D	$\text{km}^2\text{day}^{-1}$	diffusion coefficient
v	km day^{-1}	advection coefficient
ΓS_{t_0}	day^{-1}	transmission coefficient scaled by initial population
r	day^{-1}	per capita recovery rate
d	day^{-1}	per capita death rate due to infection
a	day^{-1}	per capita birth rate

Table 7.1: Summary of parameters used in the RHD model.

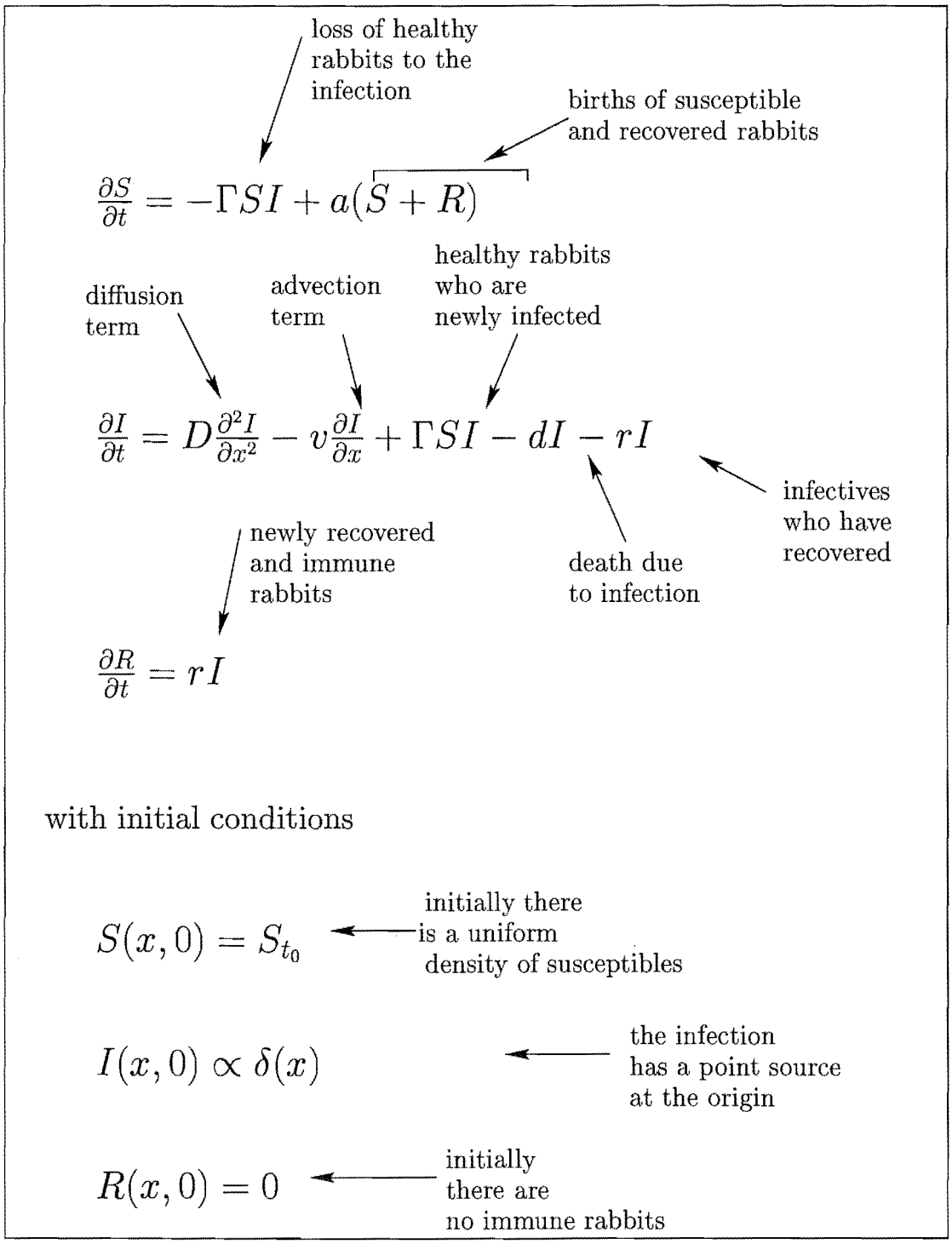

Figure 7.1: Partial differential equations and initial conditions for susceptibles, infectives and recovereds ($-\infty < x < \infty$).

7.3.1 The case of no immunity ($R(x,t) = 0$) and no breeding ($a = 0$)

As a first step to understanding the system of equations, it is assumed that there is no immunity, (i.e. $R(x,t) = 0$) and that the release of the virus is not in the breeding season

$(a = 0)$. Therefore, the system becomes:

$$\frac{\partial S}{\partial t} = -\Gamma SI \tag{7.8}$$

$$\frac{\partial I}{\partial t} = D\frac{\partial^2 I}{\partial x^2} - v\frac{\partial I}{\partial x} + \Gamma SI - dI \tag{7.9}$$

$$S(x,0) = S_{t_0} \tag{7.10}$$

$$I(x,0) \propto \delta(x) \tag{7.11}$$

which is discussed in [66] (with $v = 0$) in terms of the spread of rabies in foxes. It is shown that the system has a travelling wave solution (Figures 7.2, 7.3 and 7.4) of the form $I(x,t) = f(x \pm ct)$ and $S(x,t) = g(x \pm ct)$.

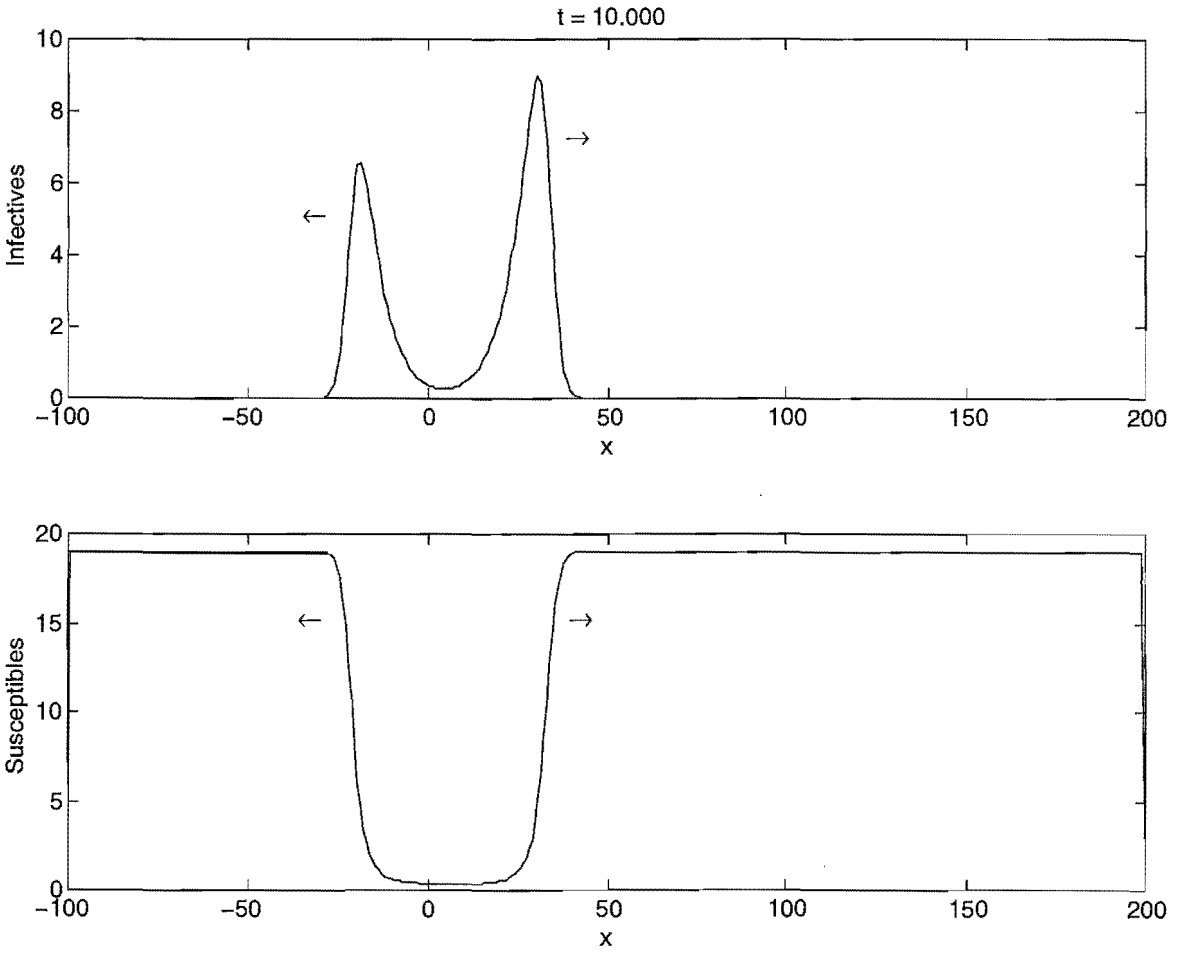

Figure 7.2: An example of travelling wave solutions ($t = 10$) of the system where there is no immunity and no breeding. The arrows indicate the direction the wave is travelling. Arbitrary parameter values are $\Gamma = 0.14, d = 0.67, D = 1.5, v = 0.5, S_{t_0} = 19, I(0,0) = 1, \triangle t = 0.1, \triangle x = 1.5\sqrt{2D \triangle t}, t_{\min} = 0, t_{\max} = 25, x_{\min} = -100, x_{\max} = 200$. The units of parameters are summarised in Table 7.1.

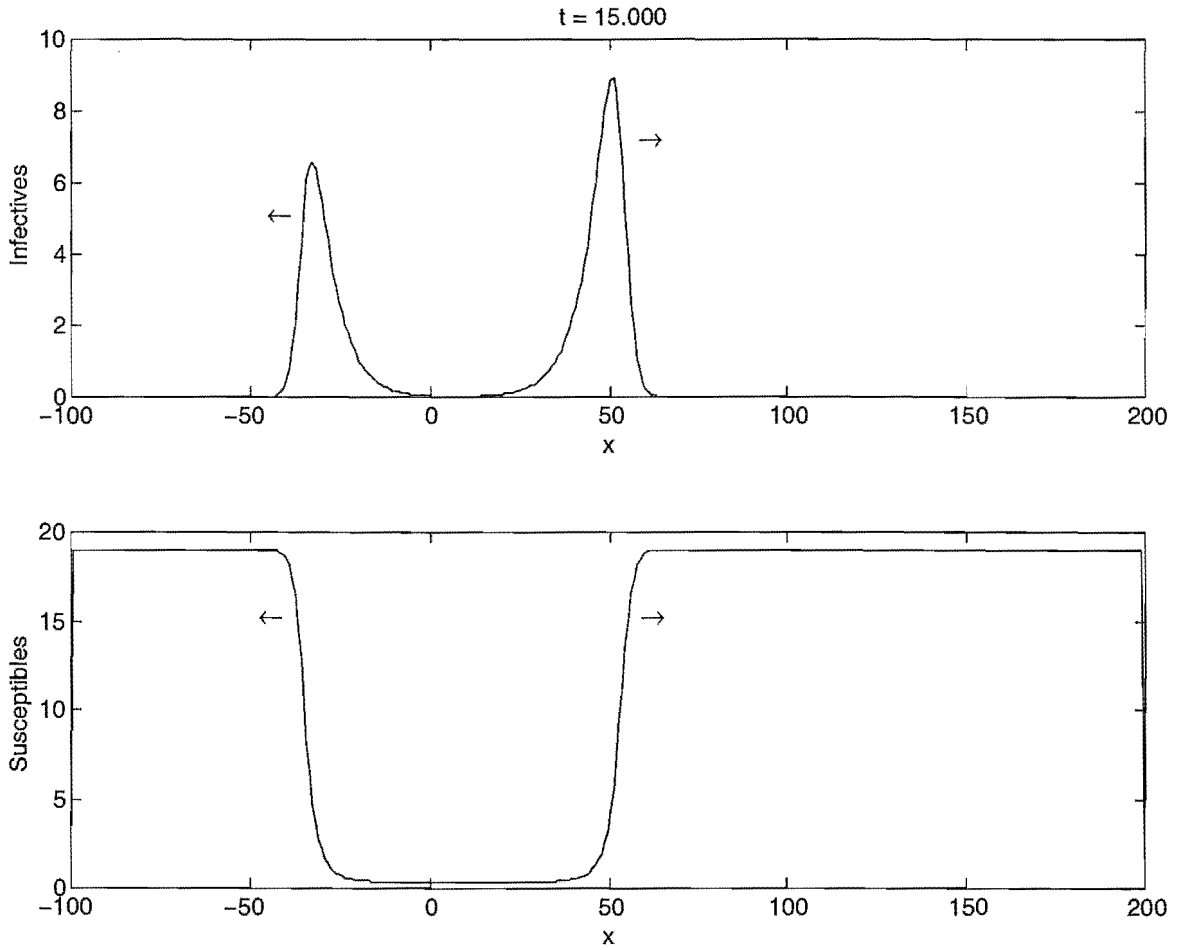

Figure 7.3: Same as for Figure 7.2 except $t = 15$.

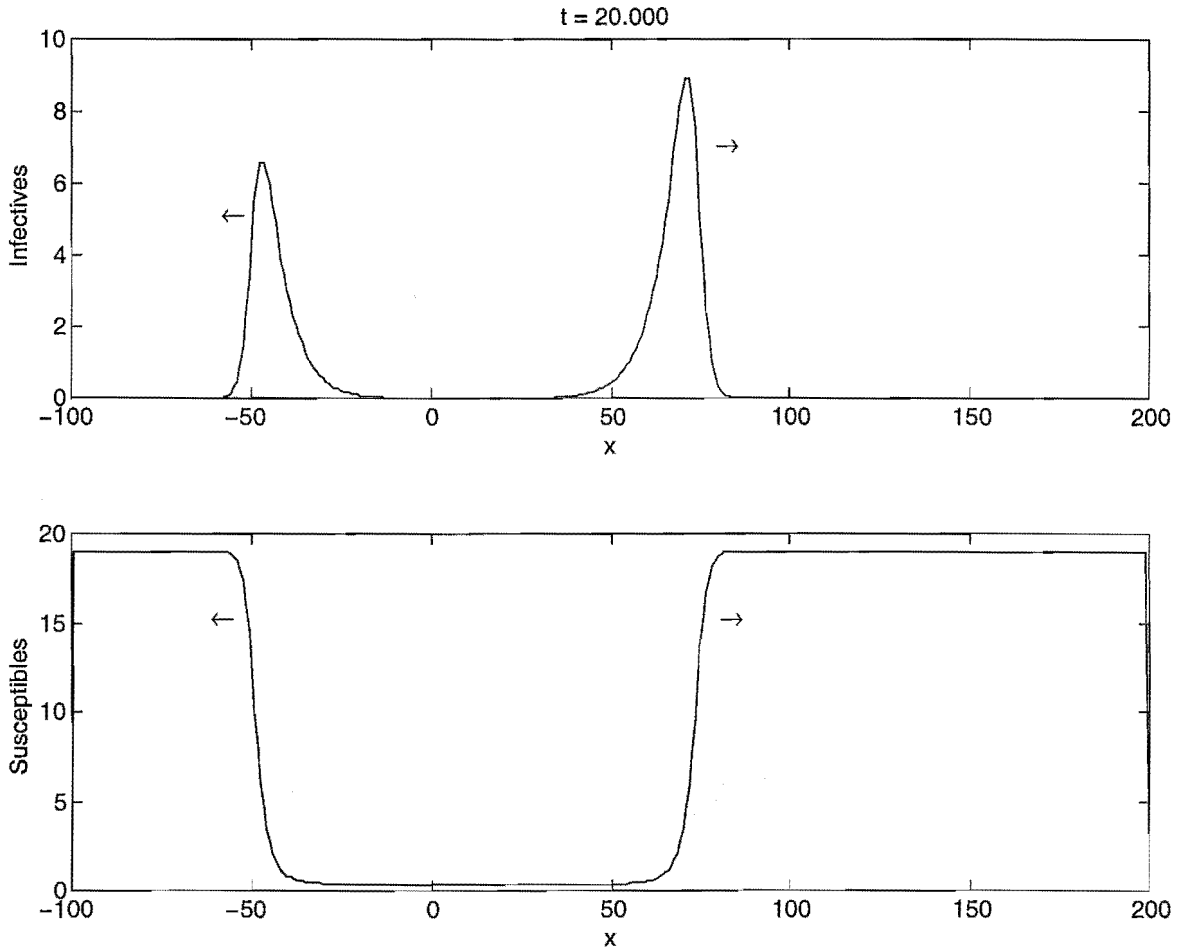

Figure 7.4: Same as for Figure 7.2 except $t = 20$.

In order to find the speed of the wave of infection analytically, [66] assumes that the rate of change of susceptibles is much slower than the rate of change of infectives (i.e. at the wave front, the density of susceptibles is approximately constant). It is then possible to solve the system of equations analytically by linearising about S_{t_0}. That is, let $S(x,t) = S_{t_0}$ be a constant. Using Fourier transforms ([84]), the solution for the density of infected rabbits at location x and time t is

$$I(x,t) \sim \frac{1}{\sqrt{t}} e^{\frac{-(x-vt)^2}{4Dt}} e^{(\Gamma S_{t_0} - d)t}$$

which is plotted in Figure 7.5. Note that is only an approximate solution of the system and it does not have travelling waves but it can still be used to find the speed of infection which can then be numerically verified.

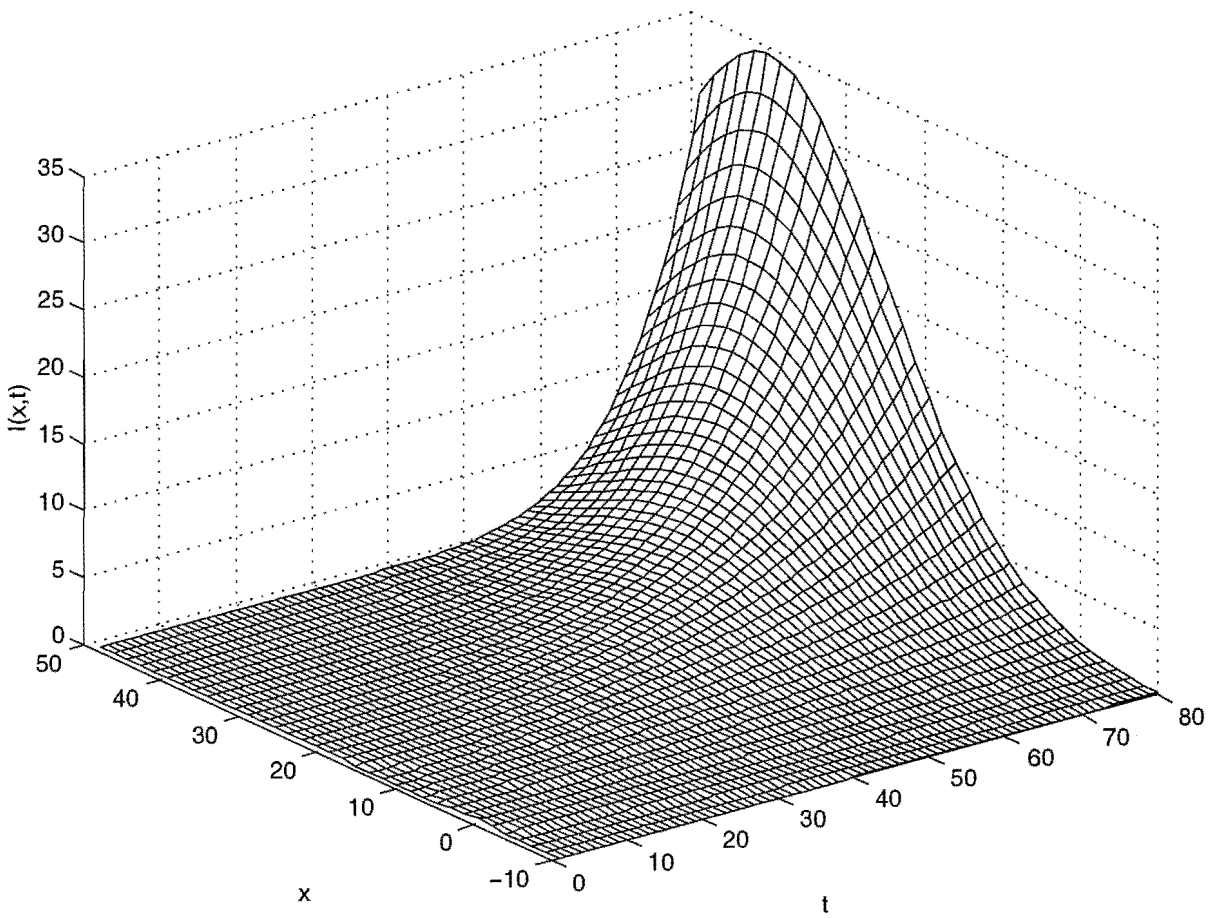

Figure 7.5: An example of the analytic solution for arbitrary parameter values $\Gamma = 0.04, d = 0.67, a = 0, D = 1.5, v = 0.5, S_{t_0} = 19, \triangle t = 1, \triangle x = 1.5\sqrt{2D \triangle t}, t_{\min} = 0, t_{\max} = 80, x_{\min} = -100, x_{\max} = 200$. The units of parameters are summarised in Table 7.1.

To find the speed of infection analytically, note that since $I(x,t) \to 0$ as $t \to \infty$, $I(x,t)$ cannot oscillate about 0. Thus it is required that

$$\begin{aligned} (\Gamma S_{t_0} - d)t &< \frac{(x - vt)^2}{4Dt} \\ \Rightarrow \quad c = \frac{x}{t} &> |v \pm 2\sqrt{D(\Gamma S_{t_0} - d)}|. \end{aligned}$$

Therefore the centre of the wave travels with speed $c = v$, the front of the wave (travelling to the right) travels with speed $c > v + 2\sqrt{D(\Gamma S_{t_0} - d)}$ and the front of the wave (travelling to the left) travels with speed $c > |v - 2\sqrt{D(\Gamma S_{t_0} - d)}|$.

These analytical wave speeds ($c > v \pm |2\sqrt{D(\Gamma S_{t_0} - d)}|$) have been found assuming that $\frac{\partial S}{\partial t} = 0$. If this assumption is dropped then numerics must be resorted to in order to solve the system.

Explicit finite difference numerical methods can behave pathologically when solving dif-

fusion equations and are dependent on the step size for convergence ([24]). Therefore an implicit method is employed by taking the difference quotient for the second derivative and first derivatives ($\frac{\partial^2 I}{\partial x^2}$ and $\frac{\partial I}{\partial x}$) centred at (x_i, t_{j+1}) ([24],[87]) i.e.

$$\begin{aligned}\frac{\partial I(x_i,t_j)}{\partial x} &= \frac{I(x_{i+1},t_{j+1}) - I(x_{i-1},t_{j+1})}{2 \triangle x},\\ \frac{\partial^2 I(x_i,t_j)}{\partial x^2} &= \frac{I(x_{i+1},t_{j+1}) - 2I(x_i,t_{j+1}) + I(x_{i-1},t_{j+1})}{(\triangle x)^2}.\end{aligned}$$

Boundary conditions that $I(x_{\min}, t) = I(x_{\max}, t) = 0$ are also added. To numerically approximate the initial condition $I(x, 0) \propto \delta(x)$ it is assumed that there is a density of I_0 infected rabbits in a neighbourhood of the origin. The force of the infection, $F(t)$, is defined as the total amount of infection present at time t. i.e. $F(t) = \int_{-\infty}^{\infty} I(x,t)dx$. Initially, $(t = 0)$, the force of infection is approximated numerically (using a step size $\triangle x$) by $F(0) = \int_{-\infty}^{\infty} I(x,0)dx = 2I_0 \triangle x$ (Figure 7.6).

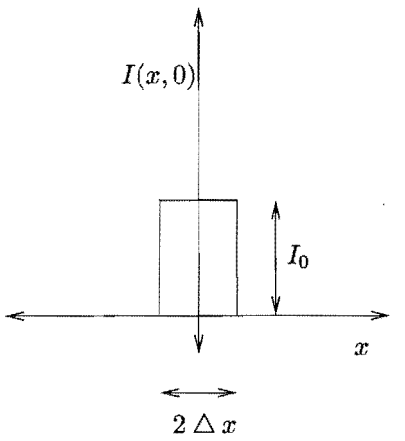

Figure 7.6: Numerical approximation of the initial force of the infection, assuming that the density of infectives is $I_0 2 \triangle x$ in a neighbourhood, $\triangle x$, of the orgin.

Numerically it can be seen that when $\Gamma \neq 0$ a wave split occurs (Figure 7.7) which represents waves travelling to the left and right of the origin. In Figure 7.8 it is evident that the wave speeds to the left and right attain their minimum, i.e. the wave speed is $c = |v \pm 2\sqrt{D(\Gamma S_{t_0} - d)}|$. Note that in Figure 7.8, a negative wave speed indicated that the wave is travelling to the left. (Similarly Figures 7.9 and 7.10.)

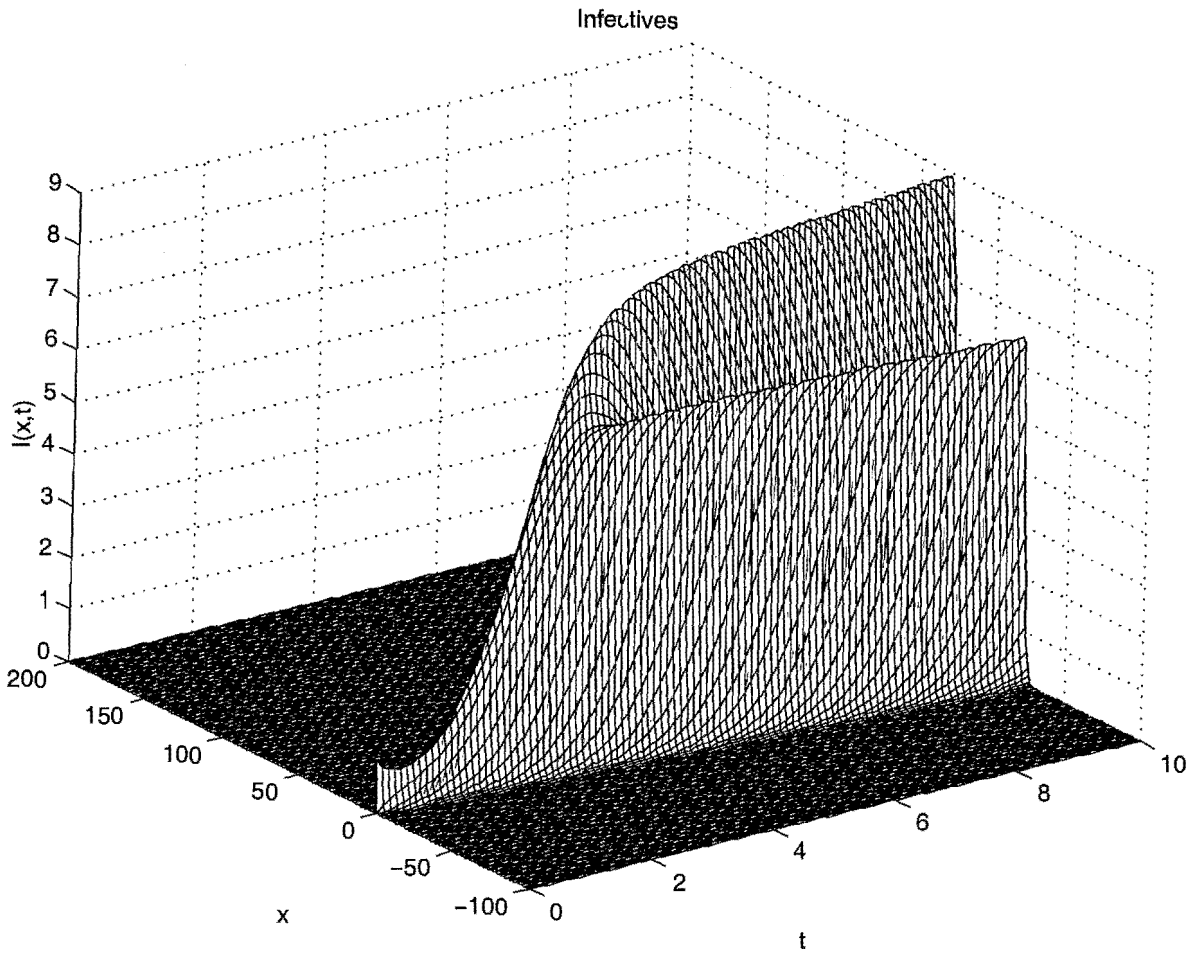

Figure 7.7: An example of the numerical solution of the system showing the wave split when $\Gamma \neq 0$. Arbitrary parameter values are $\Gamma = 0.14, d = 0.67, a = 0, D = 1.5, v = 0.5, S_{t_0} = 19, I(0,0) = 1, \triangle t = 0.1, \triangle x = 1.5\sqrt{2D \triangle t}, t_{\min} = 0, t_{\max} = 10, x_{\min} = -100, x_{\max} = 200$. The units of parameters are summarised in Table 7.1.

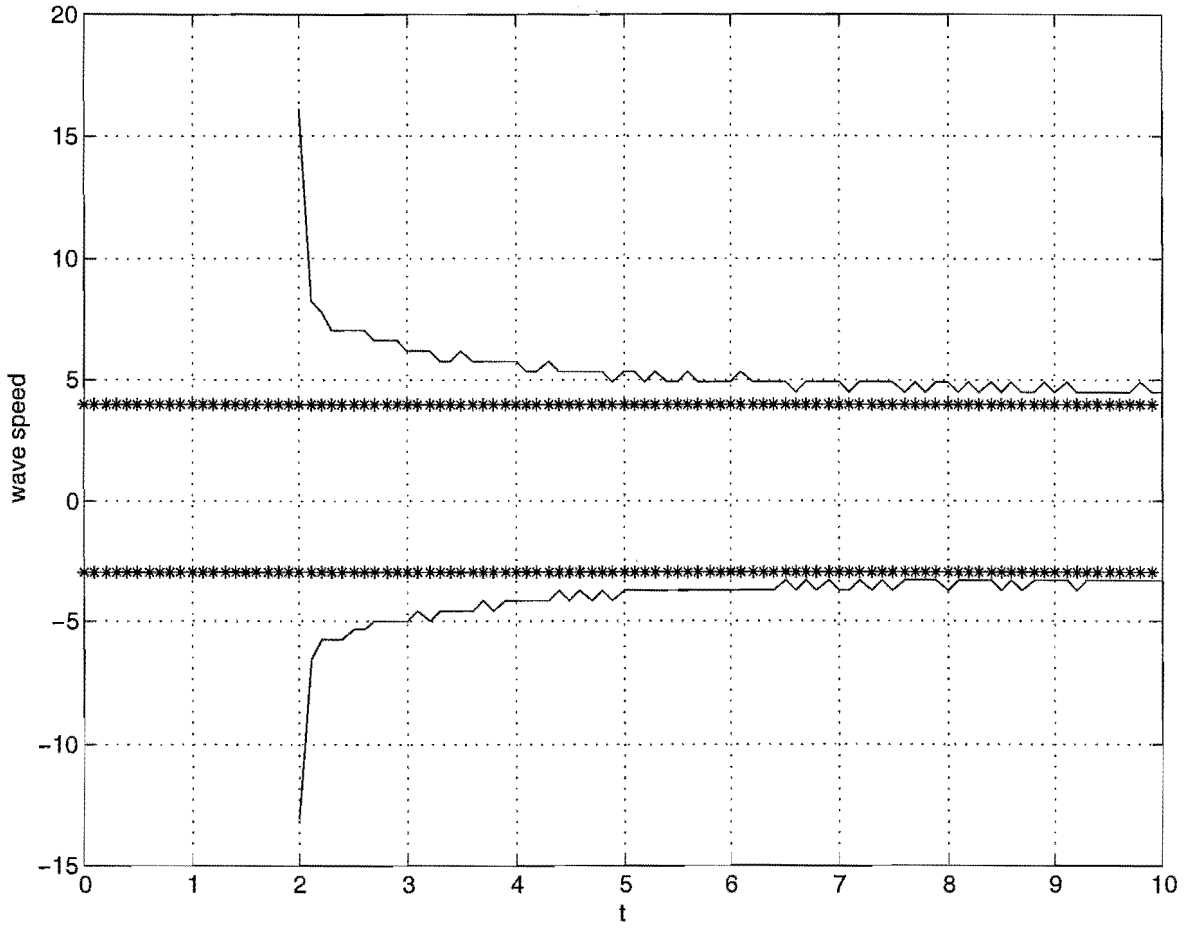

Figure 7.8: An example of the comparison of $v \pm 2\sqrt{D(\Gamma S_{t_0} - d)}$, the analytical wave speed, (**) and the numerical wave speed (-). The arbitrary parameter values are $\Gamma = 0.04, d = 0.67, a = 0, D = 1.5, v = 0.5, S_{t_0} = 19, I(0,0) = 1, \triangle t = 0.1, \triangle x = 1.5\sqrt{2D \triangle t}$, $t_{\min} = 0, t_{\max} = 10, x_{\min} = -100, x_{\max} = 200$. The units of parameters are summarised in Table 7.1.

Thus the wave speed $c = \frac{x}{t}$ is moving faster than the wind speed v, providing S_{t_0} is big enough. If $S_{t_0} < \frac{d}{\Gamma}$ then the wave of infection will not propagate. This is the same critical density as found in [5] using a non-spatially structured model.

7.3.2 Assuming breeding ($a \neq 0$) but no immunity ($R(x,t) = 0$)

As soon as breeding occurs, a becomes non-zero and there are no longer travelling wave solutions. Similarly the wave speed cannot be calculated as before since it is not possible to make the assumption that $S(x,t)$ is constant at the wave front. However it can be seen numerically (Figure 7.9) that the speed of the infection at time t is travelling at approximately $v \pm 2\sqrt{D(\Gamma \times \max(S(x,t)) - d)}$ where $\max(S(x,t))$ is the maximum number of susceptibles

at location x and at a fixed time t.

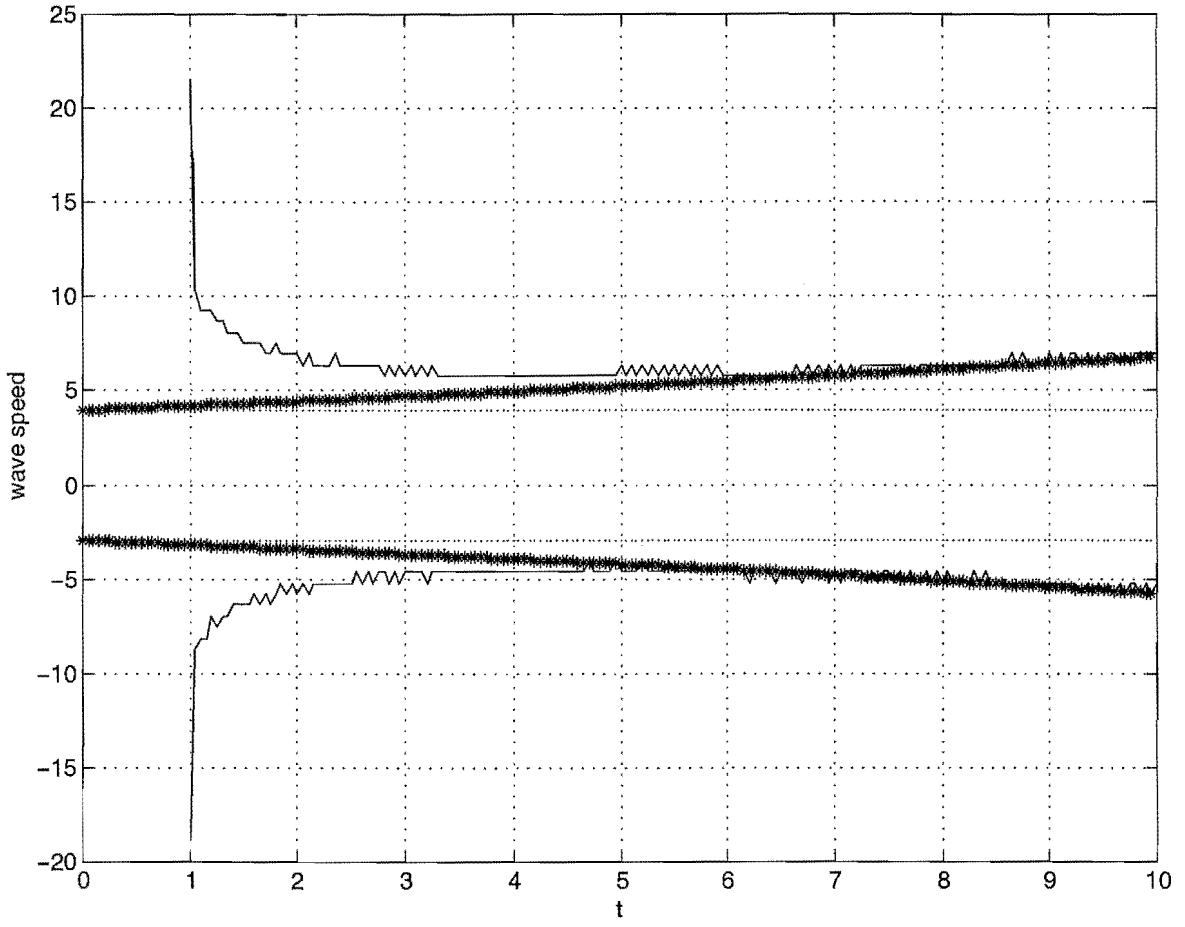

Figure 7.9: An example of the comparison of $v \pm 2\sqrt{D(\Gamma \times \max(S(x,t)) - d)}$, the analytical wave speed, (**) and the numerical wave speed (-). The arbitrary parameter values are $\Gamma = 0.14, d = 0.67, a = 0.1, D = 1.5, v = 0.5, S_{t_0} = 19, I(0,0) = 1, \triangle t = 0.1, \triangle x = 1.5\sqrt{2D \triangle t}, t_{\min} = 0, t_{\max} = 10, x_{\min} = -100, x_{\max} = 200$. The units of parameters are summarised in Table 7.1.

7.3.3 Field data parameter values

Because RHD has only been in New Zealand for such a short time, there is very little data available. Scarcity of data is a common problem especially in biological modelling situations. As more data becomes available the model can be further validated and refined. In the meantime, there is some data from Earnscleugh station, Central Otago in the South Island of New Zealand where RHD arrived naturally. Spotlight counts prior to the arrival of RHD were 35 rabbits per one kilometre of transect. After the epidemic had swept through (around about 80 days with an average speed of approximately 200 meters per day) spotlight

counts had reduced to 12 rabbits per one kilometre of transect. This is a reduction of about 67% ([68]).

The life expectancy of a rabbit who has contracted the virus is $T = 1.5$ days ([5]) therefore the value of d, the mortality rate due to the virus, is $d = \frac{1}{T} = 0.667$ per day.

The transmission coefficient, Γ, is calculated in [5] using combined data from Spain and four sites in Gum Creek Australia. The initial number of susceptibles that were infected by one infected rabbit was $\Gamma S_{t_0} = 2.1$ per day. This value is combined with the value of S_{t_0} from the Earnscleugh site in New Zealand where densities, prior to the introduction of RHD, were 35 rabbits per kilometre of transect. Thus $\Gamma = 0.06$ per day per density of infectives.

Using the values of d and Γ it can be predicted that the critical density of susceptibles below which the disease will no longer propagate is $\frac{d}{\Gamma} \sim 11$ rabbits per kilometre of transect. Post RHD densities at Earnscleugh were 12 rabbits per kilometre of transect and there have been no further outbreaks of RHD. However $\frac{d}{\Gamma}$ is extremely sensitive to values of Γ close to zero. Γ, which may not necessarily be constant, is also sensitive to values of S_{t_0}. Clearly, further analysis of data sets, in cases where RHD spread and in cases where it did not, is needed.

To find the actual speed of the wave requires the calculation of the diffusion coefficient, D, and the advection coefficient, v. There are a number of ways to calculate diffusion coefficients for example, via the random walk derivation of the diffusion equation ([34], [70],[37]) or the Fokker-Planck approach ([27],[70]). Other methods are discussed, in relation to practical problems, in [70].

A way of calculating D is shown in [79] and [66] and will be discussed here. This method is practical in the field and has been used by [72], [70], [47] and [70].

Firstly consider the basic 2-dimension diffusion equation which has a corresponding 2-dimensional diffusion coefficient D_2

$$\frac{\partial N}{\partial t} = D_2 \left(\frac{\partial^2 N}{\partial x^2} + \frac{\partial^2 N}{\partial y^2} \right)$$

with the initial condition $N(x, y, 0) \propto \delta(x, y)$. This has the solution ([84])

$$N(x, y, t) = \frac{1}{4\pi D_2 t} \exp\left(\frac{-(x^2 + y^2)}{4D_2 t} \right)$$

which is the 2-dimensional normal distribution of mean $\mu = (0, 0)$ and variance $\sigma^2 = 2D_2 t$. In polar co-ordinates (where $\rho^2 = x^2 + y^2$)

$$N(\rho, t) = \frac{1}{4\pi D_2 t} \exp\left(\frac{-\rho^2}{4D_2 t} \right).$$

$N(\rho, t)$ can be thought of as the probability density function that an individual is at location ρ at time t, rather than as a population density function. Then $< \rho^2 >$, the mean square displacement by an individual's random walk during time t, is given by

$$< \rho^2 >= \int_0^\infty \rho^2 N(\rho, t) 2\pi\rho d\rho = 4D_2 t.$$

This gives a way of calculating a 2-dimensional diffusion coefficient

$$D_2 = \frac{< \rho^2 >}{4t}.$$

To calculate a one-dimensional diffusion coefficient it is noted that $D_1 = 2D_2$ ([70], [37]) and so

$$D_1 = \frac{< \rho^2 >}{2t}.$$

To calculate the (one dimensional) diffusion coefficient, D, for the RHD model let

$$D = \frac{\begin{array}{c}\text{mean square displacement of a rabbit} \\ \text{from its original location during time interval} \quad t\end{array}}{2t}.$$

Home ranges of rabbits vary depending on season, time of day or night, topography, distances to feeding grounds and density of rabbits but are approximately one hectare (100 m $\times$ 100 m) ([35]). It is therefore assumed that the maximum distance is 140 m per day which gives a diffusion coefficient of $D = \frac{0.14^2}{2} = 0.0098$ km^2 per day.

The advection coefficient, v, in diffusion models is the drift velocity or the convective flux ([34]), in the model discussed here, v is the wind speed. If it is assumed that there was no wind speed at Earnscleugh then it is predicted that the speed of infection will travel at $c = 2\sqrt{D(\Gamma S_{t_0} - d)} = 2\sqrt{0.0098(0.06 \times 35 - 0.667)} \sim 237$ m per day. It was, however, observed at Earnsleugh that the speed of infection was on average 200 m per day ([68]) and travelled in the direction of the prevailing wind. The predicted speed is therefore a rough estimate. D could be too high and immunity has not been taken into account which could slow down the speed of the wave of infection.

7.4 Immunity

There are a number of different types of immunity. Firstly, young rabbits have natural resistance because of their age (0-8 weeks.) Secondly, if the mother has been exposed to the disease and survived then the maternal antibodies are passed across the placenta and

the young rabbit is immune. But this maternal immunity only lasts 10 weeks and then the rabbit becomes susceptible. Thirdly, adult rabbits can have antigen immunity. When they are challenged with RCD they produce antibodies and are subsequently tested as seropositive. This immunity is for life. There could be other types of immunity for example cellular immunity. For the purposes of modelling only life immunity is considered. Let r be the per capita rate of immunity in the rabbit population. The system of partial differential equations and initial conditions is the same as that given in Figure 7.1.

Using the previous results it can be numerically verified (see Figure 7.10) that the analytical wave speed is $c(t) = |v \pm 2\sqrt{D(\Gamma \times \max(S(x,t)) - (d+r))}|$ giving a threshold density of $\max(S(x,t)) = \frac{d+r}{\Gamma}$.

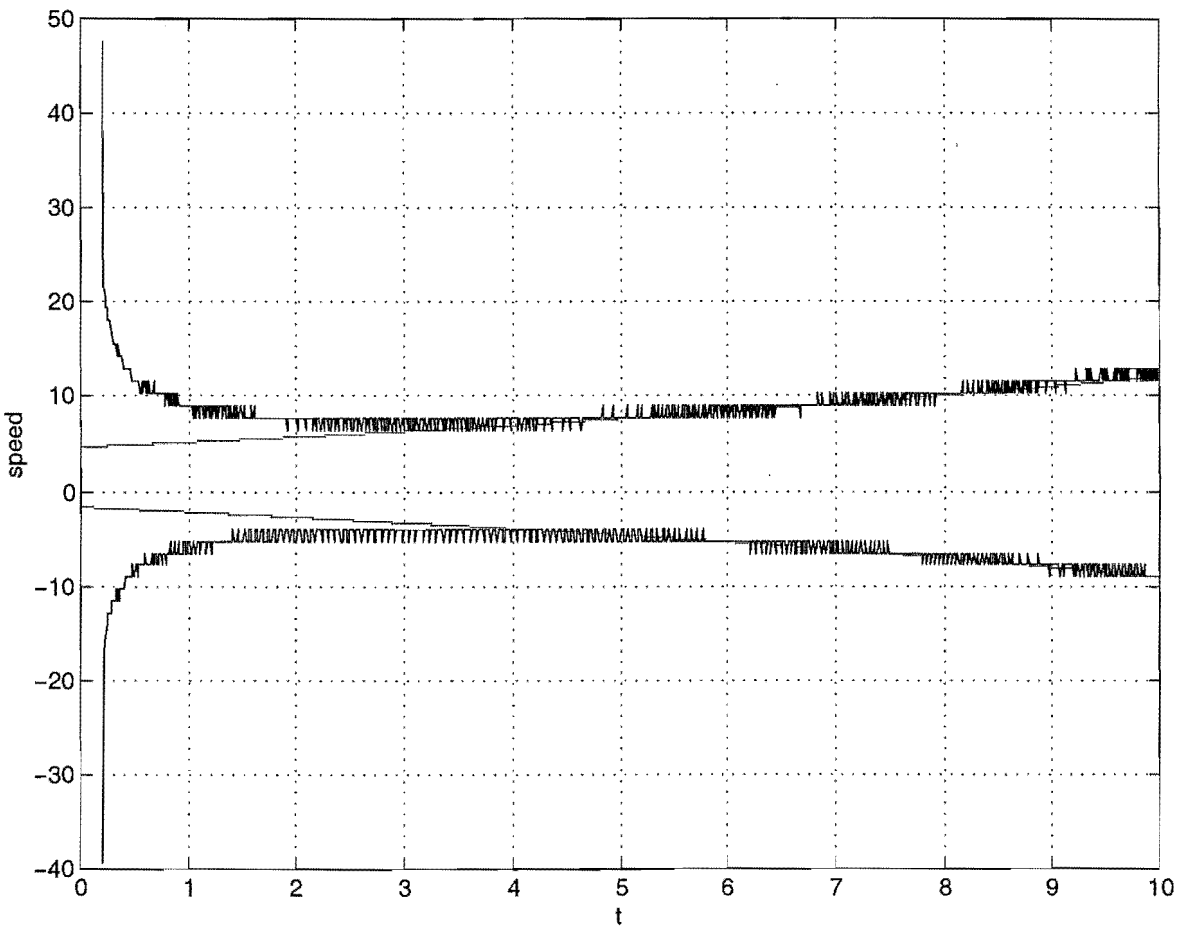

Figure 7.10: An example of the comparison of the analytical wave speed (depicted by a smooth line), $c(t) = v \pm 2\sqrt{D(\Gamma \times \max(S(x,t)) - (d+r))}$, and the numerical wave speed (jagged line). The arbitrary parameter values are $\Gamma = 0.14, d = 0.67, a = 0.2, r = 0.2, D = 1.5, v = 1.5, S_{t_0} = 19, I(0,0) = 1, \triangle t = 0.01, \triangle x = 1.5\sqrt{2D \triangle t}, t_{\min} = 0, t_{\max} = 10, x_{\min} = -150, x_{\max} = 150$. The units of parameters are summarised in Table 7.1.

Figure 7.11 shows an example of the solution of the system from Figure 7.1 where immunity is taken into account. It can be seen that once the infection has passed through, the immune rabbits breed producing further susceptibles. The density of susceptibles that remain after an RHD epidemic may be below the threshold required for the disease to persist. Predators may keep densities low but the need to cull immune rabbits is evident.

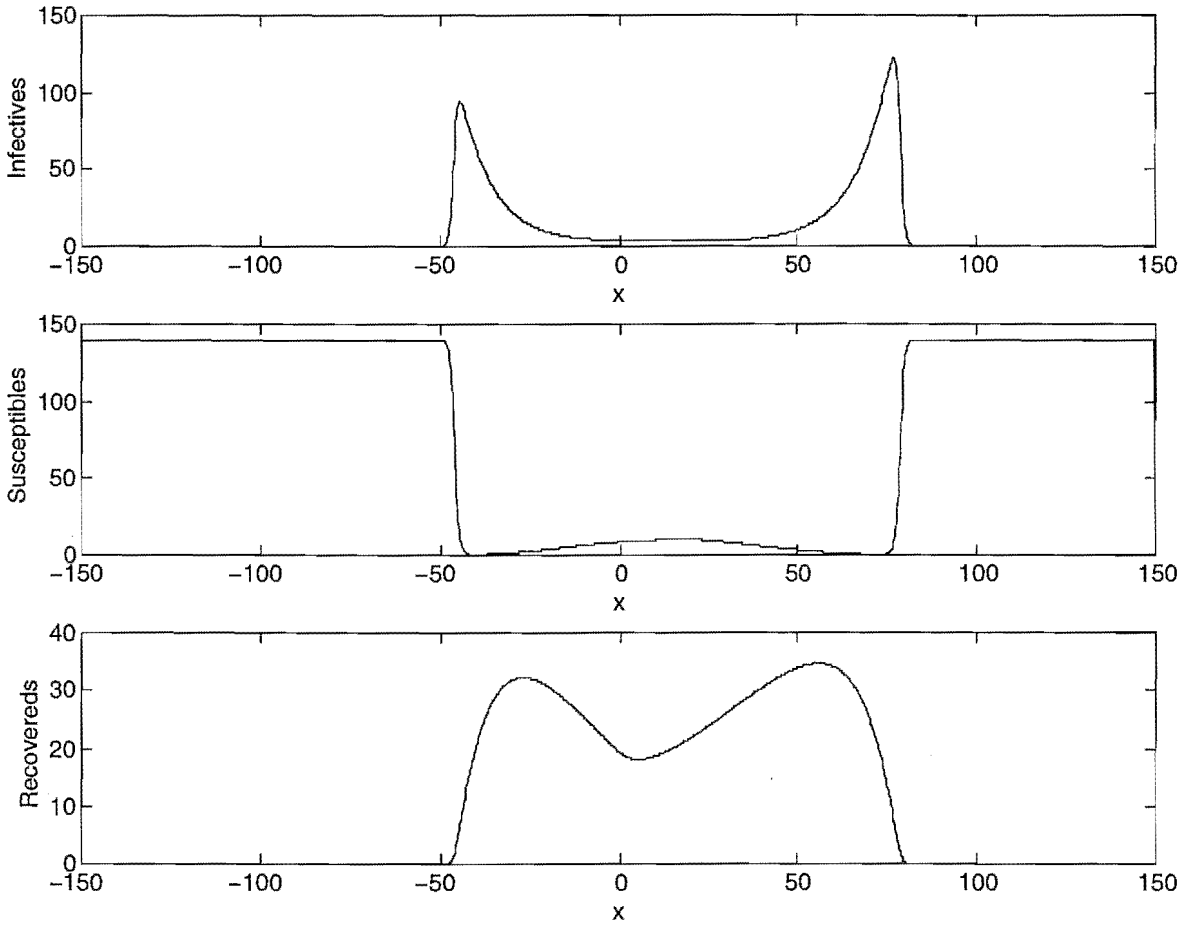

Figure 7.11: An example of the solution, at an arbitrary time $t > 0$, of the system from Figure 7.1 where immunity has been included into the model. Parameter values are the same as in Figure 7.10.

7.5 Results and conclusions

This work has given a quantitative formula for the speed of the wave of infection which depends on the density of susceptibes, the wind speed, the diffusion coefficient, the transmission coefficient, the recovery rate and the death rate due to infection. From this it is possible to calculate the threshold density below which the infection will not spread. This

threshold density is the same as that concluded in a non-spatial SIR model by [5]. The actual calculation of the speed is dependent on the accurate calculation of parameter values which is difficult in New Zealand given the short time span RHD has been present in the country.

The model predicts that for the RHD virus to spread through a property there must be a sufficiently high density of susceptibles. Thus, the best time to seed RHD would be when the entire population is challenged (i.e. when young no longer have immunity and have left the nest). After the RHD epidemic has passed through, the remaining population needs to be culled in order to eradicate any immune rabbits. The limiting factor in this study has been the paucity of data. This will take time to collect. The model developed here appears to make predictions consistent with observations made in the field.

7.6 Further work

As in previous chapters, there is plenty of scope for refinement in the model. Some possible extensions to the current work are listed.

- Further research using different data sets as they become available is essential in verifying the model.

- Model and hence compare the case of releasing RHD as a biocide (where wide scale baiting is used to spread RHD) and bio-control (where the epidemic is allowed to spread naturally from small virus seeding points) ([25]). This would be done by using a distribution over position as the initial condition for the infectives rather than as a point source. It would be important to see how the initial profile affects the outcome for the wave speeds in the model.

- It would be important to re-examine the effect of the possible diffusion of the susceptible population. This would replace equation (7.3) by a diffusion equation similar to equation (7.2). The mathematical complication introduced would make it difficult to obtain an analytical expression for the wave speed. It is possible for some diseases that the diffusion coefficient in the susceptible cohort is different to that for the infective cohort. This needs to be considered.

- In the Canterbury region, New Zealand, it was found that most of the survivors with

immunity were females ([25]). It would be interesting to try and incorporate gender structure into the model to find out why this is the case. This would mean the model would have gender classes for both susceptible and infective cohorts adding two further diffusion-advection equations. The contact between these classes would need to be initially examined.

- Consider the reality of non-constant parameter values reflecting different physical environments and climatic conditions.

All these refinements will lead to the same kind of analysis and outcomes albeit complicated by the increased detail of the new models.

Chapter 8

Conclusion of thesis

In this thesis it has been shown that mathematical modelling can make a valuable contribution to biological conservation issues. A predictive analysis using a mathematical model before a field trial is undertaken can provide advantages both economically and environmentally. For example, it is not always possible to test and compare different conservation strategies. This may be due to the monetary expense of implementing a trial. Even monitoring population densities on a medium scale can be prohibitively expensive. With species on the brink of extinction, there may be limited time for field work and the field work itself may impact adversely on the species.

A mathematical model can give an insight into, and an understanding of, the dynamic behaviour of the system which sometimes cannot be gained from observations. Important parameters can be identified and this can motivate the need of field work and focus it on salient issues. Conversely, field work often motivates the modelling and may pinpoint parameters or state variables of a model which are difficult to estimate in reality. Consequently, there should be a healthy combination of preliminary analysis and complimentary field trials.

In chapters 2 to 5, each of the derived mathematical models pertained to the survival of northern brown kiwi in mainland forests of New Zealand. Because of its generic nature, the modelling could also apply to other species of kiwi or any population which can be divided into age classes with approximately constant predation or recruitment in each age class.

In chapter 2, a deterministic mathematical model of population numbers for different age and gender classes was derived. Two continuous partial differential equations (*McKendricks'* equations) were solved in order to gain expressions for the numbers of chicks and juveniles of age a at time t. These were, in turn, substituted into ordinary differential equations for female and male adults. The resulting differential delay equation for female kiwi was solved using Laplace transform techniques. The temporal solution for the number of female kiwi at time t depended on the control parameter for combined chick and juvenile predation. The critical predation rate for the combined immature kiwi age classes was estimated to be $\gamma_c = 0.6$ per capita per year. The mathematical expression for γ_c is given in equation (8.1) where a_2 is the age that a juvenile becomes an adult, b is the number of successful hatchings per female per year, f_2 is the adult female per capita death rate and α is the natural death rate for immature kiwi (chicks and juveniles).

$$\gamma_c = \frac{1}{a_2} \log\left(\frac{b}{2f_2}\right) - \alpha. \tag{8.1}$$

The value of γ_c in equation (8.1) represents the division between survival and extinction of female adults and hence the entire cohort. Using this critical predation rate, it was found that the chick to adult recruitment rate required for survival of the species was approximately 19%. Any level of recruitment lower than this will imply that, on average, a female will not be able to replace herself in her lifetime.

The modelling in chapter 2 has quantitatively estimated values for critical predation of immature birds and adult recruitment. In mainland forests of New Zealand, where there is currently no predator control, the percentage of chicks surviving to become adults is well below the 19% estimated by the model. Similarly, predation of immature birds is much higher than the critical value estimated. Stoats have been identified as the main cause of death amongst immature kiwi in these areas. It is evident that stoat densities must be reduced to an acceptable level and maintained at this level. Stoat densities fluctuate with changing seasons and years in response to food availability. The modelling in chapter 3 calculated an approximation of what an acceptable stoat density would be. The age structured model from chapter 2 was refined by assuming that the predation rate of immature kiwi depends linearly on stoat density. The critical stoat density was estimated to be a value less than two animals per square kilometer. These results support the view that even during times when stoat densities are naturally at their lowest, they are still too abundant to allow adequate adult recruitment of kiwi. From a management perspective this implies that ongoing stoat control is of paramount importance for kiwi survival.

Stoats are elusive and difficult to trap or poison directly. For this reason and because native forest in New Zealand is dense and the terrain often rugged, these current methods of stoat removal are inefficient and expensive. In chapter 4, secondary poisoning of stoats was considered as an alternative method. Secondary poisoning is when an animal is poisoned by eating poisoned prey, rather than by directly ingesting a bait containing poison. A system consisting of five ordinary differential equations was derived with three equations representing poison in the environment, poison in the mice and stoat pools and two equations for mice and stoat densities. Stochasticisty was introduced into the model via a contact rate dependant on the probability of a stoat encountering a poisoned mouse. This was necessary to ensure that an optimal poisoning regime also had a high probability of an encounter.

The aim of the modelling was to reduce stoats to 90% of their initial density of 25 animals in a 500 hectare area. This was a reduction within the interval of the estimate for critical

stoat density predicted in chapter 3. The objectives of the modelling were to minimise negative environmental impact by poisoning as few mice as possible while also minimising the use of poison and maintaining mice population densities for subsequent poisoning. It was concluded that the initial use of poison was minimised when all mice were poisoned with very small amounts of poison, however this did not satisfy the other objectives so it was decided to poison as few mice as possible.

It was found that an acute secondary poisoning regime could be successful even during a non-mast year, when densities of mice are low, if at least approximately 90% (or about 1800 out of 2000) of mice are poisoned. In a mast year, when densities are high, at least approximately 54% (26,930 mice) of the initial density (50,000 mice) must be poisoned for successful secondary poisoning. Overall, the minimum amount of poison required is much less in a non-mast year (4304.3 mg) than in a mast year (64,579 mg) because there are fewer numbers of mice that need poisoning.

The control parameters, μ, the initial proportion of mice poisoned, and P_0, the initial amount of poison distributed, were not sensitive to changes in the value of the lethal dose required to kill 90% of a group of stoats (the LD_{90}). The identification of these control parameters will assist in the formulation of future field trials.

Ethical, environmental and economic concerns indicate that an analysis of any poisoning regime is extremely important before its implementation. An accurate mathematical model has advantages over field trials because it is cost effective and can identify ways of minimising environmental impacts. Verification of any model is essential and so, at some stage, field trials are needed to check the validity of the assumptions in the model.

The area considered for the secondary poisoning regime was 500 hectares. Larger scale stoat eradication could easily be considered since it would only change initial stoat and mice densities in the model. Economically, it is desirable to perform stoat removal operations within an area as small as possible without compromising the kiwi population in a wider region. In chapter 5, a simulation incorporating sub-adult dispersal was used to approximate a minimum treatment area. A treatment area is a block of land contained within a national park for example, subject to intensive stoat control. Different sub-adult dispersion scenarios were considered and it was found that there was a quadratic relationship between the average distance travelled by sub-adults over four months and the critical treatment block size. Scenarios that restricted movements of sub-adults resulted in a smaller treatment block

size. Under all movement scenarios, the minimum treatment block area predicted by the simulation was much greater than areas currently undergoing intensive stoat trapping in the field. This information could be useful from a management point of view by using natural boundaries in an attempt to limit sub-adult dispersal and increasing current treatment areas. On a 750 hectare peninsular at Lake Waikaremoana on the North Island of New Zealand, management are considering fencing across the peninsular so that sub-adults re-settle within the treatment area.

The modelling in this thesis in chapters 2 to 5 has shown that for northern brown kiwi, *Apteryx mantelli*, in mainland forests of New Zealand, current recruitment rates of chicks to adults are too low, predation on immature birds is too high, predator densities are too high and predator eradication is on too small a scale. All these situations are common knowledge, however the mathematical modelling has formalised these intuitive ideas and quantified them. This is useful for management goals and decisions for all kiwi species and gives a foundation for the allocation of funds for stoat eradication. It is unfortunate that economics is the driving force behind whether or not New Zealand retains its national icon.

Chapter 6 used a modified version of the simulation program from chapter 5 to look into possible pulsed management strategies for kiwi and the North Island kokako, the latter being another endangered bird in New Zealand. Under the assumptions of the simulations from chapter 5 it appears that pulsed management, where a centered square block is eradicated of pests every second year, is not a viable option for kiwi. However, it may be possible to maintain a core area and perform stoat control in the surrounding area once every n years. The remainder of chapter 6 used a generalised and discretised form of the age structured model from chapter 2. Six different pulsed management strategies for kokako were compared. The productivity rate was sampled randomly from a normal distribution and simulations were run. A snapshot of female population numbers at year ten gave an approximately normal distribution slightly skewed to the right. A Wilcoxin rank sum test indicated that each strategy is significantly different at the 5% level of significance. The modelling itself has identified certain parameters as being of greater importance than others. For example, knowledge of recruitment in certain age classes is of greater value to the modelling as opposed to estimating the number of eggs hatched per season per breeding pair. The latter is more time consuming and entails climbing tall trees to gain access to nests at the risk of disturbing birds and injuring the climber.

Chapter 7 branched out from the topic of endangered species and considered a SIR model (with diffusion) representing the spread of Rabbit Haemorrhagic Disease (RHD) in the rabbit population in New Zealand. Despite an apparent diversion from the topics in the previous chapters, the mathematical model used in this chapter was still a system of conservation equations of the form discussed in chapter 1 and had a generic nature that could be applied to many different areas.

The mathematical model in chapter 7 was used to find an expression for the speed of the wave of infection and a threshold population density of susceptible rabbits below which infection no longer propagated. The model verified previous alternative models and it identified that a critical density was indeed necessary for the virus to spread. This was useful for advising when RHD should be used as a biocide, however, the threshold density was sensitive to changes in the values of the transmission coefficient. The latter parameter was especially difficult to estimate given the short time frame that RHD had arrived in the country and the corresponding paucity of data. In this situation additional field work and model revision are required before further conclusions can be made. Such a re-examination of the model and its assumptions is consistent with the modelling process outlined in chapter 1. Recall from chapter 1, the steps to mathematical modelling were categorised as: aims and objectives; formulate; solve; interpret. This procedure being repeated until model and reality concur. Although all steps are imperative, perhaps the interpretation can be singled out as the crux. It is easy to get caught up in the mathematical detail of the solution but the most difficult part of modelling is surely to keep ones feet in the real world. Throughout the thesis it has become evident that at all stages of the modelling process it is essential that there is a close association and frequent communication between all multi-disciplinary parties involved. Like pieces in a puzzle, the theoretical ecologist, the field worker and the modeller must work together to obtain the whole picture. Constant reassessment, revision and reformulation of theories and ideas, as knowledge comes to hand, are essential.

Appendix A

MATLAB programs for chapter 5 simulations

```
% main.m  Main simulation program
clear all
close all
format compact
newgraphics='n'

NumSims = 50;
% Number of years that the simulation runs for.
NumYears = 50;
movementscenario=1;

% DEFINE TREATMENT BLOCK LENGTH AS A GLOBAL VARIABLE
global TreatmentBlockLength
global ControlBlockLength
global graphics

% Length of blocks in km. Assume they are square.
TotalBlockLength = 16;  % Blocklength in km's
ControlBlockLength=10;

TreatBlockMin =6.0;
TreatBlockMax = 6.4;
TreatBlockStep = 0.1;
TreatBlockSize =[TreatBlockMin:TreatBlockStep:TreatBlockMax]';

extinctionvector = zeros(1,length(TreatBlockSize));
AveRecforeachTBS=zeros(3,length(TreatBlockSize));

t0 = clock;
for TreatmentBlockindex = 1:length(TreatBlockSize),
 TreatmentBlockLength=TreatBlockSize(TreatmentBlockindex);
 % INITIALIZE ALL VARIABLES AND CONSTANTS FOR THIS PARTICULAR TREATMENTBLOCKSIZE.
 etime(clock,t0)
 CarryingCapacityT=TreatmentBlockLength*TreatmentBlockLength*50;
 % Carrying capacity is 50 birds per square km in the treatment block.
 AverageYearlyRecruitsMatrix=[];
 for simulation =1:NumSims;
   initialtreatblocksize
   YearlyRecruitmentRatesMatrix=[];
   TreatmentBlockLength
   simulation
   for year = StartYear:NumYears,
     for month = startmonth:12,
       NumRecruitsVector=[0;0;0;0;0;0;0;0;0];
       startmonth=1;
       ageandclassify
       newbirths
       alldeaths
       SubAdults=[SubAdultsT ; SubAdultsC ;SubAdults0];
       if ~(isempty(SubAdults))
         [SubAdults]=subadultsmoving(SubAdults,length(SubAdults(:,1)),...
           movementscenario,MaxSubAdultRange,TotalBlock,month);
         [SubAdultsT SubAdultsC,SubAdults0] = ...
           treatorcontrol(SubAdults,TreatBlock,ControlBlock,TotalBlock);
       end
       % ADD NEW JUVENILES ONTO JUVENILES.
       if month == 8,
         JuvenilesT = [JuvenilesT ; NewJuvenilesT];
```

```
        JuvenilesC = [JuvenilesC ; NewJuvenilesC];
        JuvenilesO = [JuvenilesO ; NewJuvenilesO];
      end
      DensityVector=[size(JuvenilesT,1); size(JuvenilesC,1); size(JuvenilesO,1);...
        size(SubAdultsT,1); size(SubAdultsC,1); size(SubAdultsO,1);...
        size(AdultsT,1); size(AdultsC,1); size(AdultsO,1)];
      DensityMatrix=[DensityMatrix DensityVector];
      % Work out the recruitment rate for the year
      if (month==10) & (year ~=0),
        YearlyRecruitmentRatesMatrix=[YearlyRecruitmentRatesMatrix ...
        NumRecruitsVector([7 8 9])./DensityMatrix([1 2 3],size(DensityMatrix,2)-14)];
      end
    end  % of month
  end % of year
  AverageYearlyRecruitsMatrix=[AverageYearlyRecruitsMatrix ...
    (mean(YearlyRecruitmentRatesMatrix.')).'];
  n=size(DensityMatrix,2);
  m=size(YearlyRecruitmentRatesMatrix,2);
  AdultYearDensityTVector=DensityMatrix([7],1:12:n);
  AdultYearDensityCVector=DensityMatrix([8],1:12:n);
  AdultYearDensityOVector=DensityMatrix([9],1:12:n);
  if newgraphics=='y',
    figure(1)
    plot(1:length(AdultYearDensityTVector),AdultYearDensityTVector,':')
    hold on
    plot(1:length(AdultYearDensityCVector),AdultYearDensityCVector,'--')
    plot(1:length(AdultYearDensityTVector),AdultYearDensityTVector+...
       AdultYearDensityCVector,'-')
    drawnow
    hold off
    figure(2)
    plot(1:m,YearlyRecruitmentRatesMatrix(1,:),':')
    hold on
    plot(1:m,YearlyRecruitmentRatesMatrix(2,:),'--')
    legend('Treatment','Control')
    xlabel('Year')
    ylabel('Recruitment Rate')
    axis([1 m 0 1])
    drawnow
    hold off
  end
  if (AdultYearDensityTVector(length(AdultYearDensityTVector))-...
     AdultYearDensityTVector(1))>=0,
    disp('This treatment block size is large enough')
  else
    disp('This treatment block size is too small')
    extinctionvector(TreatmentBlockindex)=extinctionvector(TreatmentBlockindex)+1;
  end
  AveRecforeachTBS(:,TreatmentBlockindex)=...
  [mean(AverageYearlyRecruitsMatrix(1,:));...
    mean(AverageYearlyRecruitsMatrix(2,:));mean(AverageYearlyRecruitsMatrix(2,:))];
  save output extinctionvector AveRecforeachTBS TreatBlockSize ...
    TreatmentBlockLength simulation
  clear DensityMatrix
 end % of simulations
 save output  extinctionvector AveRecforeachTBS TreatBlockSize ...
    TreatmentBlockLength simulation
end % of this treatment block size.
```

```
extinctionvector=1/NumSims*extinctionvector;
save output  extinctionvector AveRecforeachTBS TreatBlockSize ...
   TreatmentBlockLength simulation
```

```
% initialtreatblocksize.m
%
% This script file initialises the setting for
% the starting treatment block.  Initialization August year 0.
disp(sprintf('Treatment Block area is %3.2f km x %3.2fkm.',...
  TreatmentBlockLength,TreatmentBlockLength));
if newgraphics == 'y'
   figure(3)
   set(figure(3),'Position', [10,5,450,330]); % [left, bottom, width, height]
   clf reset
   figure(2)
   set(figure(2),'Position',[10,354,450,250]) % [left, bottom, width, height]
   clf reset
end
StartYear = 0;

% TreatBlockDim = [xmin xmax ymin ymax]
% Block is square and centered then:
TreatBlock = 0.5*TreatmentBlockLength*[-1 1 -1 1];
TotalBlock=0.5*TotalBlockLength*[-1 1 -1 1];
ControlBlock=0.5*ControlBlockLength*[-1 1 -1 1];

MaxSubAdultRange = 1.5;  % 50m = 0.05km per day = 1.5km per month.
% Initial numbers in the block.
InitialNumAdults = TotalBlockLength*TotalBlockLength*20; % 20 birds per km^2.
% Age Groups
MaxJuvenileAge = 9;      % Max age of a Juvenile is 9 months.
MaxSubAdultAge = 13;     % Max age of a SubAdult is 13 months.
MinAdultAge = MaxSubAdultAge + 1;
MaxAdultAge = 40*12;     % Max age of an Adults is 40 years.
% Initial position and age vectors
Adults = [0.5*TotalBlockLength*(-1 + 2*rand(InitialNumAdults,2)) ...
  round(MinAdultAge + (MaxAdultAge-MinAdultAge)*rand(InitialNumAdults,1)) ];
AdultsT=[];
AdultsC=[];
Adults0=[];
% Detail matrices for each class.
JuvenilesT=[];
JuvenilesC=[];
Juveniles0=[];
SubAdultsT=[];
SubAdultsC=[];
SubAdults0=[];
% Which Adults are in the treatmentblock??
[AdultsT AdultsC Adults0] = ...
   treatorcontrol(Adults,TreatBlock,ControlBlock,TotalBlock);
% Densities in each class [JT;JC;J0;SAT;SAC;SA0;AT;AC;A0],
% columns correspond to months
DensityMatrix=[0;0;0;0;0;0;length(AdultsT(:,1));...
  length(AdultsC(:,1));length(Adults0(:,1))];
NumRecruitsMatrix=[];
RatesMatrix=[];
DeathRates = [1-(1-0.5)^(1/9); 1-(1-0.95)^(1/9); 1-(1-0.95)^(1/9);
   1-(1-0.1)^(1/4); 1-(1-0.1)^(1/4); 1-(1-0.1)^(1/4);
   1-(1-0.082)^(1/12); 1-(1-0.082)^(1/12); 1-(1-0.082)^(1/12)];
startyear = 0;
year=0;
initialstartmonth = 8;
```

```
startmonth = initialstartmonth;
month = startmonth;
if newgraphics =='y'
   figure(1)
   % [left, bottom, width, height]
   set(figure(1),'Position',[10,625,450,250])
   hold off
   subplot(1,2,1)
   % Draw the treament block, control block,
   % total block and initial distribution.
   plot(TreatBlock([1,2,2,1,1]),TreatBlock([3,3,4,4,3]),'k',...
     ControlBlock([1,2,2,1,1]),ControlBlock([3,3,4,4,3]),'k',...
     TotalBlock([1,2,2,1,1]),TotalBlock([3,3,4,4,3]),'k')
   axis(TotalBlock)
   hold on
   plot(AdultsT(:,1),AdultsT(:,2),'b.');
   plot(AdultsC(:,1),AdultsC(:,2),'b.');
   plot(AdultsO(:,1),AdultsO(:,2),'b.');
   axis square
   axis manual
   string1 = (sprintf('Month = %3.0f. Year = %4.0f',month,year));
   title(string1)
   xlabel('kilometers')
   ylabel('kilometers')
   drawnow;
   hold off

   subplot(1,2,2)
   hist(round([AdultsC(:,3)/12;AdultsT(:,3)/12]),0:1:40);
   string2 = (sprintf('No. of Adults = %4.0f. Month = %3.0f. Year = %4.0f',...
     length(AdultsT(:,1))+length(AdultsC(:,1)),month,year));
   xlabel('Age of Adults')
   ylabel('No. in Treatment and Control')
   title(string2)
   axis square
   drawnow;
end % of graphics
```

```
% ageandclassify.m
% This script file ages each bird by 1 month and then
% calculates which age group it is now in.

% AGING OF ADULTS
  if ~(isempty(AdultsT)),
     AdultsT(:,3) = AdultsT(:,3) + 1;
     % ADULTS DYING AT AGE 40 = 480 MONTHS.
    CheckAdultsT = AdultsT(:,3) >  MaxAdultAge;
    AdultsT=AdultsT(logical(1-CheckAdultsT),:);
  end
  if ~(isempty(AdultsC)),
     AdultsC(:,3) = AdultsC(:,3) + 1;
     % ADULTS DYING AT AGE 40 = 480 MONTHS.
    CheckAdultsC = AdultsC(:,3) >  MaxAdultAge;
    AdultsC=AdultsC(logical(1-CheckAdultsC),:);
  end
  if ~(isempty(Adults0)),
     Adults0(:,3) = Adults0(:,3) + 1;
     % ADULTS DYING AT AGE 40 = 480 MONTHS.
    CheckAdults0 = Adults0(:,3) >  MaxAdultAge;
    Adults0=Adults0(logical(1-CheckAdults0),:);
  end

% AGING OF SUBADULTS
  if ~(isempty(SubAdultsT)),
    SubAdultsT(:,3) = SubAdultsT(:,3) + 1;
    % SUBADULTS BECOMING ADULTS IN THE TREATMENT
    CheckSubAdultsT = SubAdultsT(:,3) >  MaxSubAdultAge;
    NewAdultsT = SubAdultsT(logical(CheckSubAdultsT),[1 2 3]);
    NumRecruitsVector(4)=NumRecruitsVector(4)-sum(CheckSubAdultsT);
    NumRecruitsVector(7)=NumRecruitsVector(7)+sum(CheckSubAdultsT);
    AdultsT = [AdultsT; NewAdultsT];
    SubAdultsT=SubAdultsT(logical(1-CheckSubAdultsT),:);
  end
  if ~(isempty(SubAdultsC)),
     SubAdultsC(:,3) = SubAdultsC(:,3) + 1;
     % SUBADULTS BECOMING ADULTS IN THE CONTROL
    CheckSubAdultsC = SubAdultsC(:,3) >  MaxSubAdultAge;
    NewAdultsC = SubAdultsC(logical(CheckSubAdultsC),[1 2 3]);
    NumRecruitsVector(5)=NumRecruitsVector(5)-sum(CheckSubAdultsC);
    NumRecruitsVector(8)=NumRecruitsVector(8)+sum(CheckSubAdultsC);
    AdultsC = [AdultsC; NewAdultsC];
    SubAdultsC=SubAdultsC(logical(1-CheckSubAdultsC),:);
    end
  if ~(isempty(SubAdults0)),
    SubAdults0(:,3) = SubAdults0(:,3) + 1;
    % SUBADULTS BECOMING ADULTS IN THE OUTER REGION
    CheckSubAdults0 = SubAdults0(:,3) >  MaxSubAdultAge;
    NewAdults0 = SubAdults0(logical(CheckSubAdults0),[1 2 3]);
    NumRecruitsVector(6)=NumRecruitsVector(6)-sum(CheckSubAdults0);
    NumRecruitsVector(9)=NumRecruitsVector(9)+sum(CheckSubAdults0);
    Adults0 = [Adults0; NewAdults0];
    SubAdults0=SubAdults0(logical(1-CheckSubAdults0),:);
    end

% AGING OF JUVENILES
  if ~(isempty(JuvenilesT)),
```

```
     JuvenilesT(:,3) = JuvenilesT(:,3) + 1;
     % JUVENILES BECOMING SUBADULTS IN THE TREATMENT
    CheckJuvenilesT =  JuvenilesT(:,3)> MaxJuvenileAge;
    NumNewSubAdultsT = sum(CheckJuvenilesT);
    NewSubAdultsT = [JuvenilesT(logical(CheckJuvenilesT),[1 2 3]),...
       2*pi*rand(NumNewSubAdultsT,1)];
    NumRecruitsVector(1)=NumRecruitsVector(1)-sum(CheckJuvenilesT);
    NumRecruitsVector(4)=NumRecruitsVector(4)+sum(CheckJuvenilesT);
    SubAdultsT=[SubAdultsT ; NewSubAdultsT];
    JuvenilesT=JuvenilesT(logical(1-CheckJuvenilesT),:);

  end
  if ~(isempty(JuvenilesC)),
     JuvenilesC(:,3) = JuvenilesC(:,3) + 1;
% JUVENILES BECOMING SUBADULTS.
    CheckJuvenilesC =  JuvenilesC(:,3)> MaxJuvenileAge;
    NumNewSubAdultsC = sum(CheckJuvenilesC);
    NewSubAdultsC = [JuvenilesC(logical(CheckJuvenilesC),[1 2 3]),...
       2*pi*rand(NumNewSubAdultsC,1)];
    NumRecruitsVector(2)=NumRecruitsVector(2)-sum(CheckJuvenilesC);
    NumRecruitsVector(5)=NumRecruitsVector(5)+sum(CheckJuvenilesC);
    SubAdultsC=[SubAdultsC ; NewSubAdultsC];
    JuvenilesC=JuvenilesC(logical(1-CheckJuvenilesC),:);

  end
  if ~(isempty(Juveniles0)),
     Juveniles0(:,3) = Juveniles0(:,3) + 1;
% JUVENILES BECOMING SUBADULTS.
    CheckJuveniles0 =  Juveniles0(:,3)> MaxJuvenileAge;
    NumNewSubAdults0 = sum(CheckJuveniles0);
    NewSubAdults0 = [Juveniles0(logical(CheckJuveniles0),[1 2 3]),...
       2*pi*rand(NumNewSubAdults0,1)];
    NumRecruitsVector(3)=NumRecruitsVector(3)-sum(CheckJuveniles0);
    NumRecruitsVector(6)=NumRecruitsVector(6)+sum(CheckJuveniles0);
    SubAdults0=[SubAdults0 ; NewSubAdults0];
    Juveniles0=Juveniles0(logical(1-CheckJuveniles0),:);
 end
```

```
% newbirths.m
% This script file works out how many new chicks are added to the
% population
b = 0.85;
if month == 8,
 if ~(isempty(AdultsT)),
    NumAdultsT=length(AdultsT(:,1));
    NumNewJuvenilesT= round((b/2)*NumAdultsT);
    index = randperm(NumAdultsT);
    index = index(1:NumNewJuvenilesT);
    NewJuvenilesT= [AdultsT(index,[1 2]) zeros(NumNewJuvenilesT,1)];
 else
    NewJuvenilesT=[];
 end
 if ~(isempty(AdultsC)),
    NumAdultsC=length(AdultsC(:,1));
    NumNewJuvenilesC= round((b/2)*NumAdultsC);
    index = randperm(NumAdultsC);
    index = index(1:NumNewJuvenilesC);
    NewJuvenilesC= [AdultsC(index,[1 2]) zeros(NumNewJuvenilesC,1)];
 else
    NewJuvenilesC=[];
 end
if ~(isempty(Adults0)),
    NumAdults0=length(Adults0(:,1));
    NumNewJuveniles0= round((b/2)*NumAdults0);
    index = randperm(NumAdults0);
    index = index(1:NumNewJuveniles0);
    NewJuveniles0= [Adults0(index,[1 2]) zeros(NumNewJuveniles0,1)];
else
    NewJuveniles0=[];
 end
 end  % of if month == 8
```

```
% alldeaths.m
% This script file kills off Adults, SubAdults and Juveniles
% according to a death rate which depends on whether they are in the
% treatment block or in the control.

% JUVENILE DEATHS.
% IN THE TREATMENT BLOCK.
[JuvenilesT,NumJuvenileDeathsT]=deaths(JuvenilesT,DeathRates(1));
% IN THE CONTROL.
[JuvenilesC,NumJuvenileDeathsC]=deaths(JuvenilesC,DeathRates(2));
% IN THE OUTER REGION.
[JuvenilesO,NumJuvenileDeathsO]=deaths(JuvenilesO,DeathRates(3));

% SUBADULT DEATHS.
% IN THE TREATMENT BLOCK.
[SubAdultsT,NumSubAdultDeathsT]=deaths(SubAdultsT,DeathRates(4));
% IN THE CONTROL.
[SubAdultsC,NumSubAdultDeathsC]=deaths(SubAdultsC,DeathRates(5));
% IN THE OUTER REGION
[SubAdultsO,NumSubAdultDeathsO]=deaths(SubAdultsO,DeathRates(6));

% ADULT DEATHS.
% IN THE TREATMENT BLOCK
[AdultsT,NumAdultDeathsT] = deaths(AdultsT,DeathRates(7));
% IN THE CONTROL
[AdultsC,NumAdultDeathsC] = deaths(AdultsC,DeathRates(8));
% IN THE OUTER REGION
[AdultsO,NumAdultDeathsO] = deaths(AdultsO,DeathRates(9));
```

```
function [Indiv,NumDeaths] = deaths(Indiv,DeathRate)

% function [Indiv,NumDeaths] = deaths(Indiv,DeathRate)
% This functions takes Individuals = Adults, SubAdults
% or Juveniles and their respective Death rates as
% input and randomly deletes the appropriate number of
% individuals according to the death rate. The output
% is the number of deaths and the new martrix with those
% individuals who have died deleted from it.

NumIndiv = size(Indiv,1);
NumDeaths= round(DeathRate*NumIndiv);

index = randperm(NumIndiv);
index=index(1:NumIndiv-NumDeaths);
Indiv = Indiv(index,:);

function [IndivT, IndivC,Indiv0] =
   treatorcontrol(Indiv,TreatBlock,ControlBlock,TotalBlock)
if ~isempty(Indiv),
% Individuals in the treatment block.
CheckT = (Indiv(:,1) > TreatBlock(1)) & (Indiv(:,1) < ...
   TreatBlock(2)) & (Indiv(:,2)  > TreatBlock(3)) & (Indiv(:,2) < TreatBlock(4));
% Individuals in the outer regions.
Check0 = (Indiv(:,1) < ControlBlock(1)) | (Indiv(:,1) >...
    ControlBlock(2)) | (Indiv(:,2) < ...
    ControlBlock(3)) | (Indiv(:,2) > ControlBlock(4));

% Individuals in the control.
CheckC=1-(CheckT + Check0);
IndivT=Indiv(logical(CheckT),:); % Treatment.
IndivC= Indiv(logical(CheckC),:); % Control.
Indiv0=Indiv(logical(Check0),:); % Outer regions
else
   IndivT = [];
   IndivC = [];
   Indiv0=[];
end
```

```
function [SubAdults]=...
  subadultsmoving(SubAdults,NumSubAdults,movementscenario,...
  MaxSubAdultRange,TotalBlock,month)

%function [SubAdults]=
% subadultsmoving(SubAdults,NumSubAdults,movementscenario,...
% MaxSubAdultRange,TotalBlock,month)
% This function file moves subadults according to the movement scenario.

%  MOVEMENT OF SUBADULTS.
if NumSubAdults ~=0
if movementscenario==1,
 SubAdultDisplacementRadius = MaxSubAdultRange*rand(NumSubAdults,1);
 SubAdultDisplacementAngle = SubAdults(:,4) + (pi/8)*(-1 + 2*rand(NumSubAdults,1));
 SubAdults(:,[1,2]) = SubAdults(:,[1,2]) + SubAdultDisplacementRadius*[1 1].*...
      [cos(SubAdultDisplacementAngle) sin(SubAdultDisplacementAngle)];
elseif movementscenario ==2,
 if month == 6, % New SubAdults
   SubAdultDisplacementRadius = MaxSubAdultRange.*ones(NumSubAdults,1);
   SubAdultDisplacementAngle = SubAdults(:,4) + (pi/8)*(-1 + 2*rand(NumSubAdults,1));
 else
   SubAdultDisplacementRadius = MaxSubAdultRange*rand(NumSubAdults,1);
   SubAdultDisplacementAngle = 2*pi*rand(NumSubAdults,1);
 end
   SubAdults(:,[1,2]) = SubAdults(:,[1,2]) + SubAdultDisplacementRadius*[1 1].*...
     [cos(SubAdultDisplacementAngle) sin(SubAdultDisplacementAngle)];
 elseif movementscenario == 3,
  if month ==6,
    SubAdultDisplacementRadius = MaxSubAdultRange*ones(NumSubAdults,1);
    SubAdultDisplacementAngle = SubAdults(:,4) + (pi/8)*(-1 + 2*rand(NumSubAdults,1));
    SubAdults(:,[1,2]) = SubAdults(:,[1,2]) + SubAdultDisplacementRadius*[1 1].*...
      [cos(SubAdultDisplacementAngle) sin(SubAdultDisplacementAngle)];
  end
 elseif movementscenario == 4,
   SubAdultDisplacementRadius = MaxSubAdultRange*ones(NumSubAdults,1);
   SubAdultDisplacementAngle = 2*pi*rand(NumSubAdults,1);
   SubAdults(:,[1,2]) = SubAdults(:,[1,2]) + SubAdultDisplacementRadius*[1 1].*...
      [cos(SubAdultDisplacementAngle) sin(SubAdultDisplacementAngle)];
 elseif movementscenario == 5,
   SubAdultDisplacementRadius = MaxSubAdultRange*rand(NumSubAdults,1);
   SubAdultDisplacementAngle = 2*pi*rand(NumSubAdults,1);
   SubAdults(:,[1,2]) = SubAdults(:,[1,2]) + SubAdultDisplacementRadius*[1 1].*...
      [cos(SubAdultDisplacementAngle) sin(SubAdultDisplacementAngle)];
 end % of scenarios.

% MAKE SURE THEY STAY INSIDE THE WHOLE BLOCK.
CheckLeftBoundary = (SubAdults(:,1) <=  TotalBlock(1));
NumLeft = sum(CheckLeftBoundary);
SubAdults(logical(CheckLeftBoundary),[1,4])=...
   [-1*SubAdults(logical(CheckLeftBoundary),[1,4])] + ...
   [2*TotalBlock(1)*ones(NumLeft,1),pi*ones(NumLeft,1)];
CheckRightBoundary = (SubAdults(:,1) >=  TotalBlock(2));
NumRight = sum(CheckRightBoundary);
SubAdults(logical(CheckRightBoundary),[1,4])=...
   [-1*SubAdults(logical(CheckRightBoundary),[1,4])] + ...
   [2*TotalBlock(2)*ones(NumRight,1) pi*ones(NumRight,1)];
CheckBottomBoundary = (SubAdults(:,2) <= TotalBlock(3));
NumBottom = sum(CheckBottomBoundary);
```

```
SubAdults(logical(CheckBottomBoundary),[2,4])=...
   [-1*SubAdults(logical(CheckBottomBoundary),[2,4])] + ...
   [2*TotalBlock(3)*ones(NumBottom,1) zeros(NumBottom,1)];
CheckTopBoundary = (SubAdults(:,2) >= TotalBlock(4));
NumTop = sum(CheckTopBoundary);
SubAdults(logical(CheckTopBoundary),[2,4])=...
   [-1*SubAdults(logical(CheckTopBoundary),[2,4])] + ...
   [2*TotalBlock(4)*ones(NumTop,1) zeros(NumTop,1)];
end % end of if NumSubAdults ~=0
```

Bibliography

[1] H.R. Akcakaya and S. Ferson. *RAMAS/Space User Manual: Spatially Structured Population Models for Conservation Biology.* Applied Biomathematics, New York, 1990.

[2] N. Alterio and K. Brown. Secondary poisoning of mustelids in a New Zealand Nothofagus forest. *Journal of Zoology, London*, 243:863–869, 1997.

[3] Nic Alterio. Secondary poisoning of stoats (Mustela erminea), feral ferrets (Mustela furo), and feral house cats (Felis catus) by the anticoagulant poison, brodifacoum. *New Zealand Journal of Zoology*, 23:331–338, 1996.

[4] M.C. Andersen and D. Mahoto. Demographic models and reserve designs for the California spotted owl. *Ecological Applications*, 5(3):639–647, 1995.

[5] N.D. Barlow and J.M. Kean. Simple models for the impact of Rabbit Calicivirus Disease (RCD) on Australasian rabbits. *Ecological Modelling*, 109:225–241, 1998.

[6] N.S. Barrett. Short- and long-term movement patterns of six temperate reef fishes (families Labridae and Monacanthidae). *Marine and Freshwater Research*, 46(5):853–860, 1995.

[7] B. Basse, J.A. McLennan, and G.C. Wake. Analysis of the impact of stoats, Mustela erminea, on northern brown kiwi, Apteryx mantelli, in New Zealand. *Wildlife Research*, 26(2):227–237, 1999.

[8] B. Basse and G.C. Wake. Epidemic waves in animal populations: A case study. In A. Fitt and E. Cumberbatch, editors, *Modelling Case Histories.* Cambridge University Press, Cambridge, 1999. in press.

[9] B. Basse, G.C. Wake, and J.A. McLennan. Predation thresholds for survival of endangered species: An age structured model. *IMA Journal of Mathematics Applied to Medicine & Biology*, 14(3):241–250, 1997.

[10] Paul Beier. Determining minimum habitat areas and habitat corridors for cougars. *Conservation Biology*, 7:94–108, 1993.

[11] R. Bellman and K.L. Cooke. *Differential-Difference Equations.* Academic Press, New York, 1963.

[12] W.J. Boecklen. Nestedness, biogeographic theory, and the design of nature reserves. *Oecologia (Berlin)*, 112(1):123–142, 1997.

[13] W.L. Buller. Further notes on the ornithology of New Zealand. *Transactions and Proceedings of the New Zealand Institute*, 10:201–209, 1877.

[14] W.L. Buller. *A history of the birds of New Zealand*, volume 2. The Author, London, United Kingdom, 2nd edition, 1888. p359.

[15] Richard L. Burden and J.Douglas Faires. *Numerical Analysis.* PWS-KENT Publishing Company, Boston, 4th edition, 1989.

[16] M.A. Burgman, S. Ferson, and H.R. Arcakaya. *Risk Assessment in Conservation Biology.* Chapman and Hall, 1993.

[17] Lorenzo Capucci, Paola Fusi, Antonio Lavazza, Maria Lodovica Pacciarini, and Cesare Rossi. Detection and preliminary characterization of a new rabbit calicivirus related to Rabbit Haemorrhagic Disease Virus but non-pathogenic. *Journal of Virology*, pages 8614–8623, 1996.

[18] Hal Caswell. *Matrix Population Models: Construction Analysis and Interpretation.* Sinauer Associates Limited, USA, 1989.

[19] Graeme Caughley. *Analysis of Vertebrate Populations.* John Wiley & Sons, Inc., Canada, 1992.

[20] D. Choquenot, J. Druhan, B. Lukins, R. Packwood, and G Saunders. Managing the impact of rabbits on wool production systems in the central tablelands of New South

Wales: An experimental study and bioeconomic analysis. In *Proceedings of the 11th Australian Vertebrate Pest Control Conference*, Bunbury, Western Australia, May 1998.

[21] Ruel V. Churchill and James Ward-Brown. *Complex Variables and Applications.* McGraw Hill, Singapore, 1984.

[22] Brian J. Coman, Linton D. Staples, and Janine Muller. Induction of rabbit calicivirus disease (RCD) by the oral route in wild rabbits held under pen conditions. In R.K. Munro and R.T. Williams, editors, *Rabbit Haemorrhagic Disease: Issues in Assessment for Biological Control*, pages 123–125. Australian Government Publishing Service, Canberra, 1994.

[23] B.D. Cooke. Analysis of the spread of Rabbit Calicivirus from Wardang Island through mainland Australia. Technical report, CSIRO, October 1996.

[24] J.M. Cooper. *Introduction to Partial Differential Equations with Matlab.* Birkhäuser, Boston, 1998. p105-109.

[25] Otago Regional Council. RCD research in Otago. Technical report, O.R.C., February 1998.

[26] R.M. Cowling and W.J. Bond. How small should reserves be? An empirical approach in Cape Fynbos, South Africa. *Biological Conservation*, 58(3):243–256, 1991.

[27] D.R. Cox and H.D. Millar. *The Theory of Stochastic Processes.* Methuen, Great Britain, 1965. p203-251.

[28] C.T. Eason and E.B. Spurr. Review of the toxicity and impacts of brodifacoum on non-target wildlife in New Zealand. *New Zealand Journal of Zoology*, 22:371–379, 1995.

[29] L. Edelstein-Keshet. *Mathematical Models in Biology.* Random House, New York, 1988.

[30] Dilwyn Edwards and Mike Hamson. *Guide to Mathematical Modelling.* The MacMillan Press Ltd, Hong Kong, 1994.

[31] Lloyd D. Fisher and Gerald Van Belle. *Biostatistics.* John Wiley and Sons, Inc., New York, 1993.

[32] John B. Fraleigh and Raymond A. Beauregard. *Linear Algebra.* Addison-Wesley Publishing Company, USA, 3rd edition, 1995.

[33] S.H. Fritts and L.N Carbyn. Population viability, nature reserves and the outlook for gray wolf conservation. *Restoration Ecology*, 3(1):26–38, 1995.

[34] Richard Ghez. *A Primer of Diffusion Problems.* John Wiley and Sons, New York, 1988.

[35] J.A. Gibb and J.M. Williams. European rabbit. In C.M. King, editor, *The Handbook of New Zealand Mammals*, pages 138–160. Oxford University Press, Auckland, 1990.

[36] Narendra S. Goel and Nira Richter-Dyn. *Stochastic Models in Biology.* Academic Press, New York, 1974.

[37] F.C. Hoppensteadt. *Mathematical Methods of Population Biology.* New York University, Courant Institute of Mathematical Sciences, 1979. p134-136.

[38] John Innes, Kerry Brown, Paul Jansen, Rachel Shorten, and Dale Williams. Kokako population studies at Rotoehu Forest and on Little Barrier Island. Science for Conservation 30, Department of Conservation, 1996.

[39] John Innes and Ian Flux. North Island kokako recovery plan. Technical report, Landcare Reseach/ Department of Conservation, August 1999.

[40] John Innes, Rob Hay, Ian Flux, Philip Bradfield, Hazel Speed, and Paul Jansen. Successful recovery of North Island kokako, Callaeas cinerea wilsoni, populations, by adaptive management. *Biological Conservation*, 87:201–214, 1999.

[41] Robert E. Keen and James D. Spain. *Computer Simulation in Biology: A Basic Introduction.* Wiley-Liss, New York, 1992.

[42] C.M. King. The relationships between beech (Nothofagus) seedfall and populations of mice (Mus musculus) and the demographic and dietary responses of stoats (Mustela erminea), in three New Zealand forests. *Journal of Animal Ecology*, 52:141–166, 1983.

[43] C.M. King. Stoat. In C.M. King, editor, *The Handbook of New Zealand Mammals*, pages 288–312. Oxford University Press, Auckland, 1990.

[44] C.M. King and C.D. McMillan. Population structure and dispersal of peak-year cohorts of stoats (Mustela erminea) in two New Zealand forests, with especial reference to control. *New Zealand Journal of Ecology*, 5:59–66, 1982.

[45] Robert C. Lacy. Vortex: A computer simulation model for population viability analysis. *Wildlife Research*, 20:45–65, 1993.

[46] Robert C. Lacy, Kimberly A. Huges, and Philip S. Millar. *VORTEX: A Stochastic Simulation of the Extinction Process. Version 7 Users Manual.* IUCN/SSC Conservation Breeding Specialist Group, Apple Valley, MN, USA, 1995.

[47] S. Lamoureaux. *Demography and population models for Hieracium pilosella in New Zealand.* PhD thesis, Agresearch Lincoln, 1998.

[48] David B. Lindenmayer, Tim W. Clark, Robert C. Lacy, and Virginia C. Thomas. Population viability analysis as a tool in wildlife conservation policy: With reference to Australia. *Environmental management*, 17(6):745–758, 1993.

[49] K. Louie, M.G. Roberts, and G.C. Wake. Thresholds and stability analysis of models for the spatial spread of fatal disease. *IMA Journal of Mathematics in Medicine & Biology*, 10:207–226, 1993.

[50] Patrick Marchand. *Graphics and GUIs with MATLAB.* CRC Press Inc., Boca Raton, 1996.

[51] G. Martin and J. Donaldson. Rabbit control from the first RCD epidemic in New Zealand. In *Proceedings of the 11th Australian Vertebrate Pest Control Conference*, Bunbury, Western Australia, 1998.

[52] Robert M. May. On the relationship among various types of population models. *The American Naturalist*, 107(953):46–57, January-February 1992.

[53] M.A. McCarthy, D.C. Franklin, and M.A. Burgman. The importance of demographic uncertainty: An example from the helmeted honeyeater, Lichenostomus melanops cassidix. *Biological Conservation*, 67(2):135–142, 1994.

[54] P.D. McCormack. *Physical Fluid Dynamics.* Academic Press Inc., New York, 1973.

[55] A.G. McKendrick. Applications of mathematics to medical problems. *Proc. Edinburgh Math. Soc.*, 44:93–130, 1926.

[56] J.A. McLennan. Breeding of North Island brown kiwi, Apteryx australis mantelli, in Hawke's bay, New Zealand. *New Zealand Journal of Ecology*, 11:89–97, 1988.

[57] J.A. Mclennan. Survival at Waikaremoana. *Forest and Bird*, 283:16–21, 1997.

[58] J.A. McLennan and M.A. Potter. Distribution, population changes and management of brown kiwi in Hawke's Bay. *New Zealand Journal of Ecology*, 16:91–102, 1992.

[59] J.A. McLennan and M.A. Potter. Juveniles in mainland populations of kiwi. *Notornis*, 40:294–297, 1993.

[60] J.A. McLennan, M.A. Potter, H.A. Robertson, G.C. Wake, J. Reid, J. Lyall, J. Miles, L. Dew, A.J. McCann, R. Colbourne, P.J. Miller, and L. Joyce. Role of predation in the decline of kiwi, Apteryx spp., in New Zealand. *New Zealand Journal of Ecology*, 20(1):27–35, 1996.

[61] National RCD Monitoring, Surveillance Program, and Epidemiology Program. Highlights. Technical report, RCD Management Group, July 1998.

[62] Sue Moore and John Innes. North Island kokako: The cutting edge. *Forest and Bird*, (282):13–20, 1996.

[63] E.C. Murphy and J.E. Dowding. Ecology of the stoat in Nothofagus forest: Home range, habitat use and diet at different stages of the beech mast cycle. *New Zealand Journal of Ecology*, 19:97–109, 1995.

[64] E.C. Murphy and C.R. Pickard. House mouse. In C.M. King, editor, *The Handbook of New Zealand Mammals*, pages 225–242. Oxford University Press, Auckland, 1990.

[65] Elaine Murphy. Secondary poisoning of stoats in a New Zealand forest. *Rare Bits*, 27:30, 1997.

[66] J.D. Murray. *Mathematical Biology*. Springer Verlag, New York, 1989.

[67] Greg Mutze, Brian Cooke, and Peter Alexander. The initial impact of Rabbit Haemorrhagic Disease on European rabbit populations in South Australia. *Journal of Wildlife Diseases*, 34:221–227, 1998.

[68] G. Norbury, R. Heyward, and J. Parkes. Behaviour of Rabbit Calicivirus Disease in baited versus natural epidemics, Otago, New Zealand. In *Proceedings of the 11th Australian Vertebrate Pest Control Conference*, Bunbury, Western Australia, 1998.

[69] P.J. O'Hara. Decision on the application to approve the importation of rabbit calicivirus as a biological control agent for feral rabbits. Technical report, Ministry of Agriculture and Fisheries (MAF) New Zealand, 1997.

[70] Akira Okubo. *Diffusion and Ecological Problems: Mathematical Models.* Springer-Verlag, Berlin, New York, 1980.

[71] J.P. Parkes, G. Norbury, and R. Heyward. Initial epidemiology of RHD in New Zealand. *New Zealand Science Review*, 1998.

[72] R.P. Pech and J.C. McIlroy. A model of the velocity of advance of foot and mouth disease in feral pigs. *Journal of Applied Ecology*, 27:635–650, 1990.

[73] H.P. Possingham and I. Davies. Alex: A model for the viability analysis of spatially structured populations. *Biological Conservation*, 73:143–150, 1995.

[74] O. Price, J.C.Z. Woinarski, D.L. Liddle, and J. Russell-Smith. Patterns of species composition and reserve design for a fragmented species: Monsoon rainforests in the Northern Territory, Australia. *Biological Conservation*, 74(1):9–19, 1995.

[75] B. Reid and G.R. Williams. The kiwi. *Biogeography and Ecology in New Zealand*, page 689, 1975. Junk, The Hague, The Netherlands.

[76] J. Reid, L. Joyce, and J. Lyall. The monitoring of breeding and protection of the Okarito brown kiwi in Westland National Park, 1994-95. Technical report, New Zealand Department of Conservation, West Coast Conservancy, 1995.

[77] Munro R.K. and Williams R.T., editors. *Rabbit Haemorrhagic Disease: Issues in Assessment for Biological Control.* Australian Government Publishing Service, Canberra, 1994. p80-81.

[78] Rolf H. Sabersky, Allan J. Acosta, and Edward G. Hauptmann. *Fluid Flow: A First Course in Fluid Mechanics.* Macmillan Publishing Company, New York, 3rd edition, 1964.

[79] S. Shigaseda and K. Kawasaki. *Biological Invasions: Theory and Practice.* Oxford University Press, New York, 1997. p36-39.

[80] Kristina Smitalova and Stefan Sujan. *A Mathematical Treatment of Dynamical Models in Biological Science.* Ellis Horwood, New York, 1991.

[81] Maurice E. Solomon. *Population Dynamics.* Edward Arnold (Publishers) Limited, Great Britain, 1969.

[82] Murray R. Spiegel. *Theory and Problems of Laplace Transforms.* Schaum Publishing Company, New York, 1965.

[83] E.B. Spurr. The development of the long-life toxic bait and lures for Mustelid. Technical Report LC9889/26, Landcare Research Limited, 1998.

[84] Ivar Stakgold. *Boundary Value Problems of Mathematical Physics.* The Macmillan Company, New York, 1968. p58-60.

[85] Struan K. Sutherland. *Venomous Creatures of Australia.* Oxford University Press, Melbourne, 1994.

[86] Anti-Rabbit Research Foundation Trust. *Rabbit Control and Rabbit Calicivirus Disease: A Field Handbook for Land Managers in Australia*, 1997.

[87] E.H. Twizell. *Computational Methods for Partial Differential Equations.* Ellis Horwood Limited, Chichester, 1984. p52-253.

[88] H. Versteeg and W. Malalasekera. *An Introduction to Computational Fluid Dynamics. The Finite Volume Method.* Longman Group Ltd, New York, 1995.

[89] Graeme Wake. The symbiosis of mathematics and biology. *New Zealand Journal of Ecology*, 16(1):1–3, 1992.

[90] Keith Wardhaugh and Wayne Rochester. Wardang Island: A retrospective analysis of weather conditions in relation to insect activity and displacement. Technical report, CSIRO Division of Entomology, 1997.

[91] H. Westbury, C. Lenghaus, and R. Munro. A review of the scientific literature relating to RHD. In R.K. Munro and R.T. Williams, editors, *Rabbit Haemorrhagic Disease:*

Issues in Assessment for Biological Control, pages 123–125. Australian Government Publishing Service, Canberra, 1994.

[92] C.J. Wild and G.A.F. Seber. *Introduction to Probability and Statistics.* University of Auckland, Auckland, 1993.

[93] Samuel S. Wilks. *Mathematical Statistics.* John Wiley & Sons Inc., New York, 1962. p57-205.